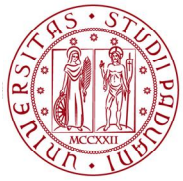

UNIVERSITÀ
DEGLI STUDI
DI PADOVA

Sede Amministrativa: Università degli Studi di Padova

Dipartimento di Territorio e Sistemi Agro-Forestali

SCUOLA DI DOTTORATO DI RICERCA IN SCIENZE DELLE PRODUZIONI VEGETALI

CICLO: XXVII.

Botrytis cinerea transcriptomic response to the active substance eugenol and role of Snf1 kinase in fungal pathogenesis

Direttore della Scuola : Ch.mo Prof. Antonio Berti

Supervisore : Ch.mo Prof. Francesco Favaron

Co-supervisori : Prof. Mathias Choquer
Prof. Luca Sella

Dottoranda : Szabina Lengyel

Declaration

I hereby declare that this submission is my own work and that, to the best of my knowledge and belief, it contains no material previously published or written by another person nor material which to a substantial extent has been accepted for the award of any other degree or diploma of the university or other institute of higher learning, except where due acknowledgment has been made in the text.

30/01/2015

Szabina Lengyel

A copy of the thesis will be available at *http://paduaresearch.cab.unipd.it/*

Dichiarazione

Con la presente affermo che questa tesi è frutto del mio lavoro e che, per quanto io ne sia a conoscenza, non contiene materiale precedentemente pubblicato o scritto da un'altra persona né materiale che è stato utilizzato per l'ottenimento di qualunque altro titolo o diploma dell'università o altro istituto di apprendimento, a eccezione del caso in cui ciò venga riconosciuto nel testo.

30/01/2015

Szabina Lengyel

Una copia della tesi sarà disponibile presso *http://paduaresearch.cab.unipd.it/*

per Giuseppe

Acknowledgements

At first, I would like to thank Prof. Francesco Favaron for the possibility that I could participate the doctoral program at the University of Padova, and for his supervision during my PhD study.

I express my deepest thanks to Mathias and Luca, for their guidance of my work, new ideas for my research, and writing of my thesis. Without their help this thesis would not have been possible.

Many thanks to the Padova-group, to Carla, Silvana, Katia, Maria Chiara, Riccardo e Sara, as well as to Anna Rita and Marta for their help in the laboratory, and to Antonio Masi for the opportunity to perform biochemical experiments in his lab. Lots of thanks for the other PhD students in Padova for their encouragement, and for the great times we passed together.

I would like to thank to the Lyon-group, especially to Christine, but also to Marie-Jo, Christophe, Nathalie, Elisabeth, Elise, Yohann, Eytham, Kelly, Jordan, and Denis; it was fantastic working at the Labo-Mixte. Many thanks to Isabelle for her help in bioinformatics. I would also thank the Université Claude Bernard Lyon 1 and Bayer CropScience, which provided me with technical support during those fifteen month I was staying in Lyon.

Finally, greatest thanks to my family: to my grandmother and my grandfather, to my mother and my father, to my sisters Betti and Alex, and to Giuseppe for their love and care, no matter how long the distance was between us. Additionally, thanks to Betti for the correction of formal errors in my thesis.

Index

Summary

Botrytis cinerea is a fungal pathogen causing grey mould on more than 240 dicotyledonous plants resulting huge economic losses. To control the disease in the field and to prevent post-harvest damages, frequent fungicidal treatments are required, thus increasing the risk of spread of resistant strains to fungicides and the negative effects on environment and human health. Therefore, new molecules with different mode of action or alternatives to fungicides should be introduced to better manage the disease, to better preserve the environment and to increase the food safety.

Several groups of natural substances can be used as alternatives to synthetic fungicides and among these compounds, plant essential oils are largely experimented for their well known antimicrobial and antifungal activity. Eugenol is an effective compound of several essential oils, the main component of clove oil, which is extracted from clove buds and used as local antiseptic in traditional medicine. The mechanism of the antifungal effect of eugenol was examined on *Saccharomyces cerevisiae* and on some plant pathogenic fungi. The main described effects of this phenolic component seem to be the disruption of integrity of fungal cell membrane and cell wall; however the precise mode of action of eugenol is unclear.

To address the mode of action of eugenol, transciptome analysis was performed using NimbleGen 4x72K arrays. Cultures of *B. cinerea* were treated with eugenol at the effective concentration (EC_{80}) of 250 µg ml^{-1}, and control (untreated) and treated mycelia were collected after 6 h and 12 h. The transcriptional response of *B. cinerea* to eugenol was statistically analyzed and the differentially expressed genes were evaluated. Significant enrichment of down-regulated genes was found in the ergosterol biosynthesis, DNA replication factors class, glutathione pathway, transmembrane transport, and botrydial toxin biosynthesis, while up-regulated genes were detected in several functional categories belonging to stress response.

A modern approach to fungicidal development is a rational design of drugs mirrored to target fundamental node of the complex cellular network.

In yeast, the Snf1 protein kinase is a global regulator and important in a glucose signalling pathway controlling the response to nutritional and environmental stresses. In order to characterize the role of *B. cinerea* Snf1 kinase, deletion mutants of the encoding gene were obtained and analyzed *in vitro* and *in vivo*. Δ*snf1* mutants grew slower with a reduction of 20-80 % on simple sugars, polysaccharides, and on lipidic carbon sources at pH 5 and mostly at pH 7. The enzyme activity produced by a mutant strains was also measured and a significant

reduction of xylanase activity and an increase of polygalacturonase activity were observed in comparison with the wild type. These results suggest that Snf1 kinase does not act as general activator of *B. cinerea* cell wall degrading enzymes but seems to be involved in a possible pH dependent regulation. In pathogenicity test, the virulence of the Δ*snf1* mutants was reduced by 60-90 % in comparison with the wild type. Δ*snf1* mutants were impaired in sporulation as well; in fact, they did not produce normal conidiophores with macroconidia, but only microconidia.

In conclusion, *B. cinerea* Snf1 protein kinase regulates conidiation, carbon source utilization and strongly affects virulence; therefore it could be a possible target for new fungicides.

Riassunto

Botrytis cinerea è un fungo patogenico che provoca muffa grigia su più di 240 piante dicotiledoni con conseguenti enormi perdite economiche. Per controllare la malattia in campo e per prevenire i danni post-raccolta, sono necessari frequenti trattamenti antiparassitari, aumentando così il rischio di diffusione di ceppi resistenti ai fungicidi e gli effetti negativi per l'ambiente e la salute umana. Pertanto, le nuove molecole con diversa modalità di azione o i fungicidi alternativi dovrebbero essere introdotti per gestire meglio la malattia, per preservare meglio l'ambiente e per aumentare la sicurezza degli alimenti.

Diversi gruppi di sostanze naturali possono essere utilizzati come alternativi ai fungicidi di sintesi e tra questi composti, gli oli vegetali essenziali sono largamente sperimentati per la loro conosciuta attività antimicrobica e antifungina. L'eugenolo è un composto efficace per diversi oli essenziali, il componente principale di olio di garofano, che viene estratto dalle gemme dei chiodi di garofano e usato come antisettico locale nella medicina tradizionale. Il meccanismo dell'effetto antimicotico dell'eugenolo è stato esaminato in *Saccharomyces cerevisiae* e su alcuni funghi patogeni vegetali. I principali effetti descritti di questo componente fenolico sembrano essere la rottura dell'integrità della membrana cellulare fungina e della parete cellulare; tuttavia non è chiara la modalità precisa d'azione dell' eugenolo.

Per affrontare la modalità di azione dell' eugenolo, l'analisi del trascrittoma è stata effettuata utilizzando matrici NimbleGen 4x72K. Le colture di *B. cinerea* sono state trattate con eugenolo alla concentrazione efficace (EC_{80}) di 250 mg ml^{-1}, e di controllo (non trattato) e i miceli trattati sono stati raccolti dopo 6 h e 12 h. E' stata analizzata statisticamente la risposta trascrizionale di *B. cinerea* all' eugenolo e sono stati valutati i geni differentemente espressi. E' stato trovato un arricchimento significativo di geni down-regolati nella biosintesi dell'ergosterolo, nei DNA classe fattori di replica, nel percorso del glutatione, nel trasporto transmembrana e nella biosintesi della tossina botrydial, mentre i geni up-regolati sono stati rilevati in diverse categorie funzionali in merito a risposta da stress.

Un approccio moderno allo sviluppo dei fungicidi è un disegno razionale di farmaci che rispecchiano il target come nodo fondamentale della complessa rete cellulare. Nei lieviti, la proteina chinasi Snf1 è un regolatore globale ed è un importante percorso di segnalazione del glucosio attraverso il controllo della risposta a stress nutrizionali e ambientali. Per caratterizzare il ruolo di *B. cinerea* Snf1 chinasi, i mutanti di delezione del gene codificato sono stati ottenuti e analizzati in vitro e in vivo. I mutanti Δ*snf1* sono cresciuti

più lentamente con una riduzione del 20-80 % su semplice zuccheri, polisaccaridi, e fonti lipidiche di carbonio a pH 5 e per lo più a pH 7. E' stata anche misurata l'attività enzimatica prodotta da ceppi mutanti ed è stata osservata una significativa riduzione dell'attività di xilanasi e un aumento dell'attività della poligalatturonasi rispetto al tipo selvatico. Questi risultati suggeriscono che la Snf1 chinasi non agisce come attivatore generale degli enzimi che degradano la parete cellulare di *B. cinerea* ma sembra sia coinvolta in un eventuale regolazione dipendente dal pH. Nel test di patogenicità, la virulenza dei mutanti Δ*snf1* è stata ridotta del 60-90 % rispetto al tipo selvatico. I mutanti Δ*snf1* sono stati alterati in sporulazione pura; in realtà, essi non producono conidiofori normali con macroconidi, ma solo microconidi.

In conclusione, la proteina chinasi Snf1 di *B. cinerea* regola la conidiazione, l' utilizzo delle fonti di carbonio e influenza fortemente la virulenza; quindi potrebbe essere un possibile bersaglio per i nuovi fungicidi.

Introduction

Botrytis cinerea biology and life cycle

Botrytis cinerea Pers. Fr. (teleomorph *Botryotinia fuckeliana* (de Bary) Whetzel) is a necrotrophic fungus causing grey mould disease on more than 240 dicotyledonous plants.

B. cinerea is member of the *Botryotinia* genus in the *Sclerotinaceae* family and in the Ascomycota phylum. Its genome contains 16 chromosomes and approximately 16,000 genes; recently, two strains have been sequenced (Amselem *et al*., 2011).

The fungus produces multinucleate macroconidia on conidiophores and uninucleate microconidia (male spermatia). Sexual crossing between microconidia and the female parent sclerotia results in the formation of apothecia containing eight ascospores. Sexual reproduction could be performed in laboratory, but this phenomenon remains undetected *in vivo*. (Williamson *et al*., 2007)

The life cycle of this pathogen is presented in Figure 1. In early spring, *B. cinerea* conidia are spread by wind or rain onto healthy plant tissue. At optimal conditions (15-20 ^{o}C and 90 % relative humidity), conidia germinate in 15 hours. After germination, hyphae penetrate leaves, blossom parts, as well as fruits causing brown necrotic lesions or softening of the tissues. The fungus then is able to live as a saprophyte organism on the necrotic tissues. Until autumn, mycelium produces conidiophores with spores and, if environmental conditions are favourable, the infection process continues. *B. cinerea* overwinters as sclerotia or as mycelium on plant debris. (Myers, 2015)

Occasionally, at dry conditions, *B. cinerea* infects ripe grapevine causing the noble rot phenotype leading to a strong concentration of sugars in the berries without production of toxic compound. These berries are used to make sweet dessert wines, such as the Hungarian Tokaji Aszú.

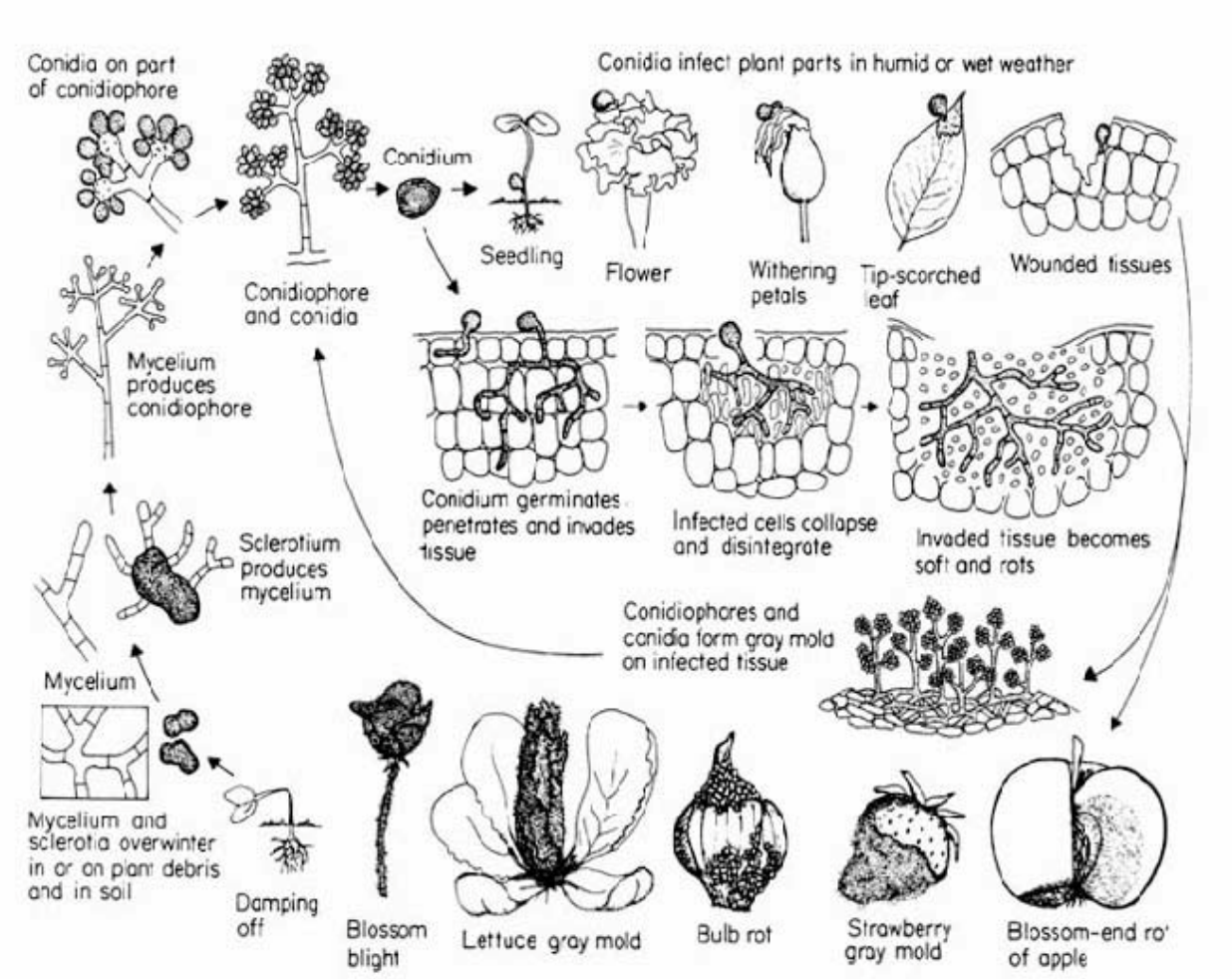

Figure 1 – Life cycle of *B. cinerea* (George N. Agrios, Plant Pathology, 4th edition, 1997).

Infection strategies

During infection, *B. cinerea* develops appressorium (hyphal tip with strong "pressing" capacity) to penetrate into the host tissue; however the physical role of this structure is disputed, because it differs from the classical appressorim formed by *Colletotrichum* and *Magnaporthe*, and it does not contain a wall that seals the appressorium from the germtube to generate high osmotic pressure (van Kan, 2006). At first, the pathogen has to breach the cuticle layer of the plant surface, which contains cutin, polyester of hydroxylated and epoxidised C_{16}- and C_{18}-fatty acids and especially on fruits, it is covered with a hydrophobic wax layer consisting of fatty alcohols. *B. cinerea* secretes cutinases, but this enzyme is not fundamental for penetration. To facilitate penetration, the pathogen secretes a spectrum of cell wall degrading enzymes (CWDEs), while by toxins and reactive oxygen species it kills the plant cells (Kars and van Kan, 2007).

The CWDEs secreted by *B. cinerea* depolymerise the diverse polysaccharide components of plant cell wall: pectin, cellulose and hemicelluloses. The role of the CWDEs in fungal pathogenesis is described with more details in the Chapter II.

Among the toxic compounds secreted by *B. cinerea,* the best studied ones are botrydial and botcinic acid derivatives. The sesquiterpene botrydial causes chlorosis and cell collapse on bean leaves (Colmenares *et al*., 2002). Botcinic acid derivatives where also identified as phytotoxic secondary metabolites, and gene clusters that are responsible for the biosynthesis of these toxins were genetically characterized (Pinedo *et al.*, 2008; Dalmais *et al*., 2011).

B. cinerea stimulates oxidative burst on the host surface (Temme and Tudzynski, 2009). Enzymes responsible for the production of ROS in the fungus are for example the NADPH oxydases (Nox) that generate superoxide; mutants in Nox genes were reduced in virulence (Siegmund *et al*, 2013). Oxidative burst is one of the defence mechanism of plants during interaction with biotrophic pathogens but the necrotrophic fungus *B. cinerea*, stimulating a rapid accumulation of ROS and inducing local cell death, benefits from this mechanism.

The control of grey mould

Grey mould caused by *B. cinerea* in one of the most important plant diseases in pre- and postharvest stage of many crops, including tomato, strawberry, grapevine, and peony. Generally, the aerial parts of plants are sprayed by fungicides with a dose of 400-500 g/ha (e.g. carbendazim, fludioxonil) to 2000-3000 g/ha (e.g. maneb, thiram) from one-two to twenty times per season (Leroux, 2007). The frequently applied fungicides can develop resistance rapidly, therefore *B. cinerea* is considered to be a "high risk" pathogen. Alternative control measures include the spray of essential oils and the use of biocontrol agents.

Chemical fungicides

Chemical fungicides against *B. cinerea* can be classified by their mode of action (MOA) and by the containing chemical group (FRAC Code List©*2014).

Benzimidazols - carbendazim, benomyl and thiophanate-methyl - inhibit hyphal growth and cause defect of germ tubes at low concentration; they were developed in the 1960s and became well known fungicides to control grey mould (Leroux, 2007). Boscalid carboxamide inhibits the succinate dehydrogenase complex (complex II) (Leroux, 2007), while azoxystrobin and fluazinam are other broad spectrum fungicides acting on the respiration system. Anilino-pyrimidines (AP) are highly active fungicides developed in the 1990s and cyprodinil - member of this group - is considered the most effective pesticide against *Botrytis* (Hahn, 2014). This molecule inhibits the methionine biosynthesis by targeting the cystathione β-lyase, which catalyses the synthesis of homocysteine from cystathione, but also affects the activity of CWDE (Waechter *et al*., 2010). Phenylpyrroles (PP) were developed from the antifungal antibiotic pyrrolnitrin, synthesized from *Pseudomonas* species; the PP-fungicide fludioxonil is used for seed and foliar treatment, as well as in post-harvest treatments (Hahn, 2014). Iprodione is a dicarboximide used against *Botrytis* and *Sclerotinia*, however in several countries these molecules are no longer registered because of resistance problems (Hahn, 2014). Phanylpyrroles and dicarboximedes act on proteins involved in the MAP kinase signalling cascades. Sterol biosynthesis inhibitors interfere with ergosterol biosynthesis by blocking several enzymes involved in this pathway. Fenhexamid is a widely used fungicide to control grey mould disease and only a low to medium resistance has been observed, developed by the site specific mutation of the target gene *erg27* (Hahn, 2014).

Biological control agents

Biological control agents (BCAs) can be utilized for crop protection. BCAs against *B. cinerea* include: *Pichia, Candida*, *Bacillus, Pseudomonas*, *Trichoderma*, *Ulocladium*, and *Gliocladium* (Jacometti *et al*., 2010). Among mycoviruses, some are known to be effective against *B. cinerea*: Botrytis virus F (BVF), Botrytis virus X (BVX), Botrytis cinerea mitovirus 1 (BcMV1), and Botrytis porri RNA virus (BpRV); BVF and BVX already exist in the international market (Pearson and Bailey, 2013).

Although biological control is a possible alternative to synthetic fungicides, the rapid growth of *B. cinerea* and the low parasitism rate of BCAs limit the widely use of classical BCAs.

Natural essential oils

Another way to control grey mould is the use of natural essential oils, which is discussed in the Chapter I.

B. cinerea is a "high risk" pathogen, therefore new control strategies and targets for fungicides should be identified in order to avoid the development of resistant populations. In the following chapters, two basic researches are presented providing knowledge useful to identify new targets for the control of this fungus.

In Chapter I, a transcriptomic approach was performed using NimbleGen microarrays to study the response of *B. cinerea* to the natural bioactive compound eugenol whose targets are poorly studied in fungi.

In Chapter II, the contribution of *B. cinerea* Snf1 protein kinase to fungal growth, development and pathogenesis was studied by deletion mutants of the encoding gene. In other fungi Snf1 regulates the fungal adaptation to carbon source and the secretion of CWDE.

Chapter I

Botrytis cinerea transcriptomic response to the active substance eugenol

1.1 Introduction

Botrytis cinerea is a necrotrophic fungus, which is able to destroy several agricultural crops (e.g.: strawberry, grapevine, onion, and tulip) on fields and after harvest as well, causing huge economic losses. Frequent treatments and huge amounts of antifungal chemicals can lead to rapid resistance of the fungus against the applied molecules and therefore *B. cinerea* is considered a "high risk" pathogen. The resistance mechanism is mediated by especially drug efflux transports and mutations of the fungicide targets (Hahn, 2014); therefore new molecules with different mode of action or alternatives to fungicides should be introduced.

Essential oils have been used for centuries as antimicrobial products. Recently, they are getting more attention in aromatherapy, in pharmaceutical products and as natural pesticides. The antifungal effect of essential oils on *B. cinerea* has been studied long ago; 49 essential oils were tested on spore germination. Palmarosa (*Cymbopogon martini*), red thyme (*Thymus zygis*), cinnamon leaf (*Cinnamomum verum*), and clove buds (*Eugenia caryophyllata*) showed the most antimicrobial activity against the fungus (Wilson *et al*., 1997). Thereafter, natural oils with great antifungal activity have been tested in post-harvest technologies and a novel method for table grape packaging using an atmosphere with natural essential oils was developed (Valero *et al*., 2010); essential oils of black caraway, fennel, and peppermint also prevented the damage caused by grey mould on sweet cherry fruit (Aminifard and Mohammadi, 2013).

Phenolic compounds contained in essential oils are known to act as antioxidants (Kamatou *et al*., 2012) and have stronger antimicrobial activity than cinnamic aldehydes, alcohols and aldehydes because of their hydroxyl group (Kalemba *et al*., 2003).

Eugenol (4-allyl-2-methoxyphenol) (Figure 1.1B), the main compound of clove oil, is a phenylpropene, extracted from clove buds (Figure 1.1A), but it is also found in cinnamon and basil (Ocimum basilicum) tissues. Its antiseptic and anaesthetic effects are already well known; in fact, clove oil is used as local antiseptic in dentistry and as an anaesthetic on aquarium fish, furthermore it is component of fragrances and food flavours.

As early as 1977, the first observations about the antifungal activity of eugenol were published; 200 ppm of this molecule completely inhibited the growth of *Aspergillus flavus* (Bullerman *et al*., 1977). The mechanism of antimicrobial effect of eugenol was studied on *Saccharomyces cerevisiae* and on two wood decay fungi suggesting that disruption of both membrane and cell wall is probably the main impact of this phenolic component (Bennis *et*

al., 2004 and Yen *et al*., 2008). This effect was also verified on *B. cinerea*: microscopic examinations showed alteration in the hyphae and large vesicles (Wang *et al*., 2010). Practical utilization of eugenol was tested on postharvest pathogens; CO_2 and O_2 gas mixture supplemented with eugenol was used inside the packages of table grape (Valverde *et al*., 2005); apple fruits were treated with eugenol mixed with tween 80 or ethoxylate or lecithin (Amiri *et al*., 2008); in both cases the positive effect of eugenol was recognized.

Despite the fact that eugenol is a well know molecule with antimicrobial effect *in vivo* and *in vitro*, little is known about mode of action and its putative targets in fungus cell. To address the mode of action of eugenol, transciptome analysis was performed on *B. cinerea* treated with EC_{80} (250 µg ml^{-1}) concentration of the molecule. So far, *S. cerevisiae* was utilized as a model system to identify the response of the pathogen to different fungicides. Now the whole genome of several important plant pathogenic fungi has been sequenced (Cools *et al*., 2013), as well as the genome of two strains of *B. cinerea* (Amselem *et al*., 2011) and when we started this work, DNA microarray chips were used to have a global overview on gene expression.

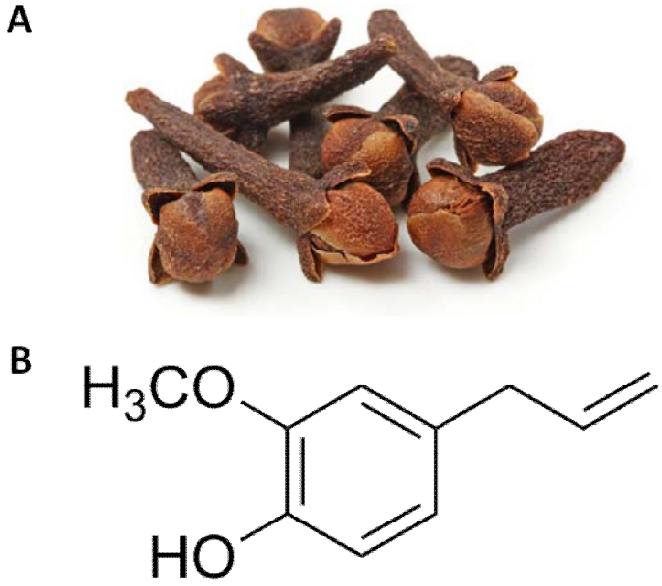

Figure 1.1 – (**A**) Clove buds (*Eugenia caryophyllata*). (**B**) Chemical structure of eugenol. (Kamatou *et al*., 2012)

1.2 Materials and methods

1.2.1 Fungal strains and materials

For further experiments, 50 ml PDB medium was inoculated with *B. cinerea* B05.10 conidia (1.5 x 10^4 ml^{-1}) and the fungus culture was grown for 48 h. Cultures were treated then with eugenol at EC_{80} dose (250 µg ml^{-1}) (data kindly provided by Riccardo Marcato). Mycelia of control (without treatment) and treated samples were harvested by filtration after 6 and 12 hours of incubation and stored at -80 ^oC. Five biological replicates were prepared for each condition.

1.2.2 Microarray preparation

The different steps for microarray preparation are shown in Figure 1.2.

1.2.2.1 RNA extraction

Total RNA was extracted using RNeasy Midi Kit (Qiagen, Germany) following the manufacturer's instructions. The RNA then was treated with DNase, using DNase kit (Ambion, Germany). The concentration of the total RNA was measured with NanoDrop (Thermo Fisher Scientific Inc., USA) and the quality was controlled with Agilent 2100 bioanalyzer (Agilent Technologies, Germany) using Agilent RNA 6000 Nano Kit (Agilent Technologies, Germany) following the user's manual. Samples of good quality were kept when the expected concentration was at least 100 ng μl^{-1} and the ratio of $A_{260}/A_{230} \geq 1.8$.

Presence of residual DNA content in samples was controlled by amplifying the actin gene; PCR conditions were as follows: initial denaturation at 95 ^oC for 3 min, then 34 cycles of denaturation at 95 ^oC for 30 sec, annealing at 60 ^oC for 30 sec, and polymerization at 72 ^oC for 1 min.

1.2.2.2 cDNA synthesis

cDNA was synthesized from 10-15 µg total RNA using double-stranded cDNA synthesis Kit (Invitrogen, USA). The RNA was concentrated in vacuum centrifuge to 9 µl and 2 µl oligo dT primer (Ambion, Germany) was added. Samples were incubated at 70 ^oC for 10 min and kept in ice-water slurry for 5 min. Master mix was prepared with 4 µl of 5X First Strand Buffer, 2 µl of 0.1 M DTT, and 1 µl of 10 mM dNTP Mix, and added to the samples. Then the mixture was incubated at 42 ^oC for 1h; after 2 minutes of incubation time, 2 µl SuperScript II enzyme was added. For the second strand cDNA synthesis a master mix containing 91 µl DEPC water, 30 µl of 5X Second Strand Buffer, 3 µl of 10 mM dNTP Mix,

1 µl of 10 U μl^{-1} DNA ligase, 4 µl of 10 U μl^{-1} Polymerase I, and 1 µl of 2 U μl^{-1} RNase H. It was added to the samples and the mixtures were incubated at 16 ^{o}C for 2 h. The incubation was elongated with 5 min after that 2 µl of 5 U μl^{-1} T4 DNA polymerase had been added to the reactions, and then the samples were kept on ice until the following step. Ten µl of 0.5 M EDTA (Sigma-Aldrich, USA) and then 1 µl of 10 mg ml^{-1} RNase A solution (Novagen, USA) were added to the samples and the mixtures were incubated at 37 ^{o}C for 10 min. Then the samples were added to previously prepared 163 µl of phenol:chloroform:isoamil alcohol solution and the vortexed mixtures were centrifuges in Phase Loch tube at 12,000 x g for 5 min. The aqueous layer was transferred into a new tube. For the cDNA precipitation 16 µl of 7.5 M ammonium acetate (Sigma-Aldrich, USA), 7 µl of 5 mg ml^{-1} glycogen and then 326 µl of ice-cold absolute ethanol were added to the samples which were then centrifuged at 14,000 x g for 25 min. The supernatant was removed and the pellet was washed two times with 500 µl 80 % (v/v) of ice-cold ethanol. The pellet was dried in Concentrator plus (Eppendorf, USA) and then rehydrated with 20 µl H_2O.

The concentration of the samples was determinded with NanoDrop and the quality was controlled with Agilent 2100 bioanalyzer using Agilent RNA 6000 Nano Kit following the manufacturer's instructions. The expected concentration was at least 100 ng μl^{-1} and the ratio of $A_{260}/A_{230} \geq 1.8$. Four biological replicates for each condition were selected for the following processes.

1.2.2.3 Labeling

2 µl β-mercaptoethanol was added to 1100 µl of random primer buffer. Cy3 labeled random nonamer primer was briefly centrifuged then diluted in 1050 µl of random primer buffer. One µg cDNA was diluted in 40 µl PCR grade water and mixed with 40 µl Cy3 random nonamer. The sample was heat-denatured at 98 ^{o}C for 10 min, then quick-chilled in an ice-water bath for 2 min. dNTP/Klenow mastermix was prepared with 10 µl dNTP mix (10 mM each dNTP), 8 µl PCR grade water and 2 µl Klenow Fragment (3'->5' exo-; 50 U μl^{-1}), and added to the sample. The mixture was incubated at 37 ^{o}C. After 2 hours the reaction was stopped adding 21.5 µl stop solution and the sample was transferred into a 1.5 ml Eppendorf containing 110 µl isopropanol. The mixture was vortexed and then incubated at RT for 10 min. After centrifuge at 12,000 x g for 10 minutes, the supernatant was removed with a pipet and the pellet was washed with 80 % (v/v) of ice-cold ethanol. The supernatant was removed

again and the pellet was dried in a vacuum centrifuge at 30 ^{o}C. At the end the pellet was rehydrated with 25 µl PCR grade water and the concentration was measured with NanoDrop.

1.2.2.4 Hybridization and washing

For microarray analysis NimbleGen 4x72K arrays (Roche NimbleGen, USA) were used, designed by the *Botrytis* consortium based on the first annotation of the *B. cinerea* genome. One array contained three 60-mer oligonucleotides of 20.885 predicted genes and non-mapping ESTs of the two sequenced *B. cinerea* strains B05.10 and T4, and 9.559 random probes, as negative controls. The microarray preparation is shown in Figure 1.2. Hybridization, washing and scanning were carried out at the laboratory of ProfileXpert facility, Genomics & MicroGenomics (Lyon, France). The chips were scanned with 3 or 4 different photomultiplier tubes (PMT) gains, with a 523 nm of wavelength (according to Cy3 nonamer).

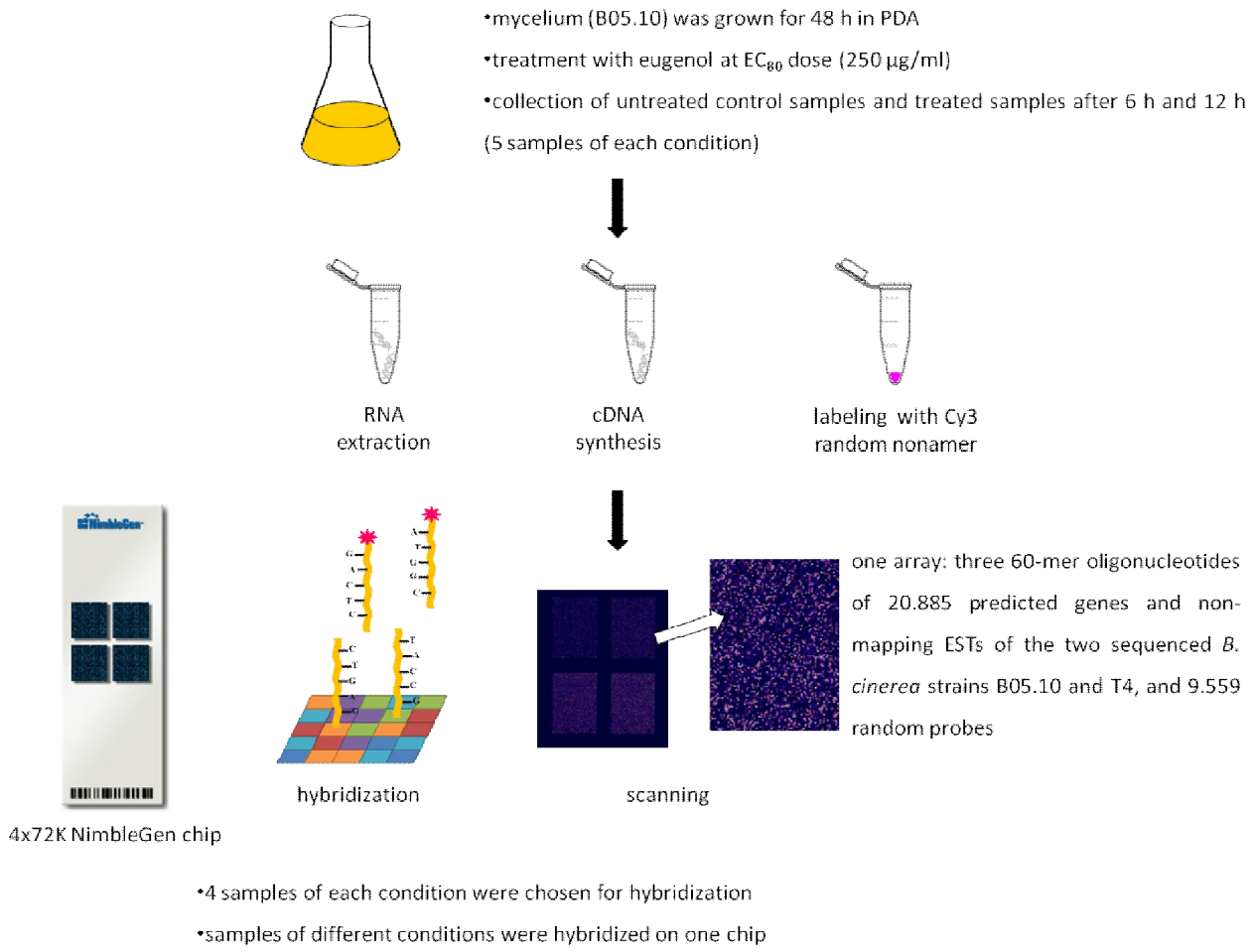

Figure 1.2 – Outline of the protocol for microarray preparation.

1.2.3 Bioinformatic analysis

1.2.3.1 Qualitative analysis of the microarrays

To avoid possible errors coming from the hybridization, wash or scanning (too low or too high intensity of hybridization) experiments with mean intensity between 4000 and 8200 were chosen (NimbleGen Software: Guide to Interpreting the Experimental Metrics Report v3, Roche NimbleGen, USA).

Hierarchical clustering and Principal Component Analysis (PCA) were performed with Genedata Analyst™ software (Genedata, Swithzerland) in order to visualize the connection and proximity between samples.

1.2.3.2 Quantitative analysis

Differential gene expression was determined using ANAIS web-based tool (Simon *et al*., 2010). Data from the two independent experiments (treatments with eugenol for 6 h and 12 h) were normalized altogether in order to decrease the difference of hybridization and scanning between slides and arrays. Intra-array (Robust Multi-Array Average (RMA) background correction) and inter-array (quantile) normalizations were chosen.

For following analysis, genes with BC1G_XXXX and BofuT4_PXXXXXX annotations and 12 experimental genes were kept, reducing the total number of genes to 15.750. Differentially expressed genes were identified with ANOVA statistical test for each gene, separating the two different conditions. Genes were considered expressed if their intensity was beyond the 99^{th} percentile values of the random probes (negative control) for at least one microarray, resulting in 13.106 expressed genes. According to large sets of genes, for multiple test correction False Discovery Rate (FDR) was used. Genes were accepted as significantly differentially expressed if they had more than a 2-fold change of expression level with a $FDR<0.05$.

1.2.3.3 Gene enrichment analysis

Global analysis of the *B. cinerea* transcriptome after 6 h and 12 h of eugenol treatments was performed. Significant enrichment in functional categories of *B. cinerea* (Amselem *et al*., 2011) was determined manually, while FungiFun web-based tool (Priebe *et al*., 2011) was used to analyze the enrichment in FunCat categories (Ruepp *et al*., 2004) and Gene Ontology (GO) biological process categories (Ashburner *et al*., 2000); in both cases, the statistical analysis was performed with Fisher's exact test ($p<0.05$).

1.2.4 qRT-PCR validation

For the validation of microarray results with qualitative reverse transcription-PCR (qRT-PCR), new control and treated samples were prepared following the protocol described above.

1.2.4.1 RNA extraction and cDNA preparation

Total RNA was extracted using RNeasy Midi Kit (Qiagen, Germany) following the user's manual with little modifications. The RNA then was treated with DNase, using DNase kit (Ambion, Germany). DNA contamination was checked amplifying the actin gene. For cDNA synthesis, ThermoScript™ RT-PCR System for First-Strand cDNA Synthesis kit (Invitrogen, USA) was utilized the manufacturer's instructions. Two µg RNA in 9 µl H_2O were used as template; 1 µl of 50 µM oligodT and 2 µl dNTP mix (10 mM each dNTP) were then added and the mixture was incubated at 65 ^oC for 5 min. For reverse transcription, 4 µl of 5X cDNA synthesis buffer, 1 µl of 0.1 M DDT, 1 µl of 40 U μl^{-1} RNaseOUT^{TM}, 1 µl of 15 U μl^{-1} ThermoScript™ RT, and 1 µl H_2O (DEPC-Treated) were added and the mixture was incubated at 51 ^oC for 1 h; then at 85 ^oC for 5 min. The obtained cDNA was treated with 1 µl of 2 U μl^{-1} RNase H at 37 ^oC for 20 min and was purified by precipitation with 2 volumes of absolute ethanol and 1/10 volume of 3 M NaAc (pH 5.2).

1.2.4.2 qRT-PCR

To verify the results of the microarray, the expression of some down- and up-regulated genes at 6 h or 12 h or at both conditions, as well as of stable genes, was checked by qRT-PCR. Primers were designed on B05.10_vankan sequences with Primer Express® Software v3.0.1 (Applied Biosystems®, USA) (Table 1.1). MicroAmp® Fast Optical 96-Well Reaction Plate with Barcode, 0.1 mL (Applied Biosystems®, USA) was used and the following reaction mix was prepared for each sample: 10 µl Power SYBR® Green PCR Master Mix (Applied Biosystems®, USA), 8.1 µl of 6.7 µM primer For and Rev, and 5 µl cDNA. The qRT-PCR was performed in 7900HT Fast Real-Time PCR System (Applied Biosystems®, USA) using SDS Software 2.3 (Applied Biosystems®, USA). Relative quantification of gene expression was determined using *pda1* gene as reference. The Ct value was calculated for each gene and then the fold change between the control and treated samples was determined using the $2^{-\Delta\Delta C_T}$ method (Livak and Schmittgen, 2001).

Table 1.1 – Primers used for the qRT-PCR.

Name	B05.10_vankan	Forward primer	Reverse primer	Product size (bp)
Erg27	B0510_226	5’ GCAAAGAAATGCGGAACCAT 3’	5’ TTAACACCCAAGACCTCAAAATCC 3’	63
Cat1	B0510_1337	5’ CGGCCACTTCACCGGTAAT 3’	5’ TGAAATCTTCCTCGCGGATT 3’	59
MFS transporter	B0510_1522	5’ TCCTCCGGCATATCCGTTT 3’	5’ TTGCGATGCCCGAGAAA 3’	55
Mcm5	B0510_2612	5’ CGCGAGCTCCAAGACGAA 3’	5’ CGGGCAACCTCTTTTTTAATTCT 3’	58
Gpa2	B0510_2668	5’ CGGTCGATCACCTCTCGAA 3’	5’ GCTGCTCTATTCAAGTCGTTTCC 3’	66
Cys4	B0510_3656	5’ AGGTGACAGACTCGTCGGTCTT 3’	5’ CGACCGCGACTAATCCAACT 3’	63
Met2	B0510_4208	5’ CAAATGCACGTCTCAGGAAGATT 3’	5’ AATTGCAACAAGAATGCATCGT 3’	61
Gsh2	B0510_5726	5’ TGGTCCCCAAGATTATACAACTGA 3’	5’ TTTGACCGCTCGATTTGAAAA 3’	63
Msm2	B0510_5850	5’ GCCGCGTCATCGTGAAGT 3’	5’ CCGGGCTTGGCTTTGTC 3’	57
Rad30	B0510_6523	5’ CGTCGAAGAGCACGATGATG 3’	5’ GCCTGGCCCGGCTAAA 3’	55
Erg6	B0510_7030	5’ TCGTCTCGGTATTGAGCAAGGT 3’	5’ GGCGATACCCTCGGAAATC 3’	64
Mcm3	B0510_7835	5’ CGAGTCGCGTACCAACACAA 3’	5’ GCCTGAGAAGCGGGTAAGG 3’	61
Sam1	B0510_7956	5’ TCACGGTGGTGGAGCTTTCT 3’	5’ GGCAGCAGATCTGTCAACCTT 3’	58
Sam4	B0510_8038	5’ CGCCCTCTCCTCTCTAAAATCC 3’	5’ TCGGCGAGGGTGTTGCT 3’	60
Erg7	B0510_9190	5’ CGCATTTTCGATGCCATTG 3’	5’ GATGCACAGCCGCCAGAT 3’	62
BcBot2 *	AY277723.2	5’ CCCAATGATTCCAGTCCAACA 3’	5’ GTGGGCCCCAGATGCA 3’	59
Act1 **	BC1G_08198	5’ CCGTGCTCCAGAAGCTTTGT 3’	5’ GTGGATACCACCGCTCTAAG 3’	61
Ef1α **	BC1G_09492	5’ TTCCCGCCCAACTGACA 3’	5’ CGTTCCAATACCACCAATCTTGT 3’	70
Pda1 **	BC1G-02852	5’ CGCTGTTAAGGCTGCTGTCA 3’	5’ CGAGGACTAATGGACCGTTACC 3’	68

*Due to the lack of B0510_van Kan annotation, BcBot2 corresponds to GenBank annotation AY277723.2. **Reference genes correspond to B05.10 annotations.

1.2.5 Determination of thiol compounds

Cysteine, cysteinylglycine, and glutathione compounds were determined following the indication of Oe *et al.* (1998).

B. cinerea was treated with 250 µg ml^{-1} of eugenol for 6, 10 and 24 h as described before; five biological replicates were prepared for each condition. One g mycelium was extracted with 2 ml of 0.1 M HCl and then centrifuged for 10 min at 12 000 rpm. Fifty µl extract from the supernatant were mixed with 175 µl of 1 M potassium borate buffer (pH 10.5) and 33 µl of 1 % Tri-n-butyl phosphine (TBP) and the mixture was incubated for 10 min at RT. After adding 33 µl ammonium 7-fluoro- benzo-2-oxa-1,3-diazole-4-sulphonate (SBD-F) (0.3 % in water), the mixture was incubated for 1 h at 60 ^{o}C. Samples were cooled on ice, and then 17 µl of 4 M HCl were added. After centrifugation for 5 min at 12,000 x g, the supernatant was injected into the HPLC system using 75 mM of sodium citrate (pH 2.9) : methanol elution buffer (98:2). Standards (glutathione, cysteine, gamma-glutamylcysteine) were injected before and after the samples. The thiol content of the samples was evaluated by fluorescence detection at 386 nm excitation wavelength, 516 nm emission wavelength and using Luna Phenomenex column with 1 ml/min of flow rate and 20 µl of loop.

Experiments were performed at the laboratory of Plant Biochemistry with the guidance of Prof. Antonio Masi (Department of DAFNAE, Padova, Italy).

1.3 Results

1.3.1 Qualitative analyses

To identify the mode of action of eugenol on *B. cinerea*, transcription analyses were performed using NimbleGen microarrays. At first, qualitative analyses of the arrays were performed to select samples with good quality for the following studies. The best scanning for each array was chosen according to the mean experimental value defined as the mean intensity of experimental features present on the array.

Roche NimbleGen user's manual advices to choose samples with mean experimental values between 4000 and 8200. For samples with lower values, the highest mean experimental value was selected. Example of a sample selection is shown below (Figure 1.3).

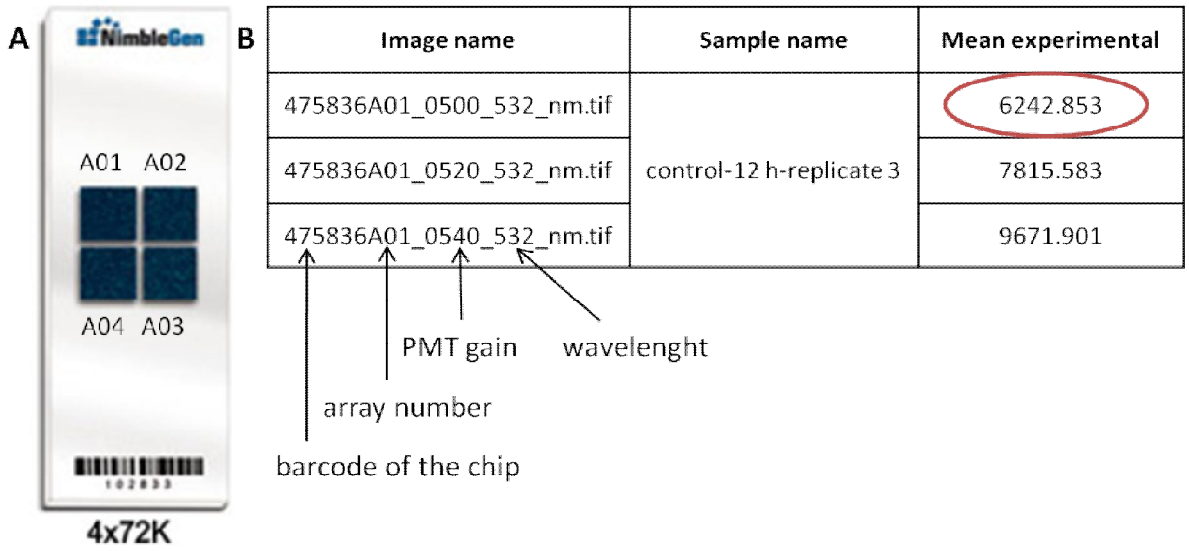

Figure 1.3 - (**A**) NimbleGen 4x72K microarray. A01, A02, A03, and A04 symbols indicate the array numbers. (**B**) Mean experimental values after scanning. The image name contains the barcode of the chip with the array number, the PMT gain representing the intensity of the fluorescence signal, and the wavelength, according to the use of Cy3 nonamer. The optimal mean experimental value – along with the chosen sample – is indicated with a red circle.

Normalization is essential to analyze multiple data, thus data from the two independent experiments (6 h and 12 h of eugenol treatments) were normalized altogether. The effect of the intra-array + inter-array (quantile) normalization is shown in Figure 1.4.

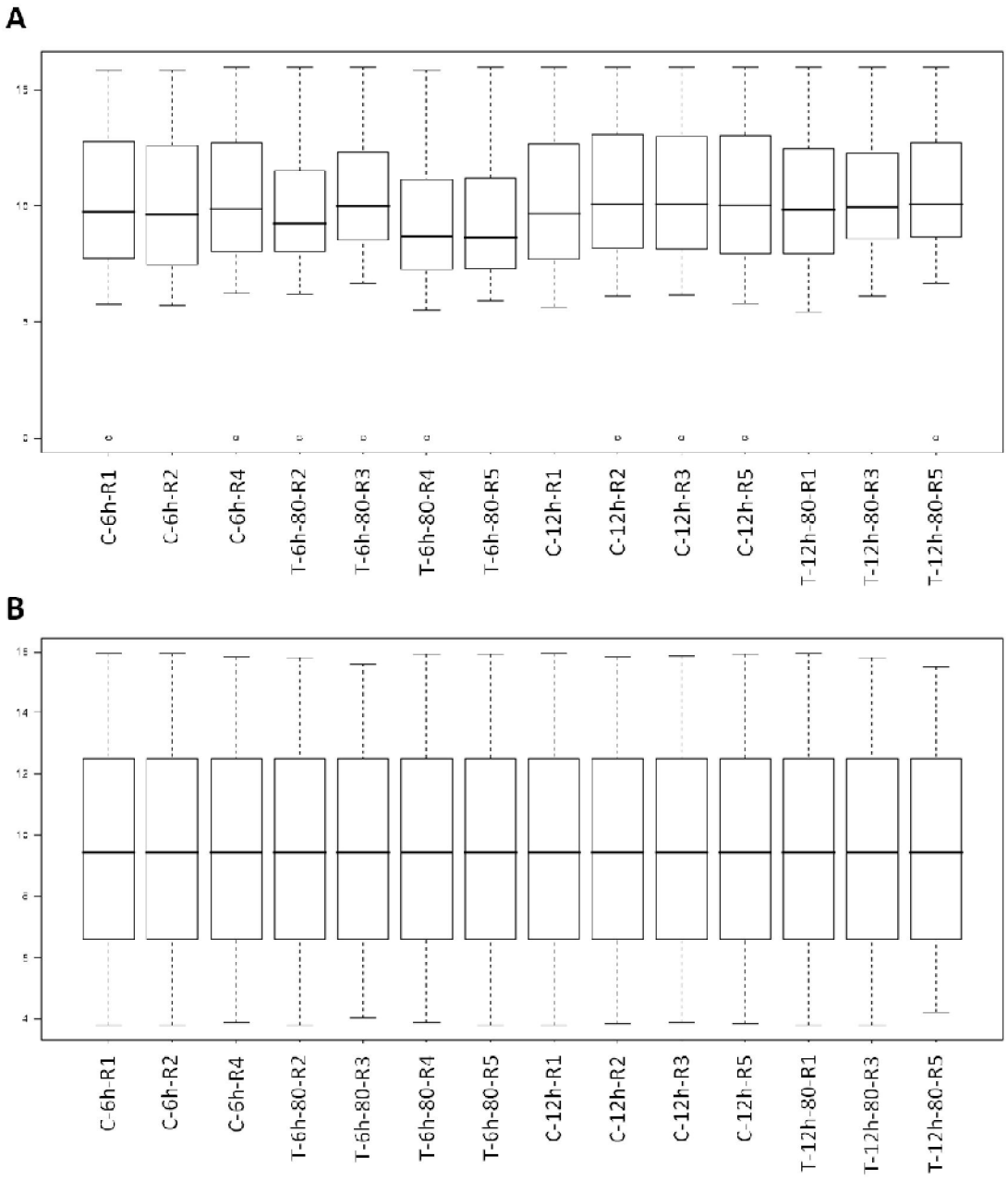

Figure 1.4 – Effect of quantile normalization: box-plots before normalization (**A**) and after normalization (**B**).

Hierarchical clustering and PCA diagram were drawn with Genedata Analyst™ software to examine if the treated samples are separated from the control samples. Samples of the two experiments (6 h and 12 h) are shown in Figure 1.5 and Figure 1.6. At 6 h, the third replicate of control samples (C-6h-R3) is separated from the other control samples on the PCA diagram; therefore this replicate was not considered for the following analyses (Figure 1.5). At 12 h, the second replicate (T-12h-80-R2) of treated samples is grouped with the control samples in the hierarchical clustering and on the PCA diagram; therefore this replicate was not considered for the following analyses. Another replicate (T-12h-80-R1) was included in the subsequent analysis even if it was not clustered with the other two treated samples in both hierarchical clustering and PCA diagram (Figure 1.6).

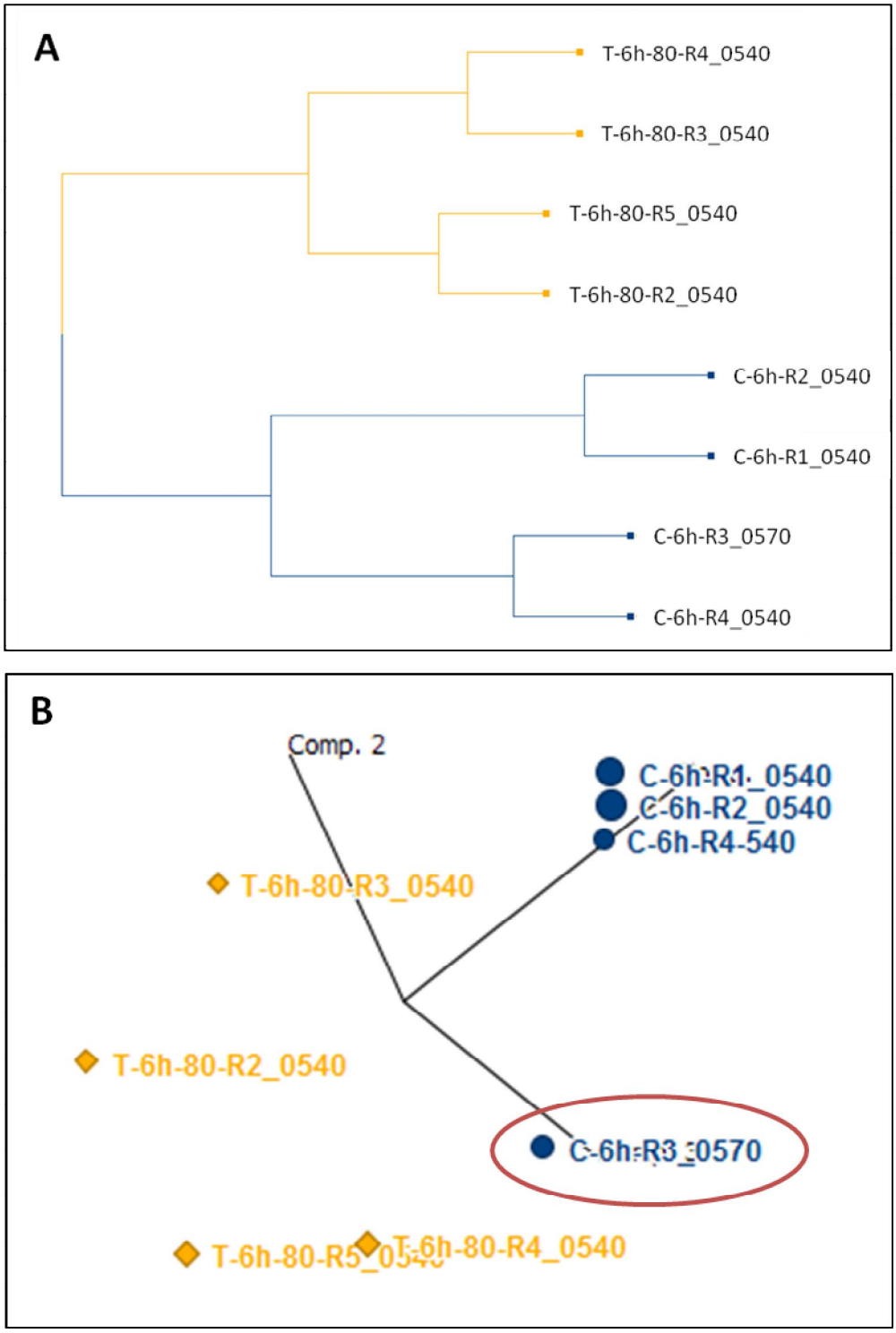

Figure 1.5 - (**A**) Hierarchical clustering of the control and treated samples at 6 h. (**B**) PCA diagram of the control and treated samples at 6 h. Blue colour indicates the control, yellow colour the treated samples. Samples' names consist of a C as control or a T as treated, 6 h as treatment for 6 h, R as replicate, and 540 as PMT gain. Sample excluded from the following analyses is indicated with a red circle.

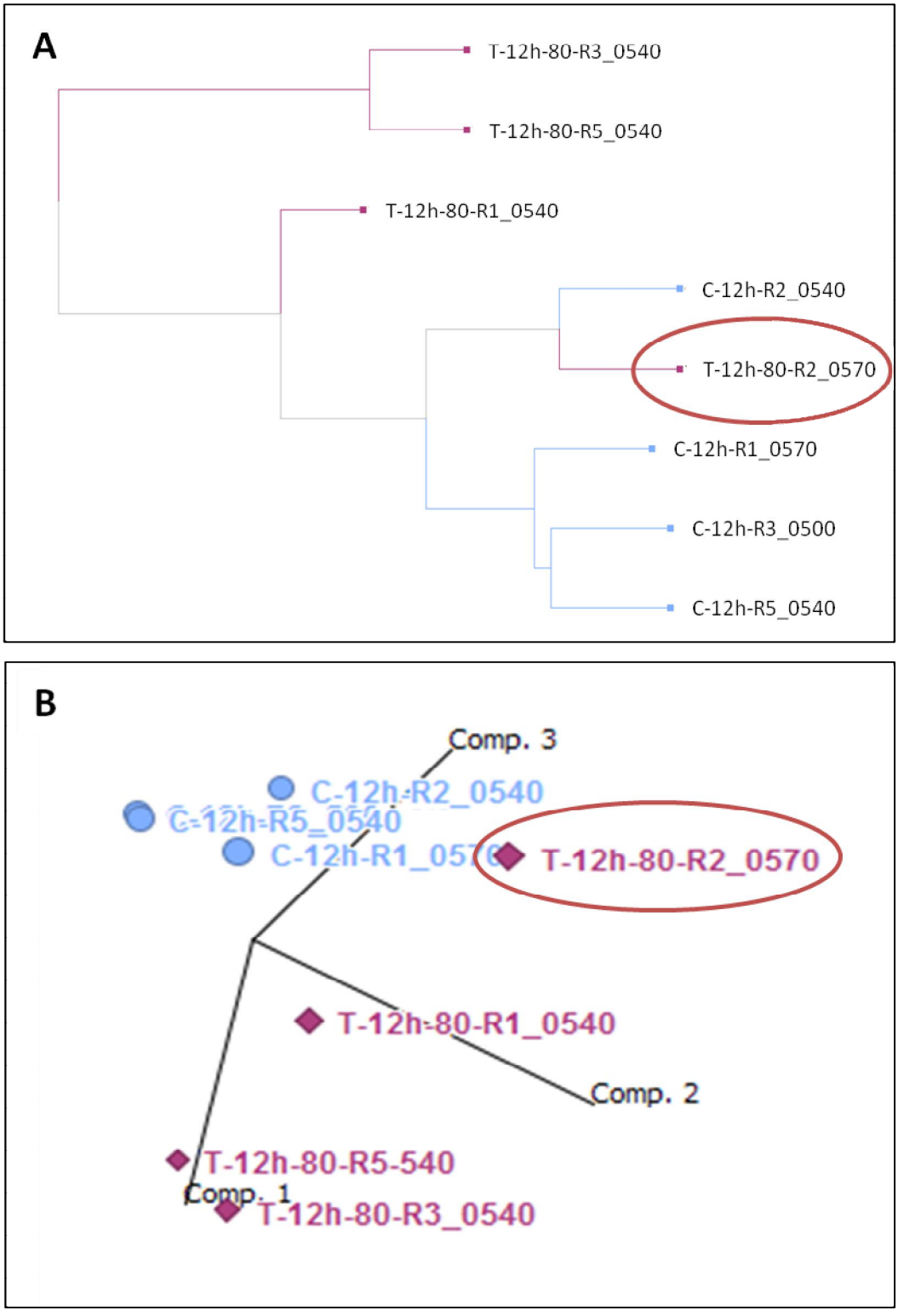

Figure 1.6 - (**A**) Hierarchical clustering of the control and treated samples at 12 h. (**B**) PCA diagram of the control and treated samples at 12 h. Blue colour indicates the control, pink colour the treated samples. Samples' names consist of a C as control or a T as treated, 12 h as treatment for 12 h, R as replicate, and 540 as PMT gain. Sample excluded from the following analyses is indicated with a red circle.

1.3.2 Quantitative analyses

For differential analysis, ANOVA for each gene was used, utilizing ANAIS software. Genes with more than 2-fold change of expression level and FDR<0.05 were accepted as significantly differentially expressed. After 6 h of treatment with eugenol, 949 up- and 1504 down-regulated genes were detected: at 12 h post treatment, 887 up- and 823 down-regulated genes were detected. Among the up-regulated genes, 281 were common for the two treatments, and 177 between the down-regulated genes. (Figure 1.7).

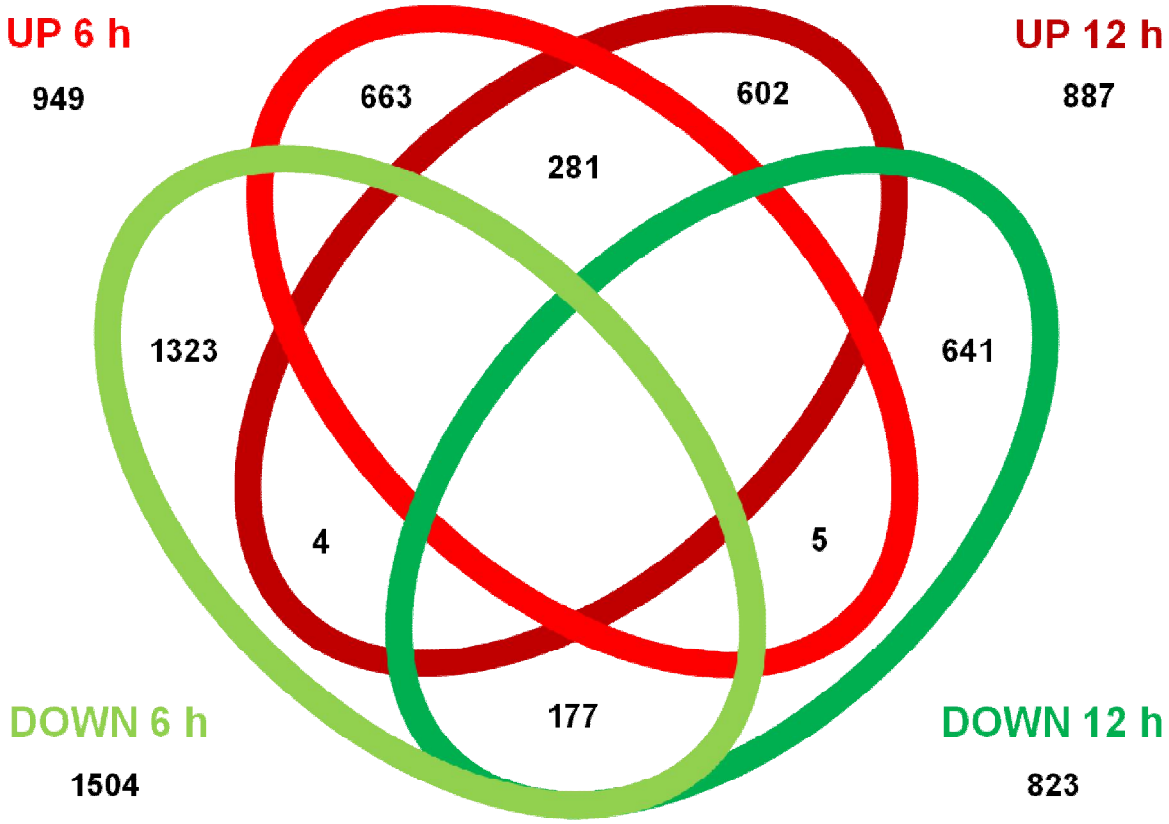

Figure 1.7 - Venn diagram representing the up- and down-regulated genes after 6 and 12 h of eugenol treatment, showing the relation between sets of the individual and common down- and up-regulated genes.

Functional categories (Amselem *et al*., 2011) were examined using Fisher's exact test ($p<0.05$) and significant enrichment in down-regulated genes was found in several classes (Table 1.2). Groups of CAZy (Carbohydrate-Active Enzymes), proteases, MFS-type (major facilitator superfamily) sugar transporters, and ergosterol biosynthesis were enriched at 6 h; groups of transcription factors, MFS efflux transporters and kinase were enriched at 12 h. The transporters functional category was enriched at both conditions.

Table 1.2 – Significantly enriched functional categories in down-regulated genes after eugenol treatment.

functional category	number of genes	DOWN at 6 h	p-value	DOWN at 12 h	p-value
Botrytis T4 CAZy	388	68	<0.001		
Botrytis T4 proteases	40	12	0.0013		
transcription factor	437			64	<0.001
transporters	394	65	0.0015	34	0.037
MFS efflux transporters	122			13	0.042
MFS-type sugar transporters	68	13	0.044		
ergosterol biosynthesis	23	9	<0.001		
kinase	220			25	0.011

Functional categories were described by Amselem *et al*. (2011). p-value of Fisher's test was determined using R statistical software.

At 6 h, from the 1504 down-regulated genes 566 could be functionally analyzed with FungiFun web-based tool choosing FunCat categories and significant enrichment was found e.g. in DNA synthesis and replication, while at 12 h, from the 823 down-regulated genes 233 could be functionally analyzed with the same tool and e.g the mitotic cell cycle and cell cycle control category was found to be significantly ernriched. From the 949 up-regulated genes only 69 were annotated in FunCat categories at 6 h, and enrichment was found e.g. in the oxidative stress response category, while at 12 h, from the 887 up-regulated genes only 95 were annotated with the same application (Table 1.3).

Analysing GO biological process classes with FungiFun tool, at 6 h, from 1504 down-regulated genes 797 were annotated and significant enrichment was found e.g. in the translation, DNA replication, transmembrane transport, cell cycle, and methionine biosynthesis categories. At 12 h, from 823 down-regulated genes 408 were detected with annotation e.g. the transmembrane transport, DNA-dependent transcription, and translation categories. Among up-regulated genes, at 6 h 142 from 949 genes were annotated belonging to oxidation-reduction process and response to oxidative stress; at 12 h 173 from 887 genes belonging to oxidation-reduction process and cellular cell wall organization categories were annotated (Table 1.4).

Some of the enriched categories were selected for further investigations. Among the functional categories determined by Amselem *et al* (2011), ergosterol biosynthesis was found to be enriched in down-regulated genes at 6 h and was examined since eugenol is know to act on the cell membrane. In methionine biosynthesis category both genes were found to be down-regulated analyzing GO categories at 6 h. Methionine biosynthesis is connected to the biosynthesis of glutathione, which has an important function by detoxifying the fungal cells from xenobiothics, therefore genes involved in the glutathione pathway were analyzed. Many transporters also play a role in the detoxification prosess and as GO transmembrane transport category and other transporter categories identified by Amselem *et al*. (2011) were enriched in down-regulated genes at 6 and at 12 h, these classes were further investigated. DNA replication factors class was analized too, as a result of enriched FunCat and GO categories in down-regulated genes connected to the cell cycle were found.

Among the up-regulated genes, enrichment was detected in both FunCat and GO functional categories related to stress response, such as oxidative stress response, pH stress response, oxygen and radical detoxification, and oxidatation-reduction process; however no individual pathways with significant enrichment in up-regulated genes were found.

Table 1.3 – FunCat functional categories (at the 3rd level) enriched in down- and up-regulated genes after eugenol treatment for 6 and 12 h.

FunCat ID	category (3rd level)	elements	hits	p-value
DOWN at 6 h				
14.07.03	modification by phosphorylation, dephosphorylation, autophosphorylation	127	6	0,0002
11.04.01	rRNA processing	137	36	0,0010
12.01.01	ribosomal proteins	133	8	0,0013
11.06.02	tRNA modification	31	12	0,0014
30.01.05	enzyme mediated signal transduction	130	8	0,0018
11.02.03	mRNA synthesis	377	38	0,0020
20.09.13	vacuolar/lysosomal transport	103	6	0,0035
42.10.07	nucleolus	3	3	0,0037
10.01.03	DNA synthesis and replication	96	26	0,0037
43.01.03	fungal and other eukaryotic cell type differentiation	228	21	0,0059
20.09.07	vesicular transport (Golgi network, etc.)	148	12	0,0102
18.01.01	regulation by modification	53	2	0,0122
02.16.11	propionate fermentation	4	3	0,0130
20.01.10	protein transport	115	9	0,0182
01.25.09	extracellular lignin degradation	8	4	0,0235
01.01.06	metabolism of the aspartate family	82	20	0,0299
01.05.03	polysaccharide metabolism	139	31	0,0304
32.07.07	oxygen and radical detoxification	37	1	0,0355
01.20.17	metabolism of secondary products derived from primary amino acids	54	14	0,0376
20.01.15	electron transport	189	19	0,0381
DOWN at 12 h				
20.01.09	peptide transport	12	5	0,0005

18.02.05	regulator of G-protein signaling	16	5	0,0024
12.01.01	ribosomal proteins	133	1	0,0030
20.09.01	nuclear transport	53	9	0,0055
42.10.07	nucleolus	3	2	0,0116
14.07.03	modification by phosphorylation, dephosphorylation, autophosphorylation	127	15	0,0157
11.04.01	rRNA processing	137	16	0,0181
01.04.04	regulation of phosphate metabolism	17	4	0,0197
40.01.05	growth regulators / regulation of cell size	12	3	0,0364
42.10.03	organization of chromosome structure	84	1	0,0419
01.07.01	biosynthesis of vitamins, cofactors, and prosthetic groups	111	2	0,0459
10.03.01	mitotic cell cycle and cell cycle control	268	25	0,0498
UP at 6 h				
32.01.01	oxidative stress response	67	6	0,0014
32.07.01	detoxification involving cytochrome P450	27	4	0,0015
32.07.07	oxygen and radical detoxification	37	4	0,0048
02.01.01	glycolysis methylglyoxal bypass	6	2	0,0050
32.07.03	detoxification by modification	40	4	0,0063
16.21.01	heme binding	21	3	0,0067
32.01.04	pH stress response	7	2	0,0069
32.10.07	degradation / modification of foreign (exogenous) polysaccharides	12	2	0,0204
01.06.05	fatty acid metabolism	87	5	0,0230
01.20.01	metabolism of primary metabolic sugar derivatives	34	3	0,0252
11.02.03	mRNA synthesis	377	2	0,0428
20.01.03	C-compound and carbohydrate transport	142	6	0,0494

UP at 12 h				
01.06.05	fatty acid metabolism	87	7	0,0068
16.21.07	NAD/NADP binding	135	9	0,0077
01.20.15	metabolism of derivatives of dehydroquinic acid, shikimic acid...	32	4	0,0088
01.20.01	metabolism of primary metabolic sugar derivatives	34	4	0,0109
01.06.02	membrane lipid metabolism	66	5	0,0271
20.01.10	protein transport	115	7	0,0284
43.01.03	fungal and other eukaryotic cell type differentiation	228	1	0,0291
01.05.08	C-4 compound metabolism	11	2	0,0314
16.19.03	ATP binding	291	2	0,0320

Table 1.4 – GO biological process categories enriched in down- and up-regulated genes after eugenol treatment for 6 and 12 h.

GO ID	category name (biological process)	elements	hits	p-value
DOWN at 6 h				
GO:0006412	translation	178	11	0,0003
GO:0042254	ribosome biogenesis	27	11	0,0012
GO:0006260	DNA replication	37	13	0,0022
GO:0009451	RNA modification	6	4	0,0062
GO:0009168	purine ribonucleoside monophosphate biosynthetic process	6	4	0,0062
GO:0001522	pseudouridine synthesis	6	4	0,0062
GO:0055085	transmembrane transport	414	83	0,0066
GO:0051301	cell division	7	4	0,0127
GO:0007049	cell cycle	15	6	0,0179
GO:0008299	isoprenoid biosynthetic process	8	4	0,0224
GO:0006555	methionine metabolic process	2	2	0,0232
GO:0009072	aromatic amino acid family metabolic process	2	2	0,0232
GO:0006269	DNA replication, synthesis of RNA primer	2	2	0,0232
GO:0009156	ribonucleoside monophosphate biosynthetic process	2	2	0,0232
GO:0009085	lysine biosynthetic process	2	2	0,0232
GO:0030261	chromosome condensation	2	2	0,0232
GO:0031119	tRNA pseudouridine synthesis	2	2	0,0232
GO:0015780	nucleotide-sugar transport	2	2	0,0232
GO:0006364	rRNA processing	33	10	0,0253
DOWN at 12 h				
GO:0008152	metabolic process	986	45	1,22E-05
GO:0055114	oxidation-reduction process	604	25	0,0002

GO:0006355	regulation of transcription, DNA-dependent	213	31	0,0006
GO:0055085	transmembrane transport	414	51	0,0008
GO:0006468	protein phosphorylation	98	17	0,0016
GO:0006351	transcription, DNA-dependent	208	29	0,0021
GO:0051056	regulation of small GTPase mediated signal transduction	9	4	0,0033
GO:0006438	valyl-tRNA aminoacylation	2	2	0,0061
GO:0006812	cation transport	30	7	0,0070
GO:0043547	positive regulation of GTPase activity	6	3	0,0079
GO:0006476	protein deacetylation	7	3	0,0130
GO:0006342	chromatin silencing	7	3	0,0130
GO:0006857	oligopeptide transport	3	2	0,0172
GO:0006412	translation	178	6	0,0220
GO:0006270	DNA-dependent DNA replication initiation	9	3	0,0277
GO:0007165	signal transduction	65	10	0,0325
GO:0071805	potassium ion transmembrane transport	4	2	0,0327
UP at 6 h				
GO:0055114	oxidation-reduction process	604	36	3,15E-06
GO:0008152	metabolic process	986	45	0,0002
GO:0042744	hydrogen peroxide catabolic process	3	2	0,0022
GO:0044237	cellular metabolic process	28	4	0,0064
GO:0042218	1-aminocyclopropane-1-carboxylate biosynthetic process	5	2	0,0069
GO:0006979	response to oxidative stress	17	3	0,0101
GO:0009611	response to wounding	1	1	0,0271
GO:0000379	tRNA-type intron splice site recognition and cleavage	1	1	0,0271

UP at 12 h				
GO:0008152	metabolic process	986	56	1,64E-05
GO:0055114	oxidation-reduction process	604	35	0,0009
GO:0045039	protein import into mitochondrial inner membrane	3	2	0,0032
GO:0006626	protein targeting to mitochondrion	4	2	0,0062
GO:0007047	cellular cell wall organization	12	3	0,0063
GO:0009058	biosynthetic process	86	7	0,0229
GO:0007030	Golgi organization	1	1	0,0331
GO:0009264	deoxyribonucleotide catabolic process	1	1	0,0331
GO:0009698	phenylpropanoid metabolic process	1	1	0,0331
GO:0000379	tRNA-type intron splice site recognition and cleavage	1	1	0,0331
GO:0015031	protein transport	58	5	0,0417

1.3.3 Ergosterol biosynthesis

Analysing the functional categories determined by Amselem *et al*. (2011), a significant enrichment of down-regulated *erg* genes involved in the ergosterol biosynthesis was found after 6 h of eugenol treatment. These genes were manually checked by bidirectional best hit (BBH) with genes implied in the ergosterol biosynthetic pathway of *S. cerevisiae* (www.yeastgenom.org). To verify the enrichment of down-regulated genes in this pathway, p-value = 0.0163 of Fisher's exact test was defined with R statistical software. Among the 14 genes involved in the ergosterol biosynthesis 5 were significantly down-regulated according to the FDR<0.05: *erg7*, *erg27*, *erg6*, *erg2*, and *erg4*. The lanosterol synthase Erg7 is a key enzyme in the ergosterol biosynthesis, which converts oxidosqualene to lanosterol. The sterol C-4 demethylation complex is composed by three enzymes: the methylsterol monooxygenase (Erg25), the sterol 4-α-carboxylate 3-dehydrogenase (Erg26) and the 3-keto sterol reductase (Erg27); these enzymes catalyze the three steps to remove two C-4 methyl groups from an intermediate. The delta(24)-sterol C-methyltransferase (Erg6) converts zymosterol to fecosterol, then the C-8 sterol isomerise (Erg2) catalyzes an intermediate step. The strongest response to 6 h of eugenol treatment was obtained with the *erg4* gene, which encodes the C-(24)28 sterol reductase, the enzyme that catalyzes the last step of the ergosterol biosynthesis (Figure 1.8, Table 1.5 and Figure 1.9).

After 12 h of eugenol treatment, no significantly down-regulated genes were found, according to the FDR<0.05 (Table 1.5, Figure 1.10).

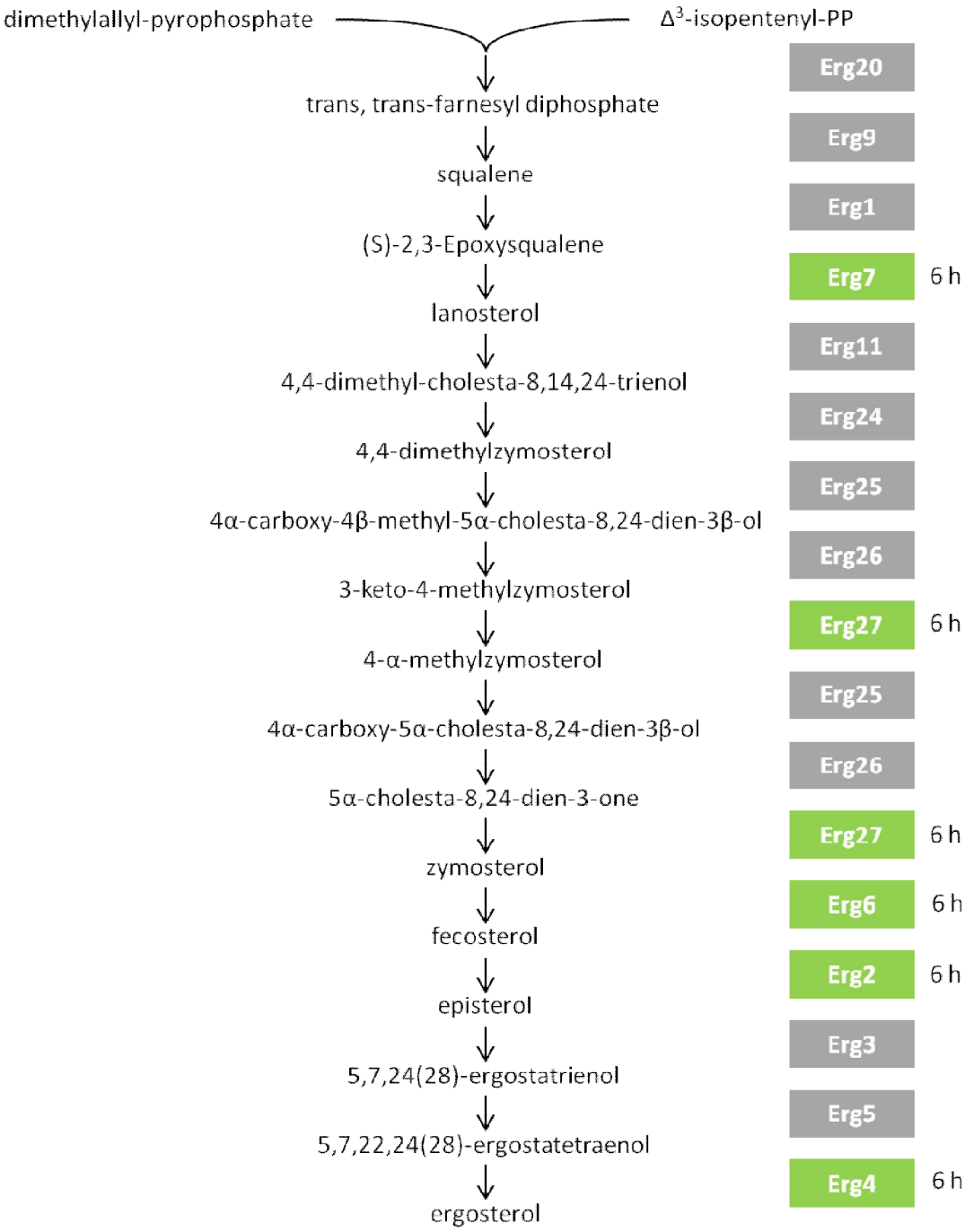

Figure 1.8 - Ergosterol biosynthetic pathway adapted from http://www.yeastgenome.org/.

Table 1.5 – Genes involved in the ergosterol biosynthesis and their transcriptional response to eugenol treatment.

Ergosterol biosynthesis		***B. cinerea* strains**		**6 h**		**12 h**	
yeast	**description**	**B05.10**	**T4**	**fold change**	**FDR**	**fold change**	**FDR**
Erg20	Farnesyl pyrophosphate synthetase	BC1G_02940	BofuT4_P003890	-3,61	0,07	-1,08	0,82
Erg9	Farnesyl-diphosphate farnesyl transferase (squalene synthase)	BC1G_01273	BofuT4_P028950	-1,41	0,31	-1,04	0,80
Erg1	Squalene epoxidase	BC1G_14066	BofuT4_P154230	-2,46	0,36	-1,23	0,49
Erg7*	Lanosterol synthase	BC1G_05572	BofuT4_P107430	-4,59	0,04	-1,25	0,55
Erg11	Lanosterol 14-alpha-demethylase	BC1G_11853	BofuT4_P161240	1,72	0,09	-1,75	0,18
Erg24	C-14 sterol reductase	BC1G_14884	BofuT4_P023670	1,02	0,98	1,28	0,41
Erg25	C-4 methyl sterol oxidase	BC1G_14068	BofuT4_P154210	-5,34	0,06	-2,62	0,07
Erg26	C-3 sterol dehydrogenase	BC1G_12399	BofuT4_P024180	1,25	0,07	1,02	0,87
Erg27*	3-keto sterol reductase	BC1G_00806	BofuT4_P019230	-3,13	0,02	-1,89	0,09
Erg6*	Delta(24)-sterol C-methyltransferase	BC1G_07905	BofuT4_P043740	-2,17	0,046	-1,32	0,20
Erg2	C-8 sterol isomerase	BC1G_03303	BofuT4_P079350	-3,23	0,04	1,76	0,04
Erg3	C-5 sterol desaturase	BC1G_12308	BofuT4_P151660	-4,51	0,07	-1,86	0,23
Erg5	C-22 sterol desaturase	BC1G_09786	BofuT4_P116330	-1,10	0,78	1,11	0,78
Erg4	C-24(28) sterol reductase	BC1G_09087	BofuT4_P100410	-17,14	0,02	-3,10	0,08

* genes verified by qRT-PCR

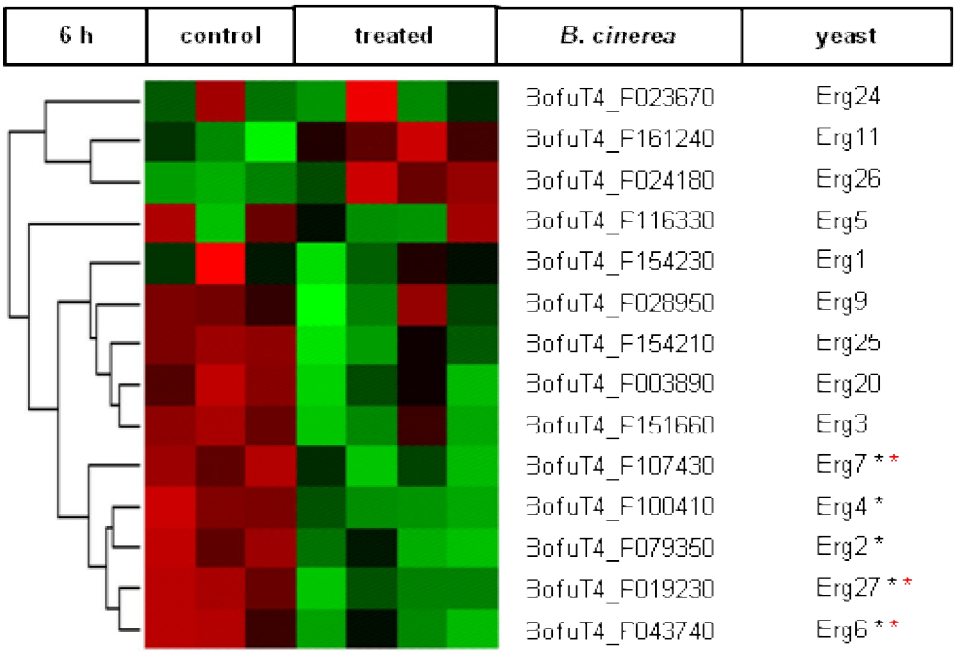

Figure 1.9 - After 6 h of eugenol treatment, the relative expression of genes involved in the ergosterol biosynthesis were clustered and visualized in a heat map. Green colour represents the under-expression and red colour the over-expression of three control and four treated samples. The enrichment of this pathway by down-regulated genes was verified by Fisher's exact test (p-value = 0.0163). (* FDR<0.05, * genes verified by qRT-PCR)

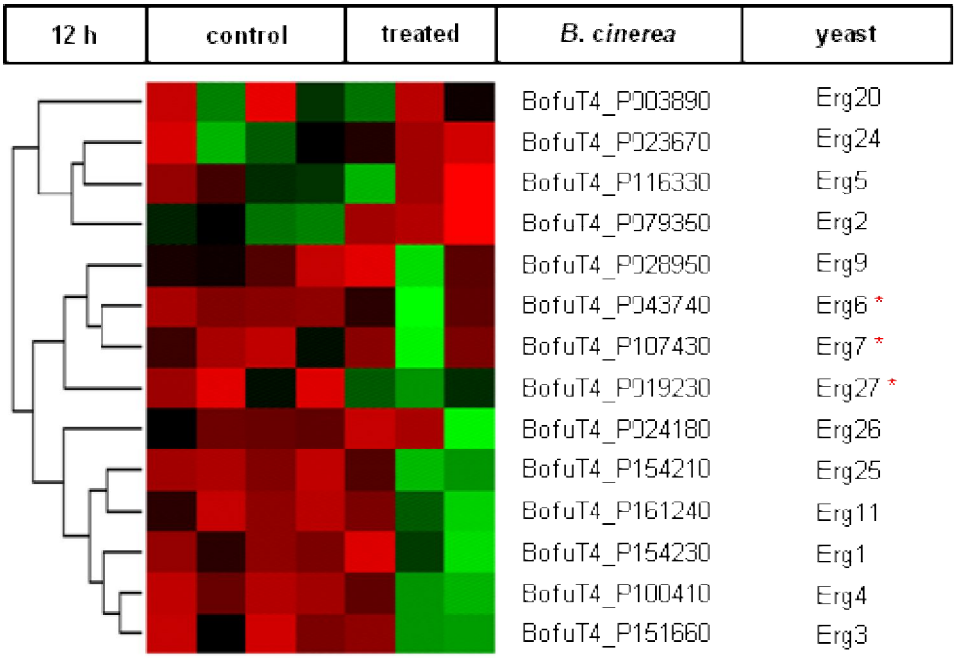

Figure 1.10 - After 12 h of eugenol treatment, the relative expression of genes involved in the ergosterol biosynthesis were clustered and visualized in a heat map. Green colour represents the under-expression and red colour the over-expression of four control and three treated samples. Significantly down-regulated genes were not found at 12 h. (* genes verified by qRT-PCR.)

1.3.4 DNA replication factors

Global analysis of FunCat categories at the 3rd level showed significant enrichment in down-regulated genes in DNA synthesis and replication, mitotic cell cycle and cell cycle control. Similar enriched categories were found in GO biological process functional categories: DNA replication, cell division, cell cycle, and transcription. Genes involved in the cell cycle of *B. cinerea* were therefore manually checked by finding putative orthologues of DNA replication factors from yeast (Enserink *et al*., 2010) using BBH. From 36 annotated genes 10 were down-regulated (FDR<0.05) after 6 h of eugenol treatment exhibiting a significant enrichment according to Fisher's test (p-value = 0.0059); 4 down-regulated (FDR<0.05) genes were found after 12 h of treatment (2 of them was down-regulated also at 6 h) and no up-regulated genes were detected. In the G1 phase of the cell cycle, in which the cell prepares itself to enter in the cell cycle by synthesizing mRNA and proteins, the following genes were down-regulated: DNA polymerase ε subunit (*dpb2*), DNA polymerase α primase (*pol12*) and its catalytic subunit (*pol1*), topoisomerase I-interacting factor (*tof1*) (part of the replication-pausing checkpoint complex), and a homologue of the B-type cyclin family members (Clb). Besides, the *dpb11* replication initiation factor gene is down-regulated after 12 h of treatment, while the *rfc2* encoding the subunit of heteropentameric replication factor is down-regulated at 6 h and 12 h after eugenol treatment. During the S phase, in which the DNA is synthesized, *orc3*, member of the origin recognition complex, is down-regulated at 12 h. In the pre-mitotic G2 phase, the largest subunit of this complex (*orc1*) is down-regulated after 6 h of treatment. Finally, in the M phase in which the mitosis occurs, three minichromosome maintenance genes (*mcm2*, *mcm3* and *mcm5*) were found to be down-regulated, which are part of the Mcm2-7 hexameric helicase complex and are important for the pre-replicative complex (Figure 1.11, Table 1.6, Figure 1.12 and Figure 1.13).

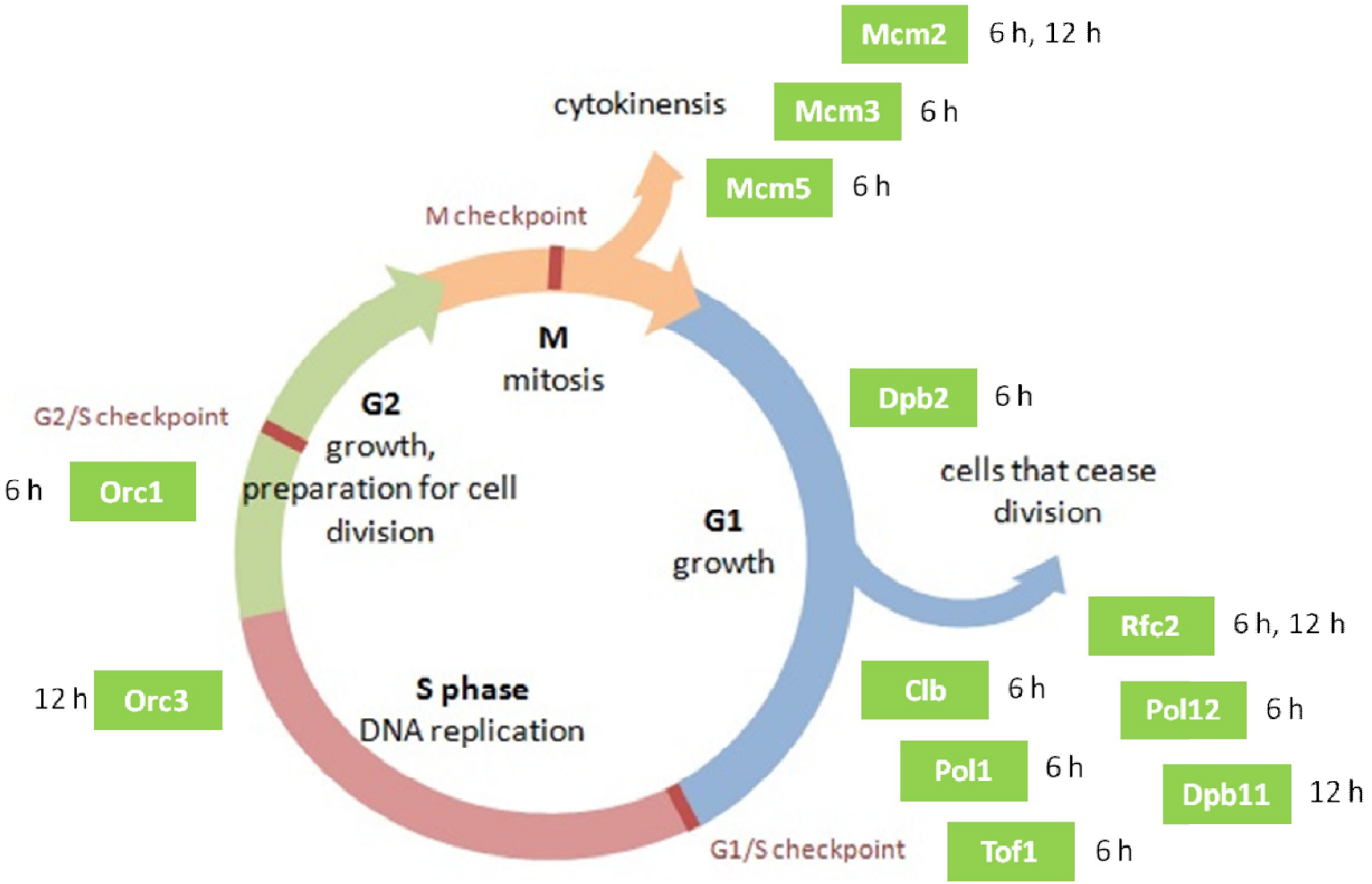

Figure 1.11 – DNA replication factor genes involved in the cell cycle.

Table 1.6 – DNA replication factor genes and their transcriptional response to eugenol treatment.

DNA replication factors		*B. cinerea* strains		6 h		12 h	
yeast	description	B05.10	T4	fold change	FDR	fold change	FDR
Orc3	Subunit of the origin recognition complex (ORC)	BC1G_00480	BofuT4_P045150	-10,13	0,06	-7,00	0,04
Orc1	Largest subunit of the origin recognition complex	BC1G_15473	BofuT4_P106240	-11,07	0,03	-5,47	0,06
Orc4	Subunit of the origin recognition complex (ORC)	BC1G_07288	BofuT4_P138560	-1,84	0,39	1,08	0,79
Mcm2*	Protein involved in DNA replication	BC1G_13345	BofuT4_P088830	-6,93	0,01	-5,38	0,04
Mcm3*	Protein involved in DNA replication	BC1G_14509	BofuT4_P077080	-8,56	0,02	-1,67	0,07
Mcm4	Essential helicase component of heterohexameric Mcm2-7	BC1G_12093	BofuT4_P090810	-2,04	0,49	-2,94	0,10
Mcm5*	Component of the Mcm2-7 hexameric helicase complex	BC1G_02916	BofuT4_P004120	-6,28	0,04	-1,32	0,42
Mcm6	Protein involved in DNA replication	BC1G_13876	BofuT4_P065300	-1,27	0,68	1,20	0,36
Mcm7	Component of the Mcm2-7 hexameric helicase complex	BC1G_05231	BofuT4_P069570	-6,75	0,06	-3,10	0,07
Cdc6	Essential ATP-binding protein required for DNA replication	BC1G_00397	BofuT4_P046120	-3,08	0,16	-1,33	0,44
Clb	B-type cyclin involved in cell cycle progression	BC1G_03287	BofuT4_P079190	-8,01	0,02	-2,42	0,12
Csm3	Replication fork associated factor	BC1G_08907	BofuT4_P075510	-3,19	0,14	1,59	0,19
Tof1	Subunit of a replication-pausing checkpoint complex	BC1G_00527	BofuT4_P021950	-8,58	0,03	1,30	0,54
Psf1	Subunit of the GINS complex (Sld5p, Psf1p, Psf2p, Psf3p)	BC1G_12096	BofuT4_P090790	1,28	0,69	-1,19	0,50
Psf2	Subunit of the GINS complex (Sld5p, Psf1p, Psf2p, Psf3p)	BC1G_14543	BC1G_14543	1,30	0,09	1,32	0,55
Dpb11	DNA replication initiation protein	BC1G_08842	BofuT4_P076210	-4,86	0,06	-4,18	0,03
Rfa1	Subunit of heterotrimeric Replication Protein A (RPA)	BC1G_13185	BofuT4_P104960	-4,91	0,12	-4,31	0,08
Rfa2	Subunit of heterotrimeric Replication Protein A (RPA)	BC1G_11483	BC1G_11483	1,03	0,91	1,24	0,17
Pol30	Proliferating cell nuclear antigen (PCNA)	BC1G_00365	BofuT4_P046430	1,10	0,86	1,17	0,42
Cdc45	DNA replication initiation factor	BC1G_14672	BC1G_14672	1,07	0,90	-5,12	0,07
Pol2	Catalytic subunit of DNA polymerase (II) epsilon	BC1G_10334	BofuT4_P092160	-3,94	0,11	-3,65	0,054
Pol3	Catalytic subunit of DNA polymerase delta	BC1G_08327	BC1G_08327	4,22	0,11	1,01	0,99

Pol31	Subunit of DNA polymerase delta (polymerase III)	BC1G_01405	BofuT4_P040880	-6,61	0,05	-2,27	0,09
Pol12	B subunit of DNA polymerase alpha-primase complex	BC1G_08381	BofuT4_P010590	-15,26	0,01	-2,68	0,16
Cdc9	DNA ligase found in the nucleus and mitochondria	BC1G_14121	BofuT4_P127690	-4,63	0,07	-1,21	0,56
Rnh201	Ribonuclease H2 catalytic subunit	BC1G_02429	BC1G_02429	-3,60	0,20	1,34	0,93
Rad27	5' to 3' exonuclease, 5' flap endonuclease	BC1G_14593	BofuT4_P123520	-2,38	0,18	1,37	0,14
Rnr1	Major isoform of large subunit of ribonucleotide-	BC1G_12274	BofuT4_P009330	-5,21	0,12	-1,78	0,08
Rfc2	Subunit of heteropentameric Replication factor C (RF-C)	BC1G_00490	BofuT4_P045030	-16,70	0,01	-2,75	0,04
Rfc3	Subunit of heteropentameric Replication factor C (RF-C)	BC1G_05602	BofuT4_P107820	1,32	0,67	2,95	0,08
Rfc4	Subunit of heteropentameric Replication factor C (RF-C)	BC1G_00671	BofuT4_P020510	-1,17	0,88	2,22	0,06
Sld5	Subunit of the GINS complex (Sld5p, Psf1p, Psf2p, Psf3p)	BC1G_02776	BofuT4_P118190	-2,41	0,05	1,54	0,34
Rnr2	Ribonucleotide-diphosphate reductase (RNR), small subunit	BC1G_12690	BofuT4_P009700	-1,63	0,36	1,24	0,47
Cdc7	DDK (Dbf4-dependent kinase) catalytic subunit	BC1G_08128	BofuT4_P102660	-1,51	0,33	-1,32	0,26
Dpb2	Second largest subunit of DNA polymerase II (DNA	BC1G_12995	BofuT4_P054560	-3,71	0,02	1,46	0,23
Pol1	Catalytic subunit of the DNA polymerase I alpha-primase	BC1G_08158	BofuT4_P033490	-23,80	0,02	-2,21	0,10

* genes verified by qRT-PCR

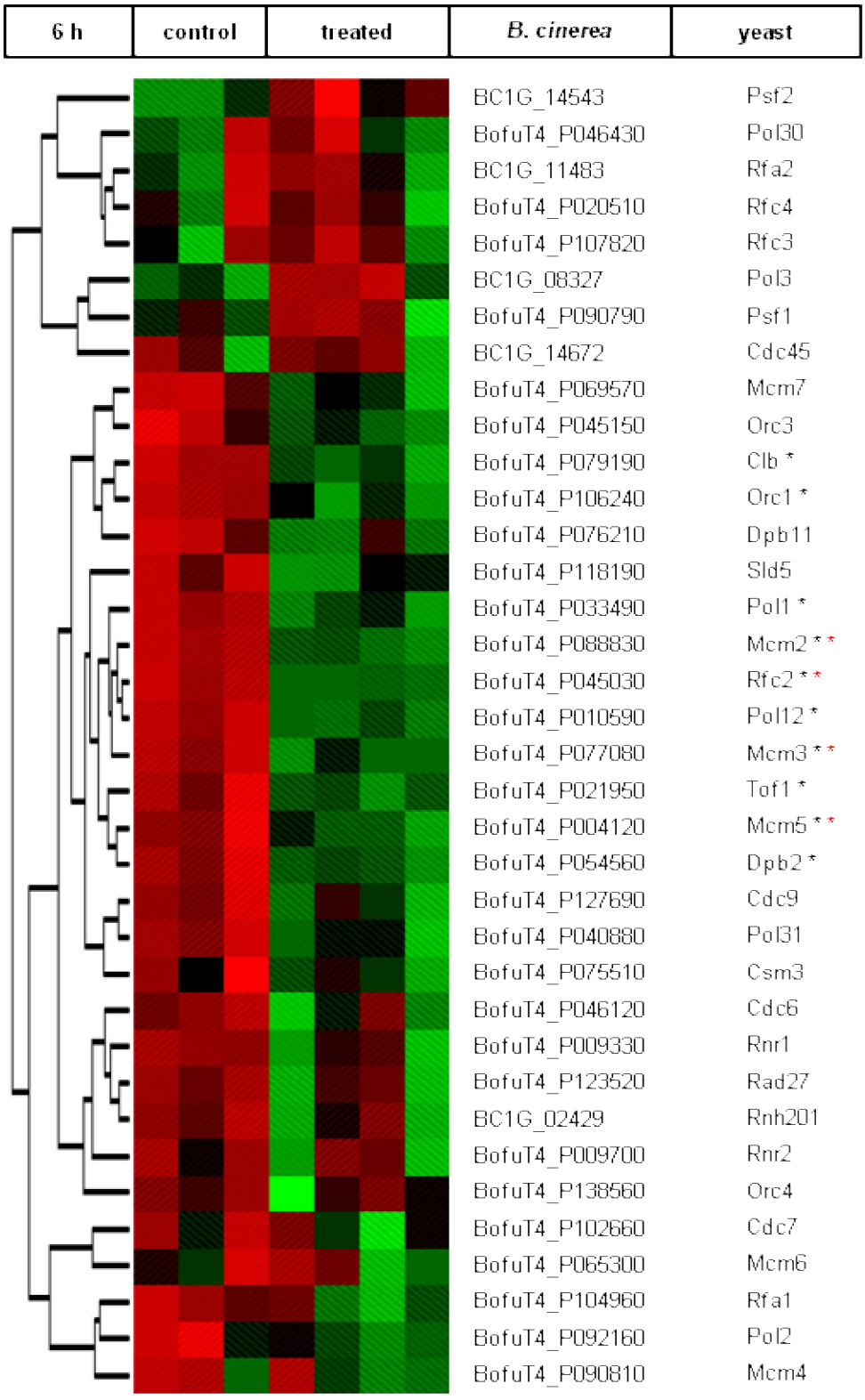

Figure 1.12 - After 6 h of eugenol treatment, the relative expression of DNA replication factor genes were clustered and visualized in a heat map. Green colour represents the under-expression and red colour the over-expression of three control and four treated samples. The enrichment of this group by down-regulated genes was verified by Fisher's exact test (p-value = 0.0059). (* FDR<0.05, * genes verified by qRT-PCR)

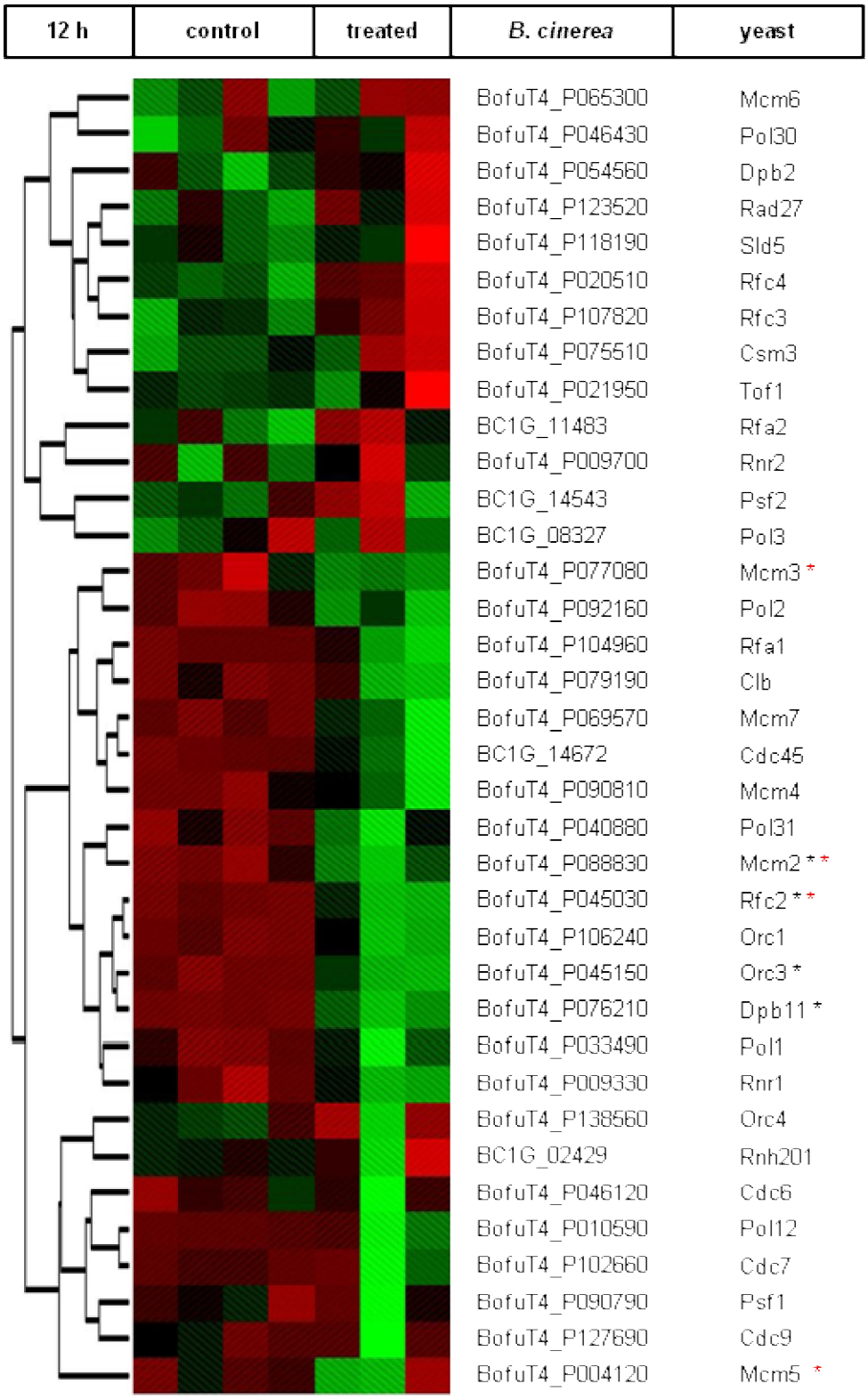

Figure 1.13 - After 12 h of eugenol treatment, the relative expression of DNA replication factor genes were clustered and visualized in a heat map. Green colour represents the under-expression and red colour the over-expression of three control and four treated samples. (* FDR<0.05, * genes verified by qRT-PCR)

1.3.5 Glutathione pathway

Global analyses of *B. cinerea* transcriptome after 6 h of eugenol treatment resulted in significant enrichment in down-regulated genes of the methionine metabolic process (GO: 0006555) functional category. Methionine biosynthesis is connected to glutathione (GSH) pathway, in which a significant enrichment in down-regulated genes was determined at 6 h (according to the p-value = 0.0164 of Fisher's exact test), but not at 12 h. In yeast, GSH synthesis starts with the formation of γ-glutamylcystein from cysteine and glutamate, catalyzed by the γ-glutamylcysteine synthetase (Gsh1). At the second step, glutathione synthase (Gsh2) ligates glycin to γ-glutamylcystein to form GSH, and the gene encoding this enzyme was down-regulated after 6 h of eugenol treatment. Two enzymes are involved in the degradation of GSH, the gamma-glutamyltranspeptidase (Ecm38) and the Cys-Gly metallodipeptidase (Dug1), both unaffected by eugenol treatment.

Linked to the glutathione biosythesis, there is an interconvertible pathway of cysteine and homocysteine, catalyzed by four enzymes: cystathionine β-lyase (Str3), cystathionine γ-synthase (Str2), cystathionine β-synthase (Cys4) and cystathionine γ-lyase (Cys3). The gene encoding Str2 was down-regulated at 6 h of treatment, while the gene encoding Cys4 gene showed down-regulation after 12 h of treatment. The biosynthesis of methionine is catalyzed by the cobalamin-independent methionine synthase (Met6), and this path is connected to the formation of S-adenosylmethionine, leaded by the S-adenosylmethionine synthetase (Sam1), which was down-regulated after 6 h of eugenol treatment. The reaction between S-adenosylmethionine and S-adenosylhomocysteine is catalyzed by the homocysteine S-methyltransferase (Mht1) and the cysteine desulfurase (Sam4). While orthologue or homologue of Mht1 in *Botrytis* genome was not found, *sam4* was down-regulated after 6 h and also 12 h of treatment. Also the L-homoserine O-acetyltransferase (Met2) and the glutamate dehydrogenase (Gdh1) encoding genes were down-regulated after 6 h of eugenol treatment (Figure 1.14, Table 1.7, Figure 1.15 and Figure 1.16).

Determination of thiol compounds with SBD-F fluorescence labelling showed significant decrease of cysteine content in the treated samples at 6 h and 24 h, of cysteinylglycine content at 10 h and of the glutathione content at 6 h. At the other time points, there was no difference between the control and the treated samples (Figure 1.17).

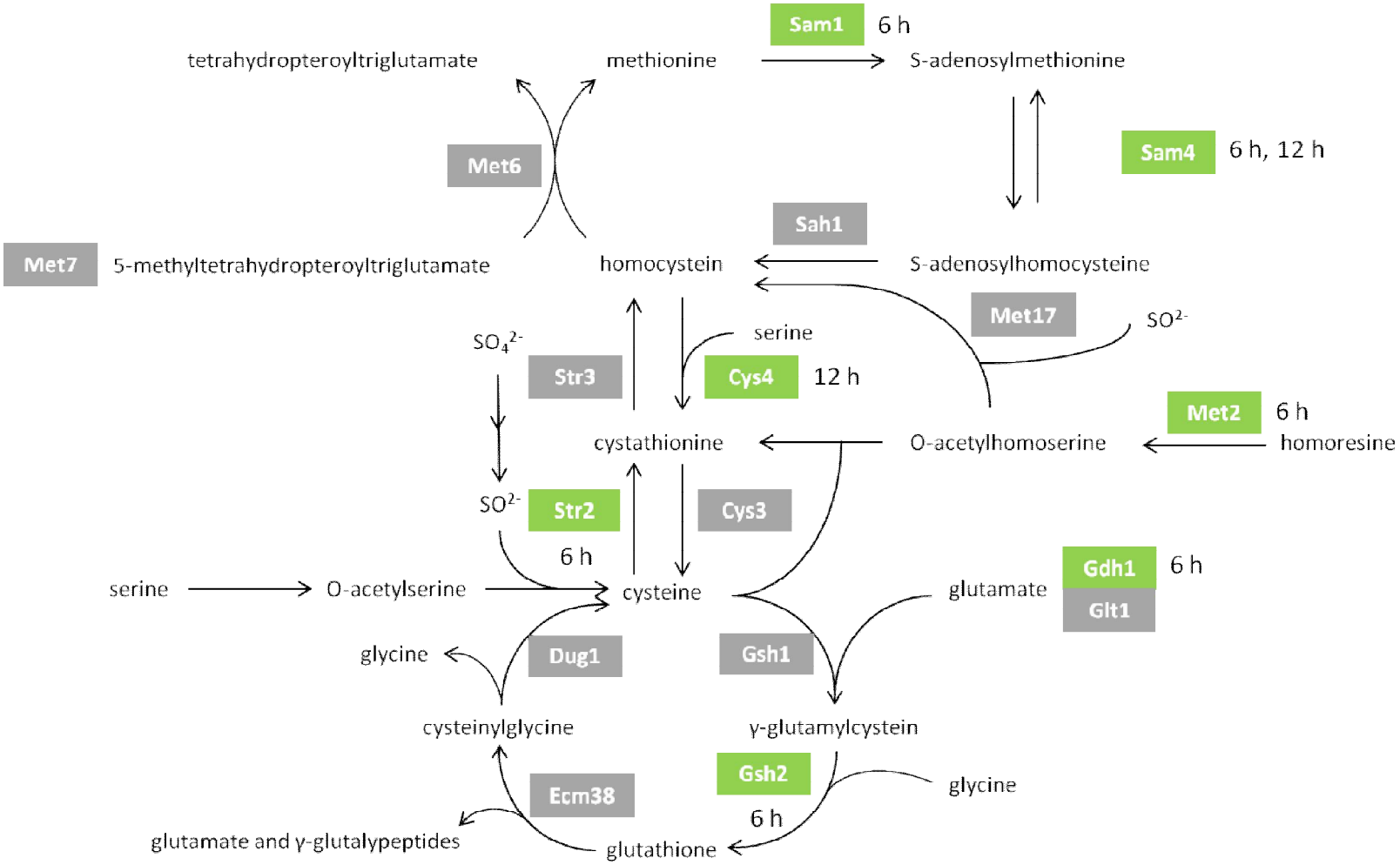

Figure 1.14 - Glutathione pathway adapted from Michel Penninckx (2000).

Table 1.7 – Genes involved in the glutathione pathway and their transcriptional response to eugenol treatment.

Glutathione pathway		***B. cinerea* strains**		**6 h**		**12 h**	
yeast	**description**	**B05.10**	**T4**	**fold change**	**FDR**	**fold change**	**FDR**
Gsh1	Gamma glutamylcysteine synthetase	BC1G_15997	BofuT4_P093480	-1,79	0,59	-1,96	0,28
Gsh2 *	Glutathione synthetase	BC1G_07364	BofuT4_P072040	-3,29	0,03	-3,54	0,07
Ecm38	Gamma-glutamyltranspeptidase	BC1G_12271	BofuT4_P009360	-1,19	0,96	-2,28	0,07
		BC1G_07620	BofuT4_P025820	-3,85	0,14	-2,27	0,27
Dug1	Cys-Gly metallo-di-peptidase	BC1G_10581	BofuT4_P115940	1,10	0,76	-1,03	0,92
		BC1G_05299	BofuT4_P068880	-1,74	0,73	-1,28	0,30
Str2	Cystathionine gamma-synthase	BC1G_11367	BofuT4_P153650	-13,40	0,02	-2,17	0,25
Str3	Peroxisomal cystathionine beta-lyase	BC1G_02862	BofuT4_P117340	-2,09	0,17	1,18	0,76
Cys3	Cystathionine gamma-lyase	BC1G_08021	BofuT4_P121420	-3,09	0,12	-1,65	0,34
Cys4 *	Cystathionine beta-synthase	BC1G_10936	BofuT4_P149990	-4,11	0,17	-3,49	0,03
Met7	Folylpolyglutamate synthetase	BC1G_12218	BofuT4_P163010	-2,36	0,14	-1,94	0,07
Met6	Cobalamin-independent methionine synthase	BC1G_12307	BofuT4_P009010	-1,75	0,43	1,32	0,56
Sah1	S-adenosyl-L-homocysteine hydrolase	BC1G_03241	BofuT4_P101990	-2,23	0,24	1,87	0,51
Met17	O-acetyl homoserine-O-acetyl serine sulfhydrylase	BC1G_07012	BofuT4_P085520	-6,21	0,07	-1,49	0,19
Met2 *	L-homoserine-O-acetyltransferase	BC1G_16012	BofuT4_P112010	-2,60	0,048	-1,44	0,38
Gdh1	NADP(+)-dependent glutamate dehydrogenase	BC1G_13490	BofuT4_P150680	-12,30	0,01	-1,48	0,32
Glt1	NAD(+)-dependent glutamate synthase	BC1G_14168	BofuT4_P004790	-6,92	0,07	-1,08	0,90
Sam1 *	S-adenosylmethionine synthetase	BC1G_04602	BofuT4_P081040	-20,03	0,02	-1,57	0,45
Sam4 *	S-adenosylmethionine-homocysteine methyltransferase	BC1G_02526	BofuT4_P109500	-39,91	0,01	-12,41	0,048

* genes verified by qRT-PCR

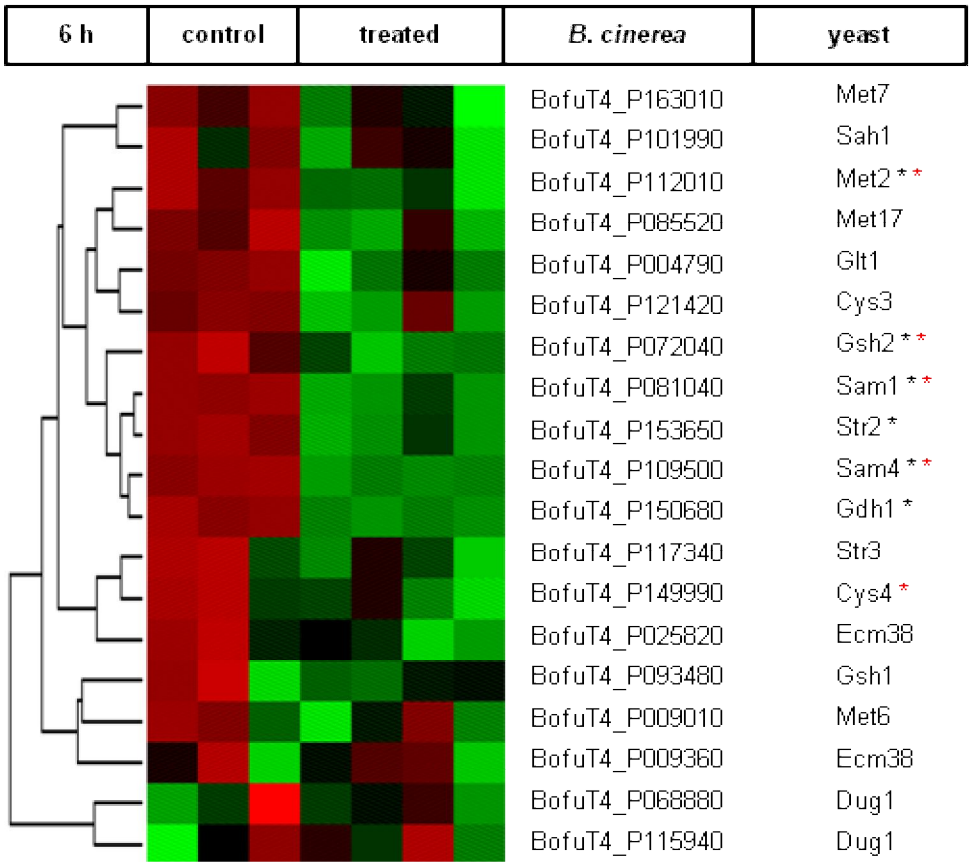

Figure 1.15 - After 6 h of eugenol treatment, the relative expression of genes involved in the glutathione pathway were clustered and visualized in a heat map. Green colour represents the under-expression and red colour the over-expression of three control and four treated samples. The enrichment of this pathway by down-regulated genes was verified by Fisher's exact test (p-value = 0.0164). (* FDR<0.05, * genes verified by qRT-PCR)

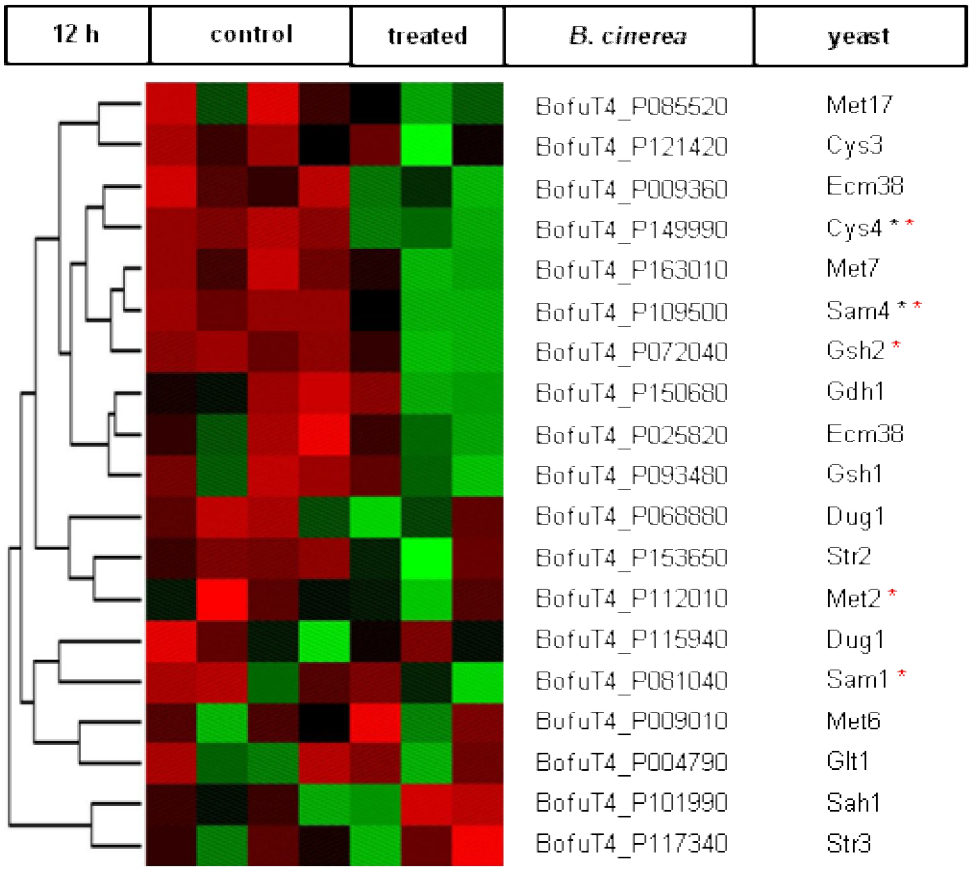

Figure 1.16 - After 6 h of eugenol treatment, the relative expression of genes involved in the glutathione pathway were clustered and visualized in a heat map. Green colour represents the under-expression and red colour the over-expression of three control and four treated samples. (* FDR<0.05, * genes verified by qRT-PCR)

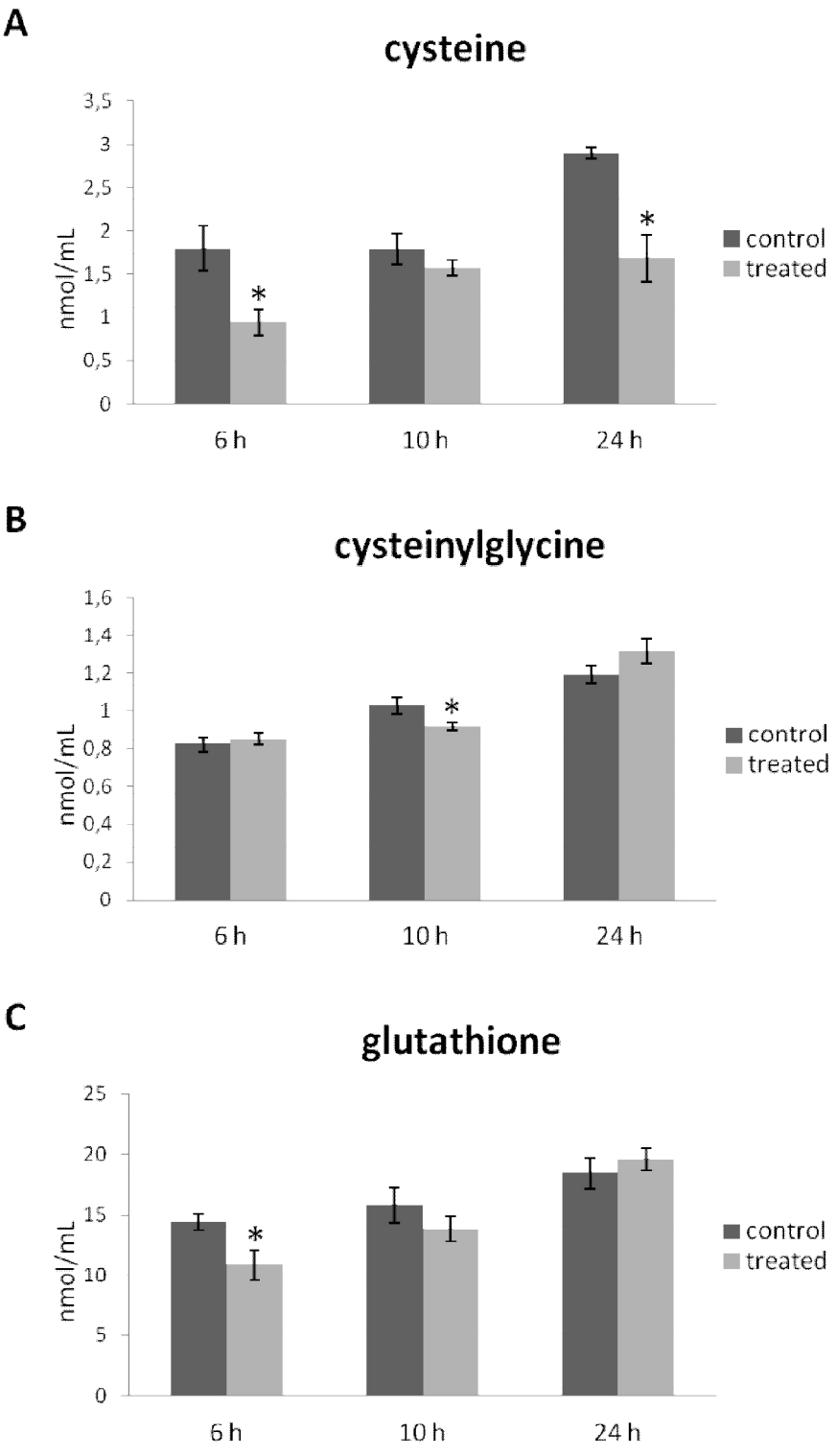

Figure 1.17 – (**A**, **B**, **C**) Histograms showing the thiol compounds in control and eugenol-treated samples at 6, 10, and 24 h. Bars indicate the standard deviation calculated from five biological replicates. Asterisks mean significant difference between control and treated samples according to Student's *t*-test (*, $p<0.05$).

1.3.6 Transporters

Global analyses of *B. cinerea* transcriptional response to eugenol treatment resulted in many enriched functional categories in down-regulated genes associated to transport. Transporters category was enriched after 6 and 12 h of treatment, while MFS sugar transporters category after 6 h and MFS efflux transporters category after 12 h (categories determined by Amselem *et al*., 2011) (Table 1.2). Similar classes were found to be enriched in down-regulated genes among FunCat categories (protein transport and electron transport at 6 h, peptide transport and nuclear transport at 12 h) (Table 1.3) and among GO categories (transmembrane transport at 6 h and 12 h) (Table 1.4). In transmembrane transport (GO: 0055085) functional category, genes were manually compared with *M. oryzae* annotation and sugar transporter, metal transporter, drug and multidrug resistance, such as azole (BC1G_01569, BC1G-03313, BC1G_12393) and fluconazole (BC1G_09265, BC1G_10524, BC1G_12176, BC1G_15172) resistance associated protein encoding genes were identified. Interestingly, protein transport functional category was found to be enriched in up-regulated genes at 12 h in both FunCat and GO categories.

1.3.7 Botrydial toxin biosynthesis

The microarray chip contained five experimental genes involved in the botrydial toxin biosynthesis. All genes showed significant down-regulation after 6 h of eugenol treatment (Table 1.8, Figure 1.18).

Table 1.8 – Genes involved in the botrydial toxin biosynthesis

Botrydial toxin biosynthesis			**6 h**		**12 h**	
name	**description**	**experimental gene**	**fold change**	**FDR**	**fold change**	**FDR**
Bot5	acetyl transferase	BCexp1_BCL5	-153,46	0,01	-1,41	0,27
Bot3	P450 monooxygenase	BCexp2_CND11	-36,78	0,04	-1,41	0,26
Bot2 *	sesquiterpene synthase	BCexp3_CND15	-14,42	0,03	-1,07	0,55
Bot1	P450 monooxygenase	BCexp4_CND5	-50,53	0,01	-1,79	0,10
Bot4	P450 monooxygenase	BCexp5_BCL4	-27,90	0,03	-1,16	0,57

* gene was verified by qRT-PCR

Figure 1.18 – Physical cluster of the botrydial toxin encoding gene *bot1* and co-regulated genes (adapted from Pinedo *et al.*, 2008).

1.3.8 Results of the qRT-PCR

Differential gene expression obtained from the microarray analysis was checked by qRT-PCR choosing some genes with different gene expression profile. Fold change was calculated for each gene at 6 and 12 h utilizing the *act1* (actin 1), *ef1α* (elongation factor 1-alpha) and *pda1* (pyruvate dehydrogenase E1 component subunit alpha) genes as references; *pda1* was then used to determine the relative expression level presented in Table 1.9.

Taken together, the qRT-PCR results confirmed the expression profile of 12 genes (75 %) at 6 h, while 4 genes were found to exhibit a different expression pattern compared to the microarray data. At 12 h, the expression of 6 genes was confirmed by qRT-PCR and of 8 genes showed a different expression profile; in addition, the expression of 2 genes could not be determined according to large standard error.

In particular, in the ergosterol biosynthetic pathway, the expression of *erg6* gene was confirmed by qRT-PCR at 6 h and 12 h; instead, the expression of *erg7* and *erg27* genes resulted from the microarray analysis was not confirmed by qRT-PCR, even if the expression of *erg7* gene at 12 h could be not determined by qRT-PCR, according to its high standard error.

Mcm2 and *mcm3* genes, belonging to the DNA replication factors class, showed the same expression profile using microarray and by qRT-PCR analysis; the expression of *mcm5* gene was confirmed by qRT-PCR at 6 h but not at 12 h when, in contrast to the microarray, it was found to be down-regulated.

Surprisingly, two genes (*met2*, *gsh2*) involved in the glutathione pathway were down-regulated at 6 h using microarray but up-regulated analyzing them by qRT-PCR, while their expression pattern was confirmed at 12 h. Furthermore, differences were found for the expression of *sam1* at 6 and 12 h. The expression of *cys4* and *sam4* genes was confirmed by qRT-PCR.

Bot2 gene, involved in the botrydial toxin biosynthesis, was found to be down-regulated at both 6 h and 12 h by qRT-PCR analysis; however it showed down-regulation using microarray only at 6 h. *Cat1* gene, up-regulated at 6 and 12 h, was found to be up-regulated by qRT-PCR only at 6 h. The down-regulation of a MFS transporter at 6 h was confirmed, but its expression could not be determined at 12 h by qRT-PCR. After microarray analysis, *rad30* and *gpa2* genes were found to be stable at 6 h and 12 h, but a down-regulation was observed at 12 h by qRT-PCR for both genes.

Table 1.9 – Comparison of the expression of selected genes with microarray and qRT-PCR.

yeast	B05.10	T4	B05.10_vankan	6 h				12 h			
				microarray		qRT-PCR		microarray		qRT-PCR	
				fold change	FDR	fold change	standard error	fold change	FDR	fold change	standard error
Erg6	BC1G_07905	BofuT4_P043740	B0510_7030	-2,17	0,046	0,18	0,052	-1,32	0,202	0,56	0,066
Erg7	BC1G_05572	BofuT4_P107430	B0510_9190	-4,59	0,045	0,72	0,072	-1,25	0,547	2,30	1,085
Erg27	BC1G_00806	BofuT4_P019230	B0510_226	-3,13	0,021	0,82	0,333	-1,89	0,085	0,35	0,130
Mcm2	BC1G_13345	BofuT4_P088830	B0510_5850	-6,93	0,009	0,40	0,052	-5,38	0,045	0,48	0,027
Mcm3	BC1G_14509	BofuT4_P077080	B0510_7835	-8,56	0,020	0,36	0,115	-1,67	0,072	0,46	0,091
Mcm5	BC1G_02916	BofuT4_P004120	B0510_2612	-6,28	0,036	0,39	0,008	-1,32	0,418	0,37	0,034
Gsh2	BC1G_07364	BofuT4_P072040	B0510_5726	-3,29	0,032	3,68	0,955	-3,54	0,065	0,95	0,102
Cys4	BC1G_10936	BofuT4_P149990	B0510_3656	-4,11	0,173	1,15	0,278	-3,49	0,028	0,42	0,016
Met2	BC1G_16012	BofuT4_P112010	B0510_4208	-2,60	0,048	2,94	0,892	-1,44	0,380	1,35	0,231
Sam1	BC1G_04602	BofuT4_P081040	B0510_7956	-20,03	0,016	1,04	0,206	-1,57	0,448	0,34	0,109
Sam4	BC1G_02526	BofuT4_P109500	B0510_8038	-39,91	0,006	0,12	0,012	-12,41	0,048	0,11	0,007
nd	BcBot2 *	BCexp3_CND15	AY277723.2	-14,42	0,032	0,30	0,147	-1,07	0,552	0,11	0,047
Cat1	BC1G_09386	BofuT4_P148250	B0510_1337	9,17	0,023	3,82	0,640	3,56	0,037	0,78	0,492
MFS transporter	BC1G_01569	BofuT4_P042550	B0510_1522	-88,76	0,043	0,21	0,060	-26,35	0,039	3,12	2,306
Rad30	BC1G_07551	BofuT4_P084300	B0510_6523	-1,11	0,670	1,15	0,460	1,73	0,042	0,20	0,064
Gpa2	BC1G_03006	BofuT4_P003150	B0510_2668	1,77	0,039	1,19	0,457	-1,18	0,710	0,18	0,047

*Due to the lack of B05.10_vankan annotation, BcBot2 corresponds to GenBank annotation AY277723.2. High standard error values are underlined.

1.4 Discussion

Eugenol is a widely used natural molecule because of its antimicrobial characteristic, nevertheless little is known about its mode of action. Since the genome of *B. cinerea* has been already sequenced (Amselem *et al*., 2011), the transcriptional response of the fungus to eugenol treatment was analysed in this study by microarray technology.

Ergosterol biosynthesis functional category defined by Amselem *et al*. (2011) was significantly enriched in down-regulated genes after 6 h of eugenol treatment. In particular, we identified 5 of 14 genes as down-regulated: *erg7*, *erg27*, *erg6*, *erg2* and e*rg4*. Ergosterol is a fungal sterol and the main component of the cell plasma membrane. It has a role in membrane integrity and fluidity, as well as in the activity of membrane-bound enzymes (Lees *et al*., 1995; Parks *et al*., 1995). Some fungicides targeting enzymes involved in the ergosterol biosynthesis are well known and they are divided in four Sterol Biosynthesis Inhibitor (SBI) classes: Class I DMI (DeMethylation Inhibitor) fungicides, that target the C14-demethylase (Erg11/Cyp51), e.g.: triazoles, imidazoles; Class II amines ("morpholines"), that target the C-14 sterol reductase (Erg24) and the C-8 sterol isomerise (Erg2), e.g.: morpholines, piperidines; Class III keto-reductase inhibitors, that inhibit Erg27, e.g.: hydroxyanilides; and Class IV squalene epoxidase inhibitors, that target Erg1, e.g: allylamines, thiocarbamates (FRAC Mode of Action Poster©, 2014). In a previous study, transcriptional analysis of *S. cerevisiae* response to SBI fungicides was performed. Class I and Class II inhibitors bind Erg enzymes and decrease the ergosterol level in the membrane. In response to this treatment, over-expression of several *erg* genes was determined in *S. cerevisiae*. Nevertheless, Class II inhibitors did not alter the transcription level of the target *erg24* gene and fenhexamid did not change the expression of its target *erg27* gene (Kagan *et al*., 2005). Transcriptome analysis of the response of *Mycosphaerella graminicola* to epiconazole showed a common up-regulation of genes involved in the ergosterol biosynthesis. On the whole, these results seem to indicate that in general treatments with SBI fungicides – binding Erg enzymes – induce over-expression of genes involved in the ergosterol biosynthesis, in order to balance the ergosterol content in the cell membrane. In contrast to fungicides, our transcriptome analysis showed down-regulated *erg* genes after 6 h of treatment with eugenol hypothesizing low ergosterol level in the cell membrane, leading to its disruption. In fact, decreased ergosterol content was measured in the plasma membrane of *Trichophyton rubrum* after eugenol treatment (De Oliveira Pereira *et al*., 2013).

Interestingly, enrichment in up-regulated genes was found in stress related functional categories, such as oxidative stress response, pH stress response, and oxygen and radical detoxyfication. In fact, eugenol seems to induce the generation of reactive oxygen species (ROS) which could cause oxidative stress and membrane damage via lipid peroxidation (Ahuja *et al*., 2014). Our transcriptomic results seem to be in accordance with a possible effect of eugenol on the antioxidant machinery system by causing oxidative stress in the fungus, thereby activating stress related genes.

After 6 h of eugenol treatment, significant down-regulation of genes involved in the glutathione pathway was determined. Glutathione is a tripeptide, synthesized from cysteine, glutamate and glycine, and has antioxidant activity. Earlier studies showed the role of glutathione in detoxification of xenobiotics, as well as its importance in the response to oxidative stress (Penninckx, 2000; Shin *et al*., 2003, Pócsi *et al*., 2004). Methionine biosynthesis is connected to the glutathione biosynthesis, and there is a group of fungicides (Anilino-Pyrimidines) which act on the cystathionine gamma-synthase gene (*str2*), what we found significantly down-regulated after 6 h of eugenol treatment. Recently, the importance of this gene in *Fusarium graminearum* was reported: decreased virulence on wheat, lower deoxynivalenol production, and increased sensitivity of Δ*str2* mutants to SBI fungicides were observed (Fu *et al*., 2013). After treatment of yeast with chlorothalonil pesticide, the role of glutathione and glutathione S-transferase in detoxification and resistance development was described (Shin *et al*., 2003). Similar results were obtained treating yeast cells with mancozeb (Dias *et al*., 2010). To validate down-regulation of genes involved in the glutathione pathway, biochemical assays were performed and decreased amount of glutathione and cysteine was observed at 6 h post treatment; however the *gsh2* gene encoding glutathione synthetase and the *met2* gene encoding L-homoserine-O-acetyltransferase were significantly over-expressed by qRT-PCR, thus the effect of eugenol on the glutathione pathway remains unclear.

The link between over production of ABC and MFS transporters and the development of multidrug resistance (MDR) in *B. cinerea* has been already proved (De Waard *et al*., 2006; Leroux and Walker, 2013). In the present microarray analysis, the ABC transporters functional category (determined by Amselem *et al*., 2011) was not enriched neither in up, nor in down-regulated genes (data not shown); on the contrary, the MFS efflux transporters functional category was enriched in down-regulated genes after 6 h of treatment. Besides, enrichment in down-regulated genes in GO transmembrane transport (GO: 0055085) functional category was found after both 6 h and 12 h of eugenol treatment. Among these

genes, some were metal transporter encoding ones or related to drug and multidrug resistance, more precisely involved in the resistance to azole and fluconazole fungicides. These observations suggest that the fungus treated with eugenol could be impaired in the detoxification process.

Analyzing our microarray data, significant enrichment in down-regulated genes encoding DNA replication factors - introduced by Enserink in 2010 – was found after 6 h of eugenol treatment. DNA replication is part of the cell cycle and is essential for all living organisms. Approximately 800 genes are involved in this process in yeast (Spellman *et al*., 1998), however no list of these genes was found for *B. cinerea*. Our result is in accordance with the observation that treatment of yeast with thiram (a fungicide with multi-site contact activity) caused the down-regulation of most of the genes belonging to "DNA" and "transcription" categories [MIPS (Munich Information Centre for Protein Sequences)]; (Kitagawa *et al*., 2002). Analyses of gene expression after copper treatment of yeast showed over-expression of genes involved in "DNA recombination and DNA repair" within the "cell cycle and DNA processing" MIPS category (Yasokawa and Iwahashi, 2010), suggesting a DNA damage by metal ion toxicity. Treatments with eugenol at higher concentration damaged the DNA of mammal cells (Özkan *et al*., 2013; Slameňová *et al*., 2009), although the effect of eugenol on fungal DNA has not been examined yet.

Botrydial is a sesquiterpene, a secondary metabolite produced by *B. cinerea* which induces chlorosis and cell collapse during plant infection (Deighton *et al*., 2001). Currently, five genes are known to be correlated with the botrydial toxin biosynthesis (Pinedo *et al*., 2008) and all showed down-regulation using microarray after 6 h of eugenol treatment. The expression level of *bot2* gene was determined also by qRT-PCR and was significantly lower at both 6 and 12 h of eugenol treatment. These results might idicate an important effect of eugenol in the biosynthesis of botrydial toxin, which might suggest a possible effect on fungal virulence.

On the whole, our microarray data presented in Venn diagram shows 1504 down-regulated genes after 6 h and 823 after 12 h of eugenol treatment but only 177 were common. Furthermore, a significant enrichment in down-regulated genes was obtained in the examined pathways only at 6 h and this suggests a possible technical problem of the microarray at 12 h. In fact, one of the treated samples at 12 h (T-12h-80-R2) was excluded from the analyses because it was grouped with the control samples in the hierarchical clustering and on the PCA diagram, and another one (T-12h-80-R1) was considered, even if it was not well clustered

with the remaining two samples. In particular, the diverse expression of this sample from the other two is clearly visible also on the heat maps. To check this hypothesis and the reliability of our microarray results, new biological replicates were prepared and qRT-PCR was performed. At 6 h, the expression level of most of the analyzed genes was confirmed, but at 12 h more differences were found and this would confirm that the experiment at 12 h is probably unreliable.

1.5 Conclusion and perspectives

In conclusion, the natural bioactive compound eugenol seems to exert its antifungal activity by affecting different targets. One of the main targets of this molecule is the fungal plasma membrane: the down-regulation of genes involved in the ergosterol biosynthesis could lead to a reduction in the ergosterol content of the membrane, which could also be damaged by ROS accumulation and consequent induction of oxidative stress determined by eugenol treatment (De Oliveira Pereira *et al*., 2013; Anhuja *et al*., 2014); the observed up-regulation of genes involved in stress related functional categories, such as oxidative stress response, is in accordance with this hypothesis. In perpective, determination of the ergosterol content in the treated mycelium might help to confirm the role of eugenol in *B. cinerea* growth inhibition. Besides, the observed under-expression of transporters encoding genes could suggest that the detoxification process of the fungus could be also affected by this molecule. According to microarray analysis, eugenol appears to negatively affect the cell cycle and the botrydial toxin biosynthesis; this latter observation could suggest a possible effect of eugenol treatment on fungal phytotoxicity, which should be further investigated by *in vivo* infections of host plant tissues after treatment with eugenol. On the other hand, the effect of eugenol on the glutathione pathway remains unclear since microarray and qRT-PCR results are in contrast and therefore biochemical data are difficult to explain; in perspective, further gene expression analyses at different times after eugenol treatment should be performed.

Chapter II

Role of the Snf1 protein kinase in *Botrytis cinerea* pathogenesis

2.1 Introduction

Botrytis cinerea is a necrotrophic fungus that affects more than 240 dicotyledonous plants in a wide variety of agriculturally important crops, causing grey mould (Staats *et al*., 2005). The infection process of *B. cinerea* is assisted by several mechanisms that include the secretion of degrading enzymes, the production of toxic compounds and the perturbation of the host defence system (Choquer *et al*., 2007). The secretion of a wide spectrum of cell wall degrading enzymes (CWDEs) by necrotrophic fungi is probably the first and most studied mechanism involved in the penetration and colonization of the host tissue and the number and type of genes encoding CWDEs in *B. cinerea* genome reflect the complexity of the plant cell wall carbohydrates (Blanco-Ulate *et al*., 2014).

Pectin, cellulose and hemicelluloses are the main polysaccharide components of the plant cell wall (Figure 2.1). Pectin is a complex polysaccharide, composed mostly by D-galacturonic acid, and it is found mainly in the middle lamella and primary cell wall (Popper *et al*., 2011; Kars and van Kan, 2007). To degrade pectin, *B. cinerea* expresses various pectinases, such as pectin methylesterase, endo- and exopolygalacturonases (endo- and exoPGs), pectin and pectate lyase. Pectin methylesterase de-esterifies pectin to pectate and the role of this enzyme during host infection by *B. cinerea* was examined by Δ*bcpme1* mutants. Disruption mutant of the Bd90 strain showed reduced pathogenicity on apple, grapevine and Arabidopsis (Valette-Collet *et al*., 2003), but mutants created by gene-replacement of the B05.10 strain did not show any reduction in virulence on five different hosts (including apple), suggesting that the pectin methylesterase activity is strain dependent (Kars and van Kan, 2007). Endo-PGs and exo-PGs, respectively, hydrolyse internal and terminal linkages of the homogalacturonan chain. *B. cinerea* secretes six endo-PGs and their role has been well defined *in vitro* and *in planta* focusing on gene expression and enzyme activity on different carbon sources and during infection. The effect of ambient pH on the secretion of these enzymes was also studied (Wubben *et al*., 2000; Ten Have *et al*., 2001). Pg1 is the mostly expressed endo-PG during fungal infection and its contribution to virulence was repeatedly verified (Ten Have *et al*., 1998, Poinssot *et al*., 2003).

Cellulose is a β-1,4-linked D-glucose polymer, forming microfibrils in lignocelluloses in the primary and secondary cell wall, while xylan, the major hemicellulose, is built up by β-1,4-linked xylose, arabinose, and glucuronic acid (Popper *et al*., 2011). To degrade these components, *B. cinerea* secretes cellulases, xylanases and arabinases (Kars and van Kan, 2007). The importance of a xylanase enzyme (Xyn11A) in *B. cinerea* pathogenicity has been

shown by testing mutants on tomato leaves and grape berries (Brito *et al*., 2005; Noda *et al*., 2010). The function of some CWDEs is still unclear since, single mutants of their corresponding genes did not show any significant reduction in pathogenicity, in comparison to the wild type; this result could be explained by the gene redundancy in multigenic families (Choquer *et al*., 2007; Kars and van Kan, 2007). In fact, in *B. cinerea*, CWDEs are encoded by multigenic families; thus defining the contribution to virulence of a particular enzyme activity is difficult.

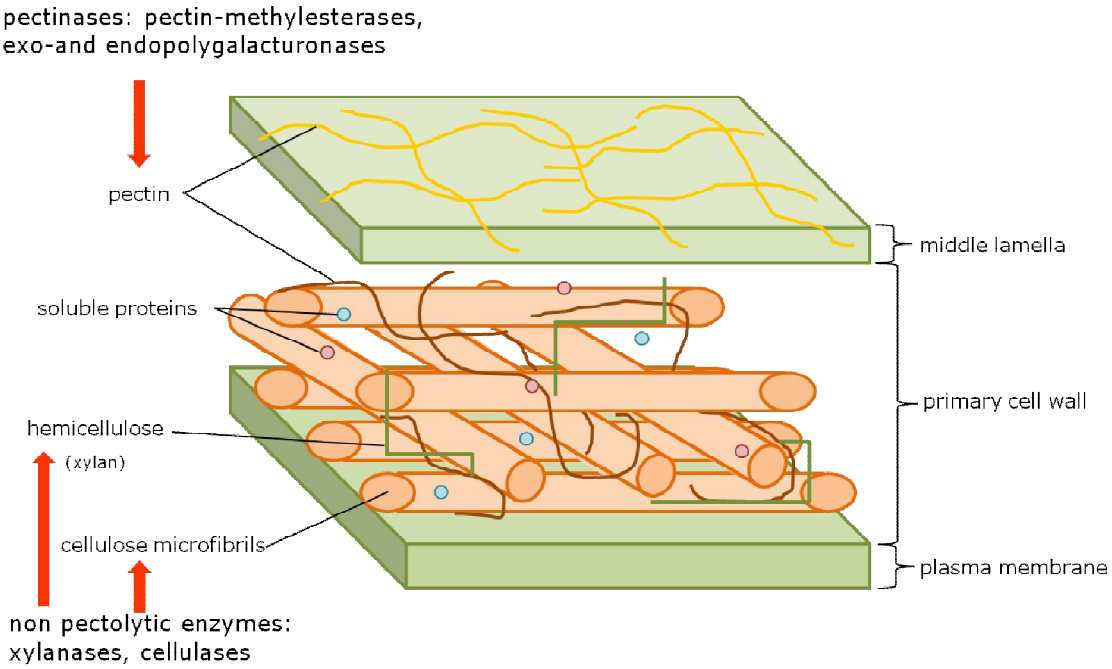

Figure 2.1 – Structure of the plant cell wall.

In fungi, the expression of several CWDEs encoding genes is known to be regulated by the Snf1 (sucrose non-fermenting 1) protein kinase. The Snf1 pathway is still unexplored in *B. cinerea*, but several other signal transduction pathways, regulated by glucose, have been well studied and their role in fungus development and pathogenicity were established (Figure 2.2) (Turrà *et al*., 2014).

Cyclic adenosine monophosphate (cAMP)-dependent pathways are involved in morphogenesis, differentiation, and virulence of *B. cinerea* (Tudzynski and Gronover, 2007). In these pathways, in presence of glucose, Gα subunits of heterotrimeric G proteins activate the adenylate cyclase (AC) enzyme, which converts adenosine triphosphate (ATP) into cAMP (Turrà *et al*., 2014). Mutants of the two genes encoding Gα subunits (*bcg1* and *bcg2*) showed

reduced virulence (Gronover *et al*., 2001). In another study, the role of protein kinase A (PKA) in pathogenicity was evaluated, comparing Δ*bcpka1* and Δ*bcpkaR* mutants with the wild type. Both mutants grew slower on bean leaves, and soft rot never occurred (Schumacher *et al*., 2008). These mutants, as well as the Δ*bcg1* and Δ*bcg2* mutants were not impaired in conidiation. AC is activated also by the fungal-specific Ras GTP-binding protein in a glucose rich ambient (Figure 2.2). Mutation of the GTPase encoding *bcras2* gene affected the germination and the growth of the fungus. This effect could be restored adding exogenous cAMP, proposing the role of Ras2 in activation of the AC (Schumacher *et al*., 2008). Ras1 and Rac small GTPases are other members of the Ras superfamily, playing role in cellular processes, differentiation, and polar growth. In *B. cinerea*, these proteins were analyzed by obtaining deletion mutants. Both strains showed decreased growth and deformed hyphae, and they did not produce conidia and were non-pathogenic. (Dub *et al*., 2013)

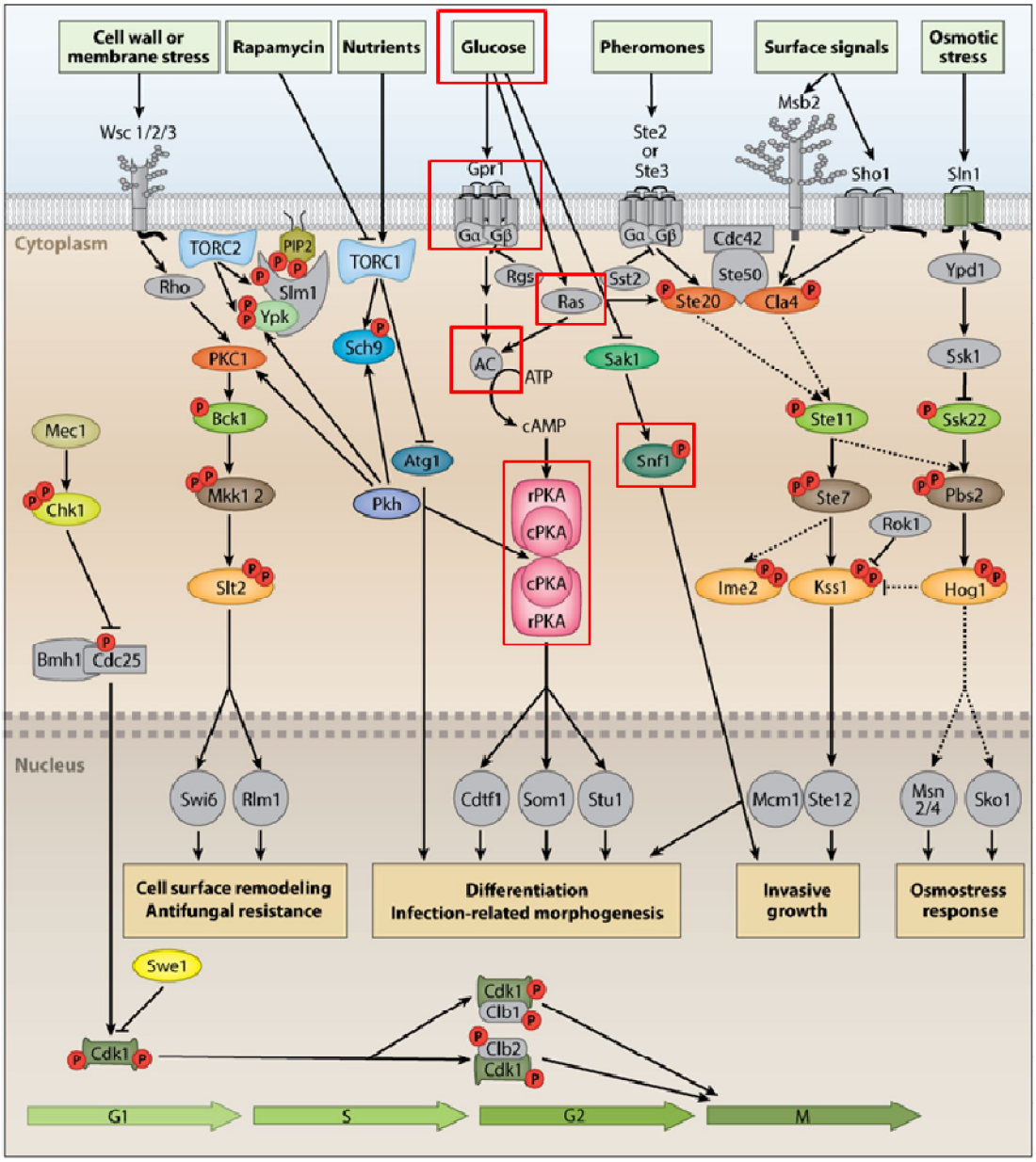

Figure 2.2 – Schematic representation of protein kinases in plant pathogenic fungi (Turrà *et al.*, 2014). Red squares indicate proteins involved in glucose-regulated signalling cascades; the role of these proteins in growth and pathogenicity is discussed above.

Although the Snf1 signal transduction in *B. cinerea* has not been characterized yet, recently, the function of this signalling pathway was studied in yeast and in several plant pathogenic fungi. In yeast, at high glucose level, the Snf1 complex (composed of an α subunit encoded by *snf1*, a β subunit encoded by *sip1* or *sip2* or *gal83*, and a γ subunit encoded by *snf4*) is inactive. Instead, in response to glucose starvation, Snf1 is activated by phosphorylation by one of its upstream kinases (Sak1, Tos3 and Elm1) and it phosphorylates the downstream kinase Mig1 [the orthologue in filamentous fungi is called CreA (Ronne,

1995)], resulting in the removal of this repressor (Rødkær and Færgeman, 2014; Hong *et al*., 2007) (Figure 2.3). In *Cochliobolus carbonum*, putative CreA binding sequences were recognized in the promoter region of three CWDE encoding genes suggesting a possible role of this transcription factor in the regulation of CWDE expression (Tonukari *et al*., 2003), while in *Sclerotinia sclerotiorum*, the expression of *cre1* gene (homologus of *creA* from *Aspergillus nidulans*) was higher at pH 3 and pH 7 than at ph 5, indicating an ambient pH dependent regulation of this gene (Vautard-Mey and Fèvre, 2002). In particular, Mig1 (CreA) would act as repressor of CWDE encoding genes expression, except when phosphorilated by Snf1.

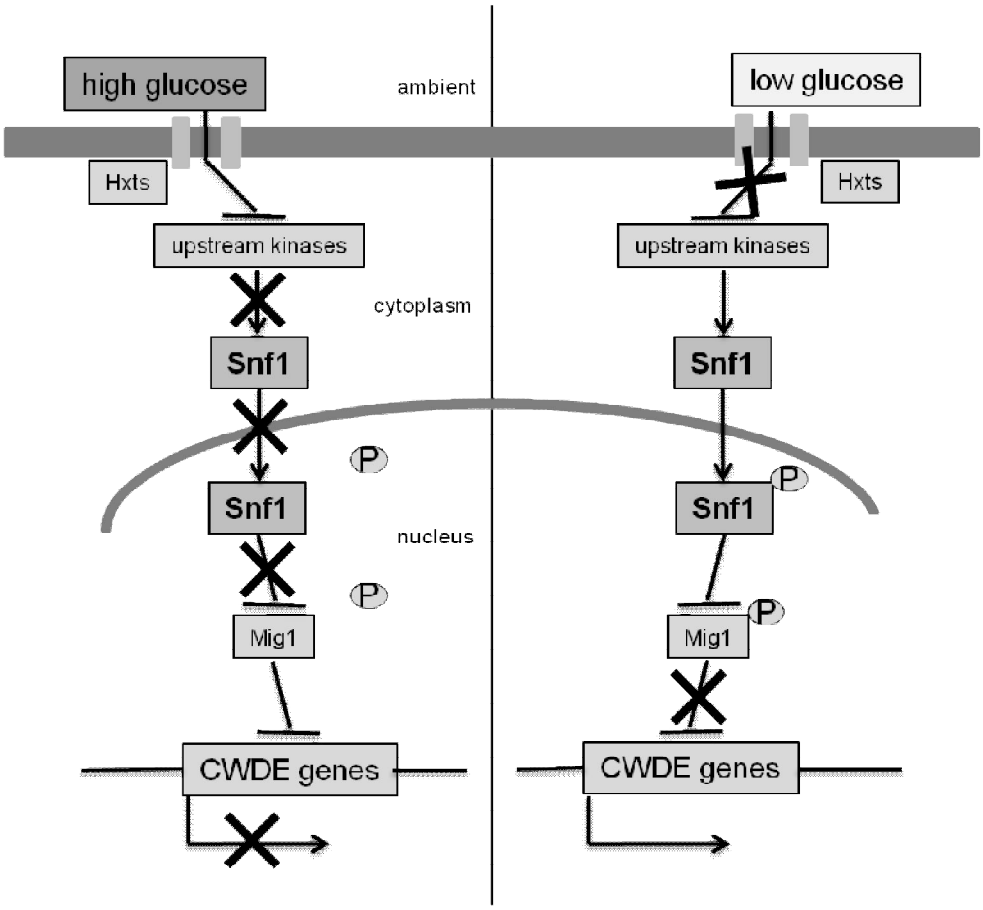

Figure 2.3 - Snf1 signalling pathway adapted from S. cerevisiae (Rødkær and Færgeman, 2014). When glucose is available, Snf1 complex is inactive and Mig1 represses the transcription of CWDEs encoding genes. When glucose is limiting, Snf1 is activated by one of its upstream kinases and phosphorylates Mig1, thereby negatively regulating its binding to the promoter of CWDEs encoding genes whose expression is thus activated.

Snf1 protein kinase is highly conserved in eukaryotes (Polge *et al*., 2007) and its function and importance in virulence were studied in different plant pathogenic fungi. Deletion mutants of *Fusarium oxyosporum* (Ospina-Giraldo *et al*., 2003), *F. graminearum* (Yu *et al*., 2014), *Magnaporthe oryzae* (Yi *et al*., 2008) and *Verticillium dahliae* (Tzima *et al*., 2011) showed reduced virulence on their respective host plants compared with the wild type strains. In several Δ*snf1* fungal mutants, the expression of PGs, other pectinases, xylanases, and cellulases encoding genes was usually significantly lower than that of the wild type, in agreement with the proposed role of Snf1 kinase in the activation of CWDEs encoding genes (Tonukari *et al*., 2000; Ospina-Giraldo *et al*., 2003; Lee *et al*., 2009; Tzima *et al*., 2011; Nadal *et al*., 2010; and Zhang *et al*., 2013). In some studies, the sporulation was also examined and abnormal shape of spores with reduced sporulation were observed (Yi *et al*., 2008, Lee *et al*., 2009, Zhang *et al*., 2013, and Yu *et al*., 2014). In *S. cerevisiae*, Snf1 kinase is also involved in adaptation to alkaline pH, oxidative and osmotic stresses (Hong *et al*., 2007).

Recently, the role of *M. oryzae* Snf1 protein kinase in response to nutrient-free environment via peroxisomal maintenance and lipid metabolism was reported. Δ*snf1* mutant grew slower on non-fermenting carbons and the peroxisomes were larger than those of the wild type strain (Zeng *et al*., 2014).

If Snf1 protein kinase has a central role in CWDEs' regulation, it probably has also other multiple roles in the fungus biology (e.g. differentiation of spores, response to different stresses, or lipid metabolism and peroxisome function). In the present chapter, two independent *snf1* mutants of *B. cinerea* were obtained by gene replacement and their CWDEs secretion, growth on various carbon sources, and virulence on several plant tissues were examined. In addition, effects on sporulation of the mutants and their adaptation to different pHs were evaluated.

2.2 Materials and methods

2.2.1 Fungal strains and growth conditions

B. cinerea strain B05.10 and mutants were kept on potato dextrose agar (PDA) (Oxoid, CM0139) at 21 °C in dark. For following growth and pathogenicity tests, three days old plates with mycelia were used; mycelium plugs were taken from the margin of actively growing fungal colonies.

For growth tests, minimal medium (MM) (2 g L^{-1} $NaNO_3$, 1 g L^{-1} K_2HPO_4, 0,5 g L^{-1} KCl, 0.5 g L^{-1} $MgSO_4 \cdot 7H_2O$, 0.01 g L^{-1} $FeSO_4 \cdot 7H_2O$) was prepared adding 1.92 g L^{-1} citric acid for a good buffering capacity (Manteau *et al.*, 2002). The medium then was supplemented with 1 % (w/v) carbon source (Table 2.1) and the pH was adjusted to 5, 6 and 7 with NaOH and 1.5 % agar (Oxoid, LP0011) was added. For inoculation, 7 mm diameter plugs with mycelium were used. Three technical replicates (three plates) were performed for each sample and the experiment was repeated independently three times obtaining three biological replicates. The Petri dishes were incubated at 21 °C in dark and the growth diameter of the wild type and the mutant strains was measured to 4 dpi.

Table 2.1 – List of the carbon source used for growth tests

simple sugars	polysaccharides	other non-fermenting carbons
• glucose (**Sigma, G-7021**)	• polygalacturonic acid (PGA) from citrus fruit (Sigma, P-3850)	• tween 80 (Sigma, P4780)
• sucrose (Merck, 107687)	• xylan from beechwood (Sigma, X-7252)	• olive oil (from the local supermarket)
• xylose (Merck, 108692)	• carboxymethyl cellulose (Sigma C-5678)	• triolein (Sigma, T7190)
• galacturonic acid (GA) (Aldrich, 85,728-9)		• NaAc (Sigma-Aldrich, S2889)

2.2.2 Gene replacement by transformation

The orthologue of the yeast *snf1* gene was identified from GenBank by bidirectional blast hit (BBH) and named *Bcsnf1* corresponding to B0510_10055 (B05.10_vankan) or BC1G_12009 (B05.10) reference gene in *B. cinerea.*

2.2.2.1 Preparation of cassettes for gene replacement

For *B. cinerea snf1* targeted replacement, the split-marker technique (Figure 2.4A) was used, as previously described by Catlett *et al*. (2003). Genomic DNA from *B. cinerea* B05.10 strain was extracted with DNeasy Plant Mini Kit (Qiagen, Germany) and used as template. In the first PCR round, the 5' and 3' flanking regions were amplified with the primer pair Snf1-5'-For and Snf1-5'-Rev, and the Snf1-3'-For and Snf1-3'-Rev. The hygromycin resistance gene was amplified with the primers Hyg-For and Hyg-Rev, using a hygromycin cassette as a template (Patel *et al*., 2008). PCR was performed with iProof ^{TM} High-Fidelity DNA Polymerase (BIO-RAD, USA) following the manufacturer's instructions and the fragments of the expected sizes (Table 2.3) were purified from agarose gel using GFX PCR and Gel Band Purification Kit (GE Healthcare, UK).

Equimolar amounts of the purified fragments were mixed in a second round of linear PCR and in a third round of PCR, the joint fragments were amplified with nested primers. The primer pair Snf1-5'-For and Hyg-Nest-Rev was used to amplify the 5' flanking region and the 5' fragment of the hygromycin gene, and the Hyg-Nest-For and Snf1-3'-Rev primers to amplify the 3' fragment of the hygromycin gene and 3' flanking region. The fragments of the expected sizes (Table 2.4) were purified from agarose gel using GFX PCR and Gel Band Purification Kit.

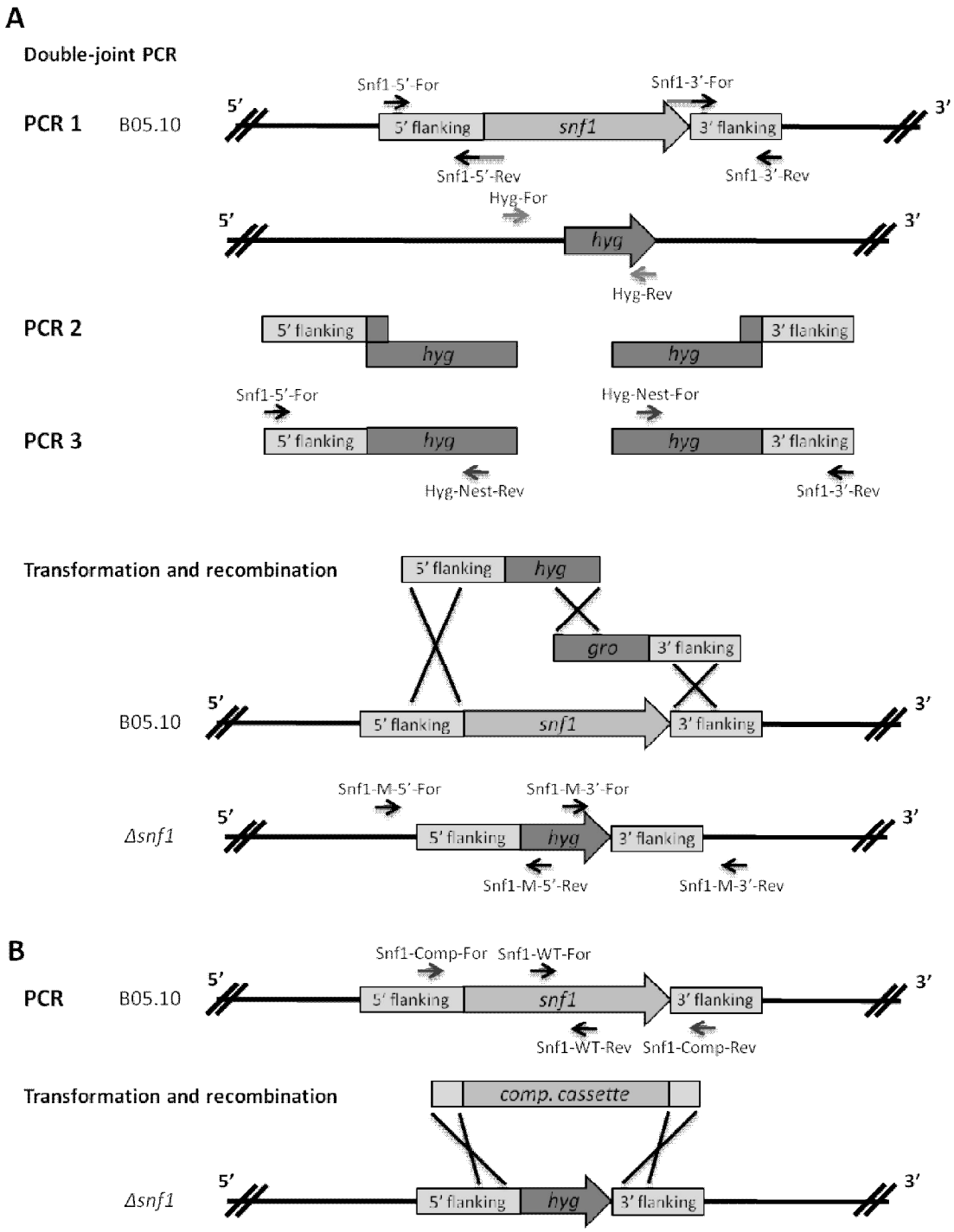

Figure 2.4 – Schematic illustration of the *B. cinerea snf1* gene replacement and complementation showing the used primers and deletion cassettes. In the Snf1-5'-Rev and Snf1-3'-For primer the identical sequences with the Hyg-For and Hyg-Rev primers are indicated with grey colour and overlaid in the primer sequences (Table 2.3) (**A**) Preparation of deletion cassettes for the *snf1* gene deletion by double joint PCR method. Primers, used for this procedure and for check the deletion mutants, are inserted. (**B**) Preparation of complementation cassettes for the complementation of the *Δsnf1* strain. Primers, used for this procedure and for check the complemented strain, are inserted.

2.2.2.2 Fungal transformation

Two weeks old sporulating mycelium of B05.10 wild type strain was scraped from plates and filtered through a 100 µm cell strainer (BD Falcon, USA). The filtered spores were transferred in a 250 ml Erlenmeyer flask containing 100 ml NY medium (2 g L^{-1} yeast extract and 20 g L^{-1} malt extract). The fungus was grown at 23 ^{o}C for 24 h at 120 rpm.

Lysing enzyme from *Trichoderma harzianum* (Sigma, USA) was prepared by dissolving 0.2 g in 10 ml of KCl/NaP buffer (Table 2.2) and preheated at 37 ^{o}C then the enzyme solution was filtered through a 20 µm filter (Sartorius, Germany) and diluted to 20 ml with KCl/NaP buffer. Mycelium from an Erlenmeyer flask was filter through a nitex bolting cloth rinsing it with KCl/NaP buffer. The spores were transferred into a 100 ml Erlenmeyer flask where the lysing enzyme was added. After 3 h of incubation at 23 ^{o}C at 70 rpm, the protoplasts obtained were filtered through a 40 µm cell strainer (BD Falcon, USA) and rinsed with 2 ml TMS buffer (1 M sorbitol and 10 mM MOPS, pH 6.3). The protoplasts were centrifuged at 4 ^{o}C for 5 min at 3500 rpm. The supernatant was carefully discarded, the pellet was diluted in 10 ml TMS buffer and the suspension was centrifuged again at 4 ^{o}C for 5 min at 3500 rpm. The pellet was diluted in 300 µl TMS buffer and the protoplast concentration was determined by Thoma cell counting chamber. For cell transformation, $2*10^7$ protoplasts were suspended in 100 µl TMSC buffer (1 M sorbitol, 10 mM MOPS, and 40 mM $CaCl_2$, pH 6.3), mixed with 2 µg of each replacement cassettes and diluted in TE $CaCL_2$ 2x buffer (20 mM Tris-HCl, 2 mM EDTA, 80 mM $CaCl_2$ * 2 H_2O, pH 7.5) and the mixture was incubated for 20 min on ice. Then 160 µl of PEG solution [1.2 g PEG6000 dissolved in 800 µl MS buffer (0.6 M sorbitol and 10 mM MOPS, pH 6.3)] was added to the mixture, and after an incubation at RT for 15 min, 1 ml pre-cooled TMSC buffer was added. The sample was centrifuged for 5 min at 5000 rpm and the pellet was resuspended in 400 µl TMSC buffer. 4 x 3 ml MMV Top medium (2 g L^{-1} $NaNO_3$, 1 g L^{-1} K_2HPO_4, 0.5 g L^{-1} KCl, 0.5 g L^{-1} $MgSO_4 \cdot 7H_2O$, 0.01 g L^{-1} $FeSO_4 \cdot 7H_2O$, 20 % (w/v) saccharose, 2 % (w/v) glucose, and 0.4 % (w/v) agar) containing 100 µg ml^{-1} hygromycin was preheated at 42 ^{o}C. 100 µl of sample was pipetted to one tube of MMV Top medium and it was poured on a Petri dish containing MMV medium (MMV Top medium with 1.5 % (w/v) agar). The plates were kept at 21 ^{o}C in dark. Transformants were transferred on MM medium containing 100 µg ml^{-1} hygromycin.

Table 2.2 – Preparation of the KCl/NaP buffer

Buffer KCl/NaP	550ml	concentration of the solution
KCl	500 ml (1)	0,6 M
NaP	50 ml (2)	0,1 M
KCl	22,37 g in 500 ml H_2O (1)	0,6 M
NaP	15,8 ml (3) + 184,2 ml (4)	1 M
$Na_2HPO4*7\ H_2O$	13,4 g in 50ml H_2O (3)	1 M
NaH_2PO4	60 g in 500 ml H_2O (4)	1 M

2.2.2.3 Verification of the transformants

Transformant colonies were first checked by PCR for insertion of the hygromycin resistance gene using the Hyg-For and Hyg-Rev primers. The positive colonies were checked for the correct insertion of the hygromycin resistance gene at the 5' and 3' Snf1 flanking regions with the primer pairs Snf1-M-5'-For, Snf1-M-5'-Rev and Snf1-M-3'-For, Snf1-M-3'-Rev. As non-transformed nuclei can maintain in hygromycin resistant transformants, we checked by PCR the presence/absence of the wild type *snf1* ORF sequence with the Snf1-WT-For and Snf1-WT-Rev primers. PCR conditions are reported in Table 2.3 according to the information sheet of Taq polymerase (MP Biomdicals, USA).

Homocaryotic transformants determined by PCR were then verified by Southern Blot analysis, utilizing the PCR DIG Probe Synthesis Kit, DIG Easy Hyb, and DIG Luminescent Detection Kit (Roche, Germany). Genomic DNA from the wild type and mutant strains were digested with *Spe*I and with *Sna*BI in two different experiments. The *Spe*I-digested genomic DNAs were hybridized with a 818 bp long hygromycin specific probe (prepared using the Hyg-Probe-For and Hyg-Probe-Rev primers) and the *Sna*BI -digested samples were hybridized with a 1167 bp long 5' flanking region specific probe (prepared using the Snf1-5'-For and Snf1-5'-Rev primers). Membranes were exposed to and X-ray film for 18 h. s*nf1* deletion mutants without additional ectopic insertion of the hygromycin cassette were selected for phenotypic characterization.

2.2.2.4 Complementation of the Δsnf1.1 strain

Genomic DNA from *B. cinerea* wild type was extracted with DNeasy Mini Plant Kit and used as template to amplify the *snf1* gene together with 1 Kb of promoter and 1 Kb of terminator region using the Snf1-comp-For and Snf1-Comp-Rev primers. The nourseothricin resistance gene was amplified from pONT-clone 16 vector with the Nourseo For and Noureo Rev primers. The PCRs were performed using iProof ^{TM} High-Fidelity DNA Polymerase

(BIO-RAD, USA) following the manufacturer's indications. Fragments of the expected sizes (Table 2.3) were purified from agarose gel using GFX PCR and Gel Band Purification Kit.

Δsnf1.1 mutant was grown on cellophane for 2 days at 21 ^{o}C. Mycelium was harvested and grinded, and then grown in 100 ml NY medium for 24 h at 21 ^{o}C at 110 rpm. Mycelium was filtered and digested to obtain protoplasts as described above. The *snf1* gene and nourseothricin resistance cassettes were transferred into the Δ*snf1.1* genome by co-transformation following the protocol reported above (Figure 2.4B). Transformants were selected on MMII medium containing 100 µg ml^{-1} nourseothricin and insertion of the *snf1* gene was verified by PCR with the Snf1-WT-For and Snf1-WT-Rev, the Snf1-5'-For and Snf1-WT-Rev, and the Snf1-WT-For and Snf1-3'-Rev primers (Table 2.3).

Table 2.3 – Primer used to create the cassettes for transformation and complementation

Name	Sequence	Annealing temperature (°C)	Purpose	Product size (bp)
Snf1-5'-For	5' TAGTACCTGGCGCTTCTGTG 3'	66	primers to amplify the s*nf1* 5' flanking region	1182
Snf1-5'-Rev	5' CCGGCCCGAATCGGGAATGTGGTTGAACGGTGGTT 3'			
Snf1-3'-For	5' CGTCCGAGGGCAAAGGAATAGGTTCGTTGGTTATTGAATCG 3'	65	primers to amplify the s*nf1* 3' flanking region	859
Snf1-3'-Rev	5' CAACCAAAGAATGAAGTTCTCAC 3'			
Hyg-For	5' TTCCCGATTCGGGCCGG 3'	60	primers to amplify the hygromycin resistance gene	1848
Hyg-Rev	5' CTATTCCTTTGCCCTCGGAC 3'			
Snf1-5'-For	5' TAGTACCTGGCGCTTCTGTG 3'	66	nested primers for the 5' flanking region-hygromycin cassette	2750
Hyg-Nest-Rev	5' GGATGCCTCCGCTCGAAGTA 3'			
Hyg-Nest-For	5' CAG CGA GAG CCT GAC CTA TTG 3'	65	nested primers for the 3' flanking region-hygromycin cassette	1617
Snf1-3'-Rev	5' CAACCAAAGAATGAAGTTCTCAC 3'			
Snf1-M-5'-For	5' GCGTGGGATCGAGTTATTGC 3'	64	primers to amplify the 5' flanking region of mutants	1719
Snf1-M-5'-Rev	3' GCCCTGACTACCTTGCTACGG 5'			
Snf1-M-3'-For	5' CAATGTCCTGACGGACAATG 3'	61	primers to amplify the 3' flanking region of mutants	1438
Snf1-M-3'-Rev	5' GATTCGGATTTCTTTTGATGAGG 3'			
Snf1-WT-For	5' GCATTTCAGCCTCGACCTAGC 3'	64	primers to amplify the s*nf1* gene	643
Snf1-WT-Rev	5' CCCATGGATCTTCTGGCAAC 3'			
Hyg-Probe-For	5' CAAGCTGCATCATCGAAATTGC 3'	55	primers used for the Hyg probe in the Southern blot	818
Hyg-Probe-Rev	5' ATCGAAAAGTCCGACAGCGTC 3'			
Snf1-Comp-For	5' CCATGATGCTAGGGGAGG 3'	68	primers to amplify the s*nf1* gene for complementation	4408
Snf1-Comp-Rev	5' GATGATATTGGCGACCCG 3'			
Nourseo-For	5' CGGTCGCCAATATCATCGAGCGGATTCCTCAGTCTC 3'	69	primers to amplify the nourseothricin resistance gene for complementation	2028
Nourseo-Rev	5' GAGTGAGCTGATACCGCTCG 3'			

2.2.3 Enzymatic assays

For enzymatic tests, the strains were first grown on potato dextrose agar (PDA) (Oxoid, CM0139) with cellophane on its surface. After three days, the cellophane with the mycelium was placed on a new Petri dish containing 10 ml liquid MM (described above), supplemented with 1 % (w/v) of PGA, xylan or cellulose and the pH was buffered to 5 and 7. The supernatant and the mycelium were collected after 4 dpi. The mycelium was lyophilized and weighted. (Figure 2.5A)

Polygalacturonase, xylanase and cellulase activities were determined by measuring the reducing end-groups with the 4-hydroxybenzoic acid hydrazide (PAHBAH) method (adapted from Lever, 1972) (Figure 2.5B). Enzymatic reaction was performed mixing 100 µl culture supernatant with 100 µl 2.5 % (w/v) of substrate (PGA, xylan or cellulose) dissolved in citrate/phosphate buffer at pH 5 or pH 7 and adjusting the volume to 400 µl with citrate/phosphate buffer. The mixtures were incubated at 37 ^{o}C for 0, 15, 30, 45, 60, 75 and 90 min, and the reactions were stopped at 95 ^{o}C (to denature enzymes). 200 µl aliquot of a reaction mixture was added to 1800 µl 0.5 % (w/v) of PAHBAH in 500 mM of NaOH and the mixture was incubated at 95 ^{o}C for 10 min. Activity was expressed as µg of reducing sugar/min/mg mycelium dry weight using GA, xylose or glucose as standard. For each substrate, three biological replicates of the wild type and Δ*snf1.1* mutant, and one of the complemented strains were prepared.

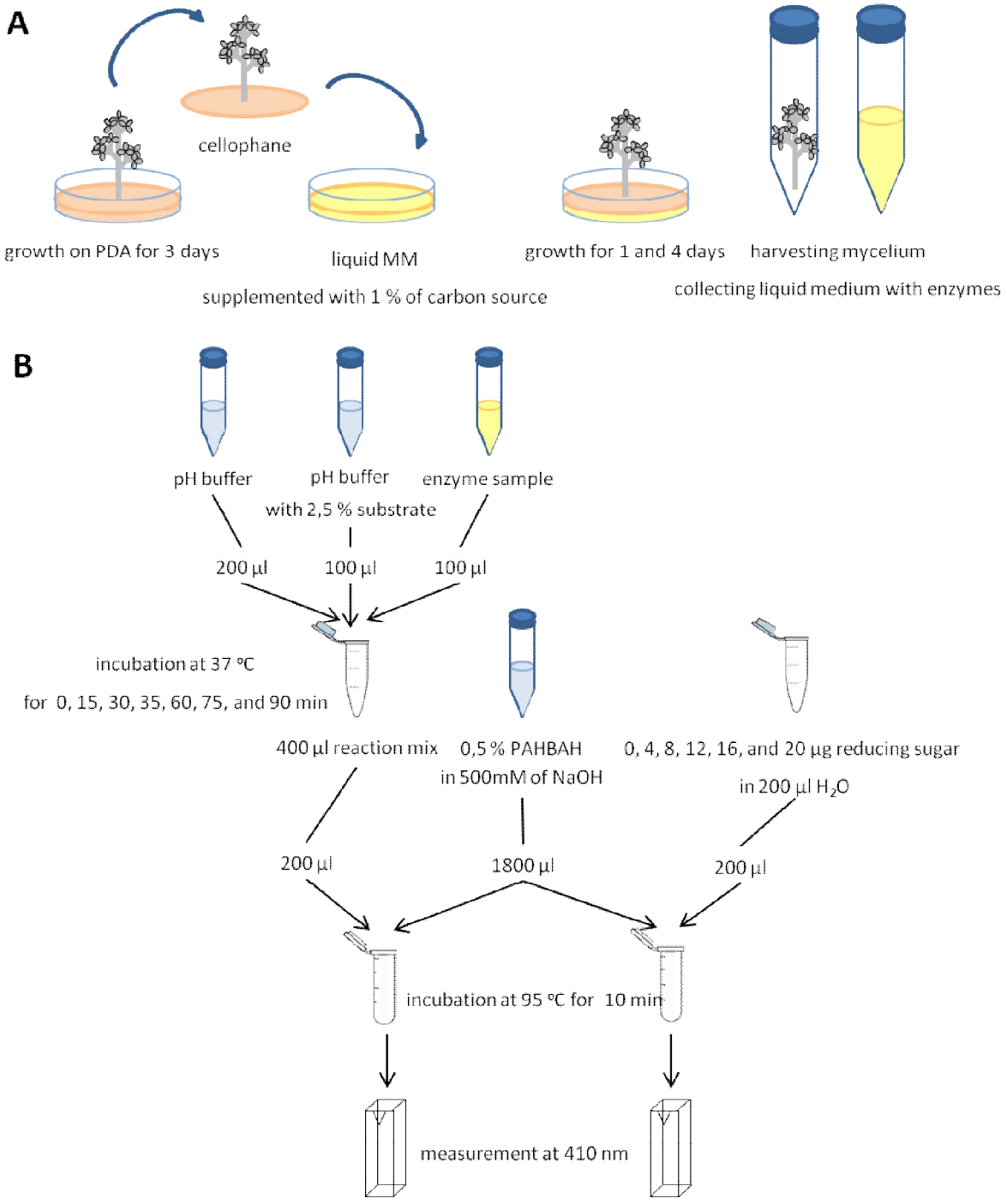

Figure 2.5 – Schematic illustration of the sample preparation (**A**) and the protocol for enzymatic assays (**B**).

2.2.4 Monitoring pH alteration *in vitro*

Mycelia of the wild type and the mutant strains were grown on sporulation malt medium (5 g L^{-1} glucose, 20 g L^{-1} malt extract, 1 g L^{-1} tryptone, 1 g L^{-1} casamino acids, 1 g L^{-1} yeast extract, 0.2 g L^{-1} ribonucleic acid sodium salt, and 15 g L^{-1} agar-agar) at 21 ^{o}C in dark. After four days of incubation, from one culture plate the medium with the mycelium was cut to small pieces and transferred into 30 µl of liquid sporulation malt medium and it was incubated at 21 ^{o}C at 110 rpm for 44 h. The mycelium was collected by centrifugation at 20 ^{o}C at 3500 rpm for 5 min and rinsed with 35 sterile ml H_2O two times. The obtained mycelium was then grown in 30 ml of non-buffered Gamborg medium (Gamborg *et al*., 1968) adjusted to pH 6, which was autoclaved with 6 days old gherkin cotyledons to mimic plant environment. Culture was incubated at 21 ^{o}C at 110 rpm and pH changes were measured at 1, 2, and 3 dpi.

2.2.5 Infection of various plant tissues

Apple fruits (cv. Golden Delicious) - purchased at a local market - were wounded superficially with a blade and mycelium plugs of 7 mm of diameter were placed above the wounds. The inoculation of French bean (cv. Saxa) was carried out by placing a 3 mm diameter plug in a drop of water on the surface of detached leaves of 7 days old plants. The inoculation of gherkin (cv. Petit vert de Paris) was performed on detached cotyledons of 6 days old plants. Inoculated leaves and cotyledons on moist filter paper in plastic boxes were put into a climate chamber with 16/8 h light/dark cycle at 21 ^{o}C and 70 – 75 % relative humidity. At 4 dpi, the fruits and leaves were photographed and the lesion areas were measured using ImageJ program (Schneider *et al*., 2012).

The pH of the lesion of the bean leaves was measured to 4 dpi with a flat contact electrode (Bioblock Scientific, Illkirch, France) (Billon-Grand *et al*., 2012). Mycelium on the leaf surface was coloured with lactic blue cotton solution and photos of the lesions were taken with SteREO Discovery.V20 microscope (Zeiss, Germany).

2.3 Results

2.3.1 Targeted deletion of the *Snf1* gene

To study the role of *B. cinerea* Snf1 protein kinase, the ORF of the encoding gene was replaced with a deletion cassette containing the hygromycin resistance gene. Hygromycin resistant transformants were first checked by PCR for the presence of the hygromycin resistance gene and for the absence of the *snf1* gene (Figure 2.6A, B, C, D); four transformants were then analysed by Southern blot and the deletion of the *snf1* gene was confirmed in two of them. In fact, *Spe*I-digested genomic DNAs hybridized with a hygromycin specific probe showed the expected band of 6.35 Kb in the mutant strains (Figure 2.6A, B); besides, *Sna*BI-digested genomic DNAs hybridized with a 5' flanking region specific probe showed the expected band of 5.57 Kb for the wild type while the mutants showed a band of 11.3 Kb, indicating insertion of the hygromycin cassette and corresponding replacement of the *snf1* gene (Figure 2.6A, C). An undetermined band of 4.90 Kb was noticed in the Δ*snf1.4* mutant (Figure 2.6C).

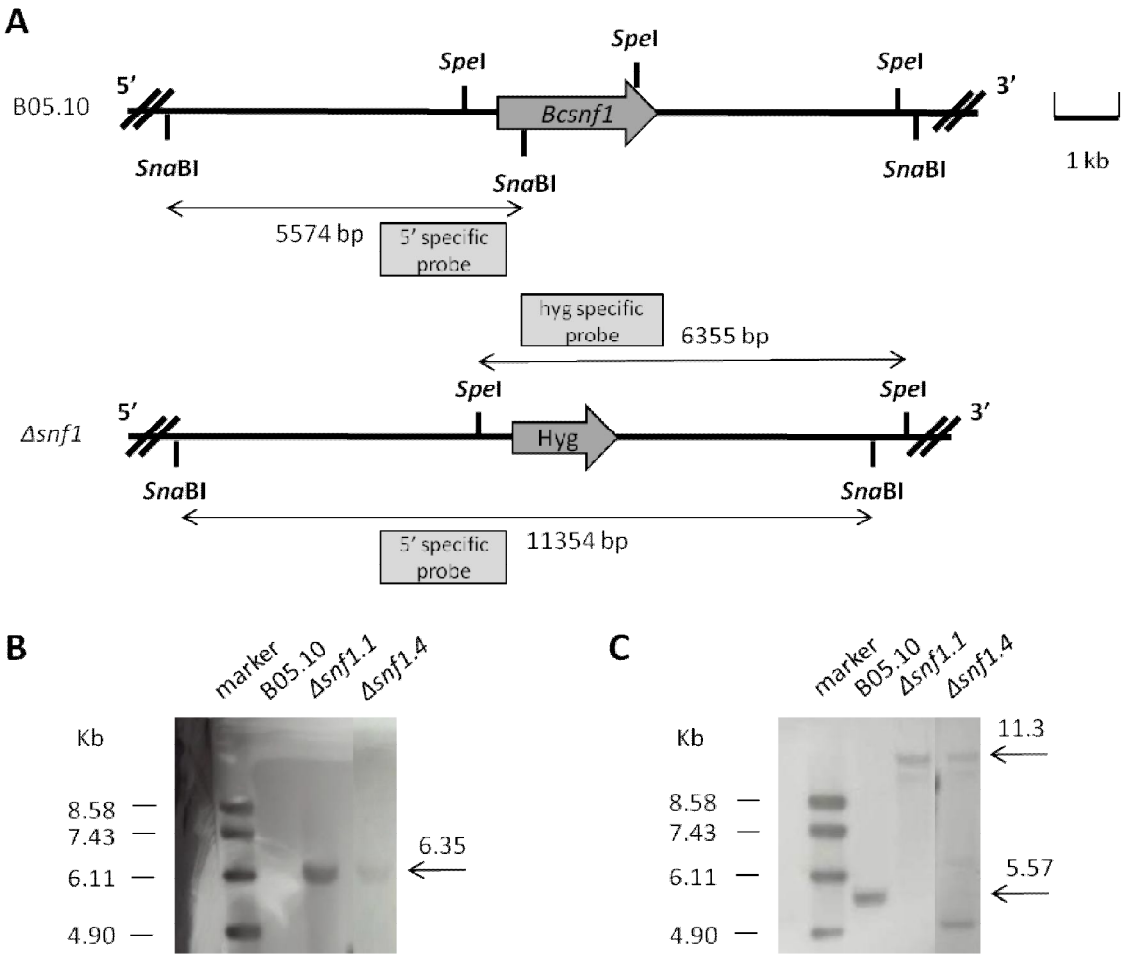

Figure 2.6 - Construction and verification of *B. cinerea* Δ*snf1* deletion mutants. (**A**) Illustration of the wild type B05.10 and mutant allele with indication of the restriction sites used in the Southern blot analysis and sizes of the probes used. (**B**) To verify the gene replacement, genomic DNA from the wild type and the mutant strains was digested with *Spe*I and hybridized with a hygromycin specific probe. Mutants show a 6.35 Kb band corresponding to the insertion of the hygromycin resistance gene. (**C**) The *Sna*BI -digested genomic DNAs were hybridized to a 5' flanking region specific probe. Wild type - as control - shows a 5.57 Kb band, while the mutant strains show a 11.3 Kb band confirming the homologous integration of the hygromycin gene at the 5' flanking region of the *snf1* gene. Δ*snf1.4* mutant shows also an undetermined band of 4.90 Kb.

2.3.2 Complementation of the Δ*snf1* mutant

In order to complement the Δ*snf1.1* mutant strain, co-transformation of the entire *snf1* gene containing 1 Kb of the promoter and 1 Kb of the terminator regions, with the nourseothricin resistance gene was performed. Mutants able to grow on medium containing nourseothricin, thus containing at least an ectopic insertion of the nourseothricin resistance

gene, were selected. The *snf1* gene replaced the hygromycin resistance gene by homologous recombination in the Δ*snf1.1-C* strain, as confirmed by PCR (Figure 2.7A, C, D).

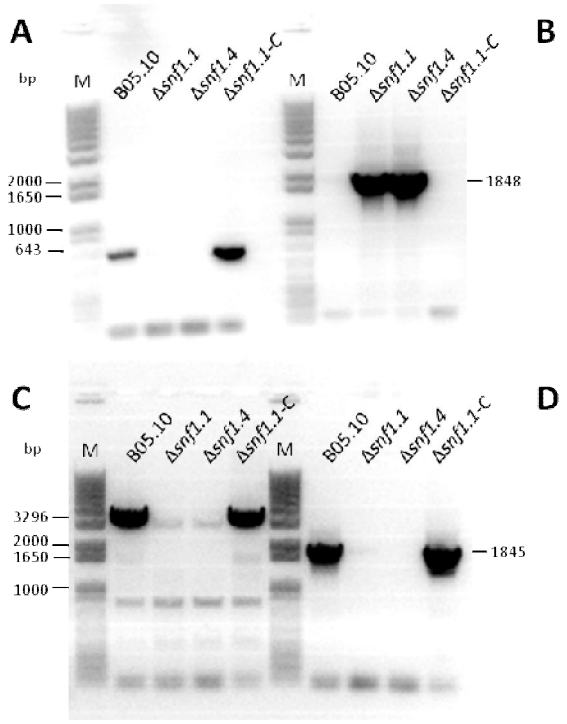

Figure 2.7 – Agarose gel electrophoresis profile of PCRs verifing the *B. cinerea* Δ*snf1* mutants and the Δ*snf1.1-C* complemented strain. (**A**) Amplification of the *snf1* gene with the Snf1-WT-For and Snf1-WT-Rev primers (643 bp). (**B**) Amplification of the hygromycin resistance gene with the Hyg-For and Hyg-Rev primers (1848 bp). (**C**-**D**) PCRs performed to confirm the proper integration of the *snf1* ORF in the complemented strain at the original *snf1* locus. (**C**) Amplification of the 5' flanking region with the Snf1-5'-For and Snf1-WT-Rev primers (3296 bp). Aspecific bands were amplified too. (**D**) Amplification of the 3' flanking region with the Snf1-WT-For and Snf1-3'-Rev primers (1845 bp).

2.3.3 Radial growth of Δ*snf1* mutants on various carbon sources

The growth of the Δ*snf1* mutants was compared with that of the wild type strain after 4 days from inoculation of plates containing 1 % (w/v) simple sugars (glucose, xylose, sucrose, and GA), or polysaccharides (PGA, xylan, cellulose) or other non-fermentable carbons (tween 80, olive oil, triolein, and NaAc). The experiments were performed at pH 5 and pH 7. At both pHs, the mutants showed reductions of colony diameter on all carbon sources (about 20-70 %), however the difference between the mutants and the wild type was not significant on 1 %

and 5 % glucose and on GA at pH 5, according to Student's t-test ($p<0.05$) (Figure 2.8). At pH 7, the growth of the mutants was much more affected on all carbon sources but the wild type strain also grew slower than at pH 5 (Figure 2.9). Interestingly, the greatest reduction at pH 5 was measured on tween 80 (about 40 %) (Figure 2.10) and at pH 7 on olive oil, triolein and NaAc (about 80 %) (Figure 2.11).

The complemented strain was tested for growth on non-fermentable carbon sources (tween 80, olive oil, triolein, and NaAc). The ability to utilize these carbon sources seem partially restored by 50-70 % at pH 7 (Figure S2.2), but not at pH 5 (Figure S2.1).

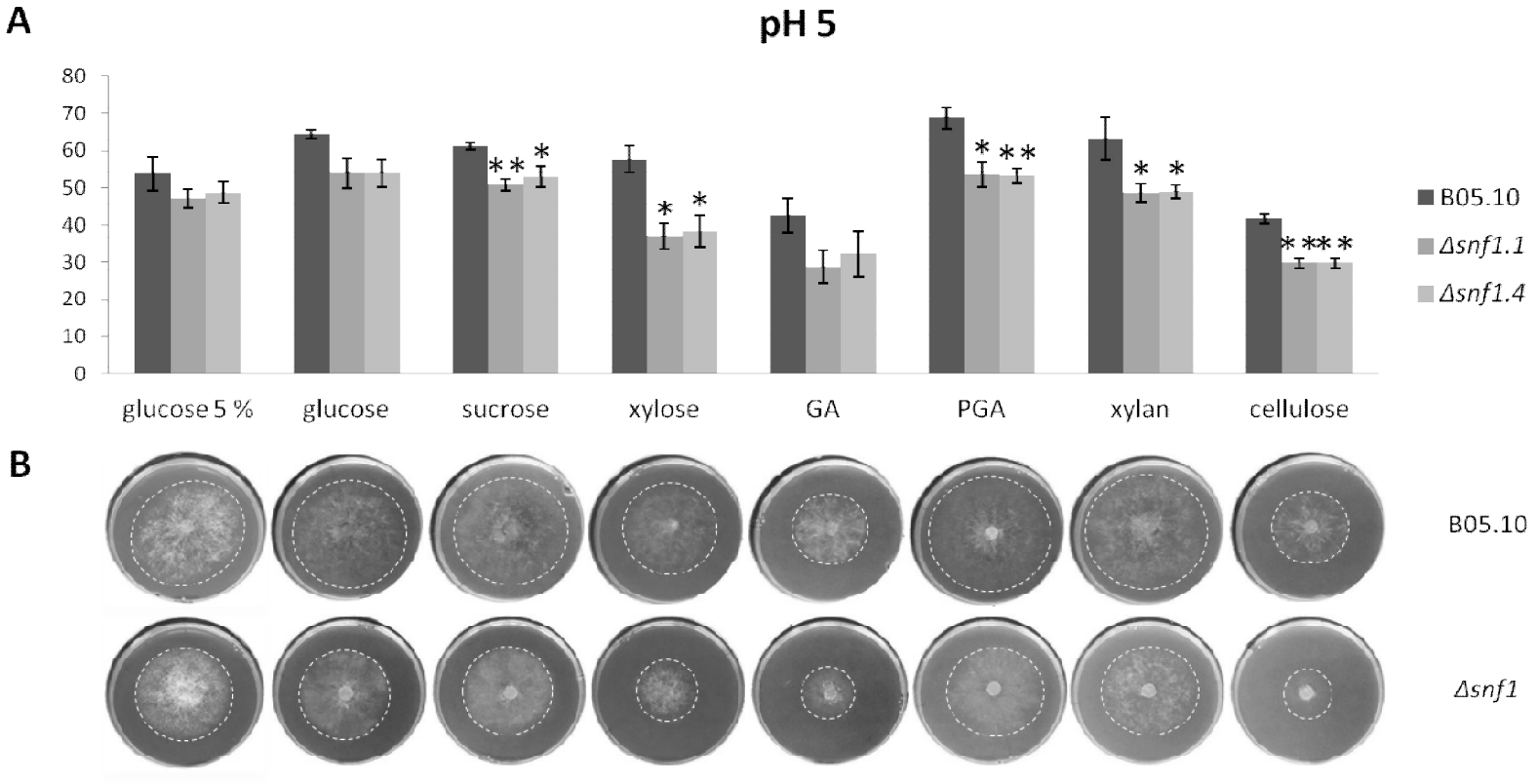

Figure 2.8 - Growth of the *B. cinerea* wild type B05.10 and the Δ*snf1* mutants on simple sugars and polysaccharides at pH 5. (**A**) Growth of 4-day-old mycelium was measured (excluding 7 mm, the diameter of the mycelium plug). Bars indicate the standard error calculated from three independent experiments. (6 growth diameter measurements of each strain per experiment were done.) Asterisks mean significant difference of growth between the wild type and the mutant strains according to Student's *t*-test (*, p<0.05; **, p<0.01). (**B**) Photos of plates were taken at 4 dpi.

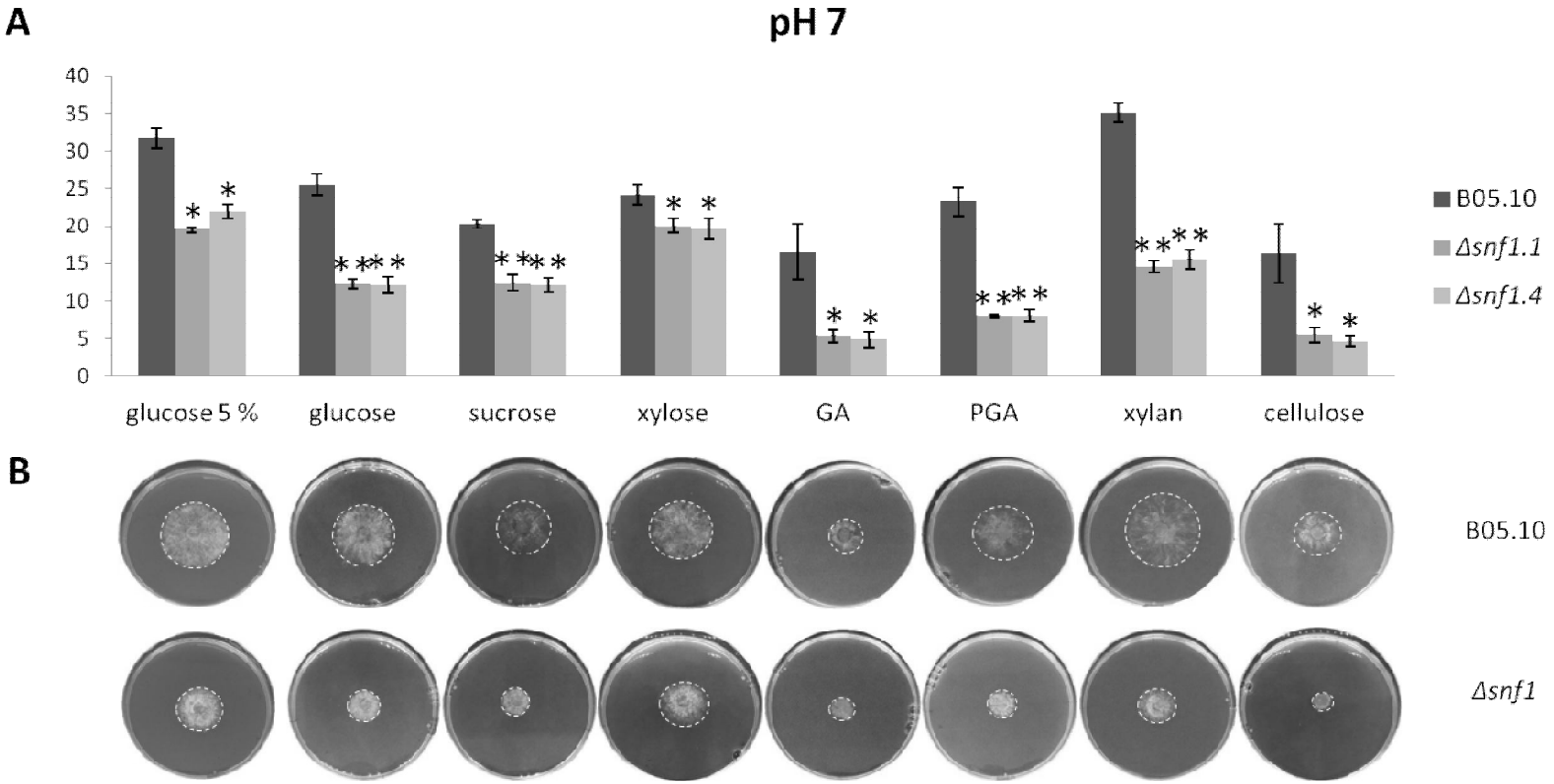

Figure 2.9 - Growth of the *B. cinerea* wild type B05.10 and the Δ*snf1* mutants on simple sugars and polysaccharides at pH 7. (**A**) Growth of 4-day-old mycelium was measured (excluding 7 mm, the diameter of the mycelium plug). Bars indicate the standard error calculated from three independent experiments. (6 growth diameter measurements of each strain per experiment were done.) Asterisks mean significant difference of growth between the wild type and the mutant strains according to Student's *t*-test (*, $p<0.05$; **, $p<0.01$). (**B**) Photos of plates were taken at 4 dpi.

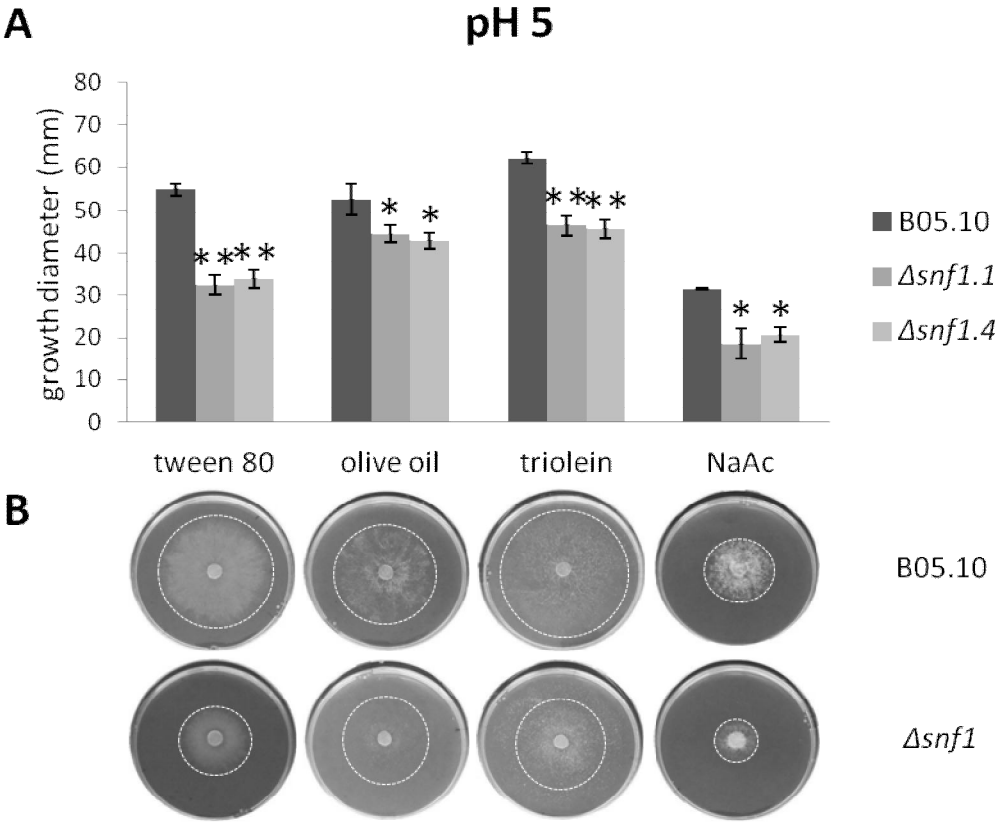

Figure 2.10 - Growth of the *B. cinerea* wild type B05.10 and the Δ*snf1* mutants on lipidic non-fermentable carbon sources at pH 5. (**A**) Growth of 4-day-old mycelium was measured (excluding 7 mm, the diameter of the mycelium plug). Bars indicate the standard error calculated from three independent experiments. (6 growth diameter measurements of each strain per experiment were done.) Asterisks mean significant difference of growth between the wild type and the mutant strains according to Student's *t*-test (*, $p<0.05$; **, $p<0.01$). (**B**) Photos of plates were taken at 4 dpi.

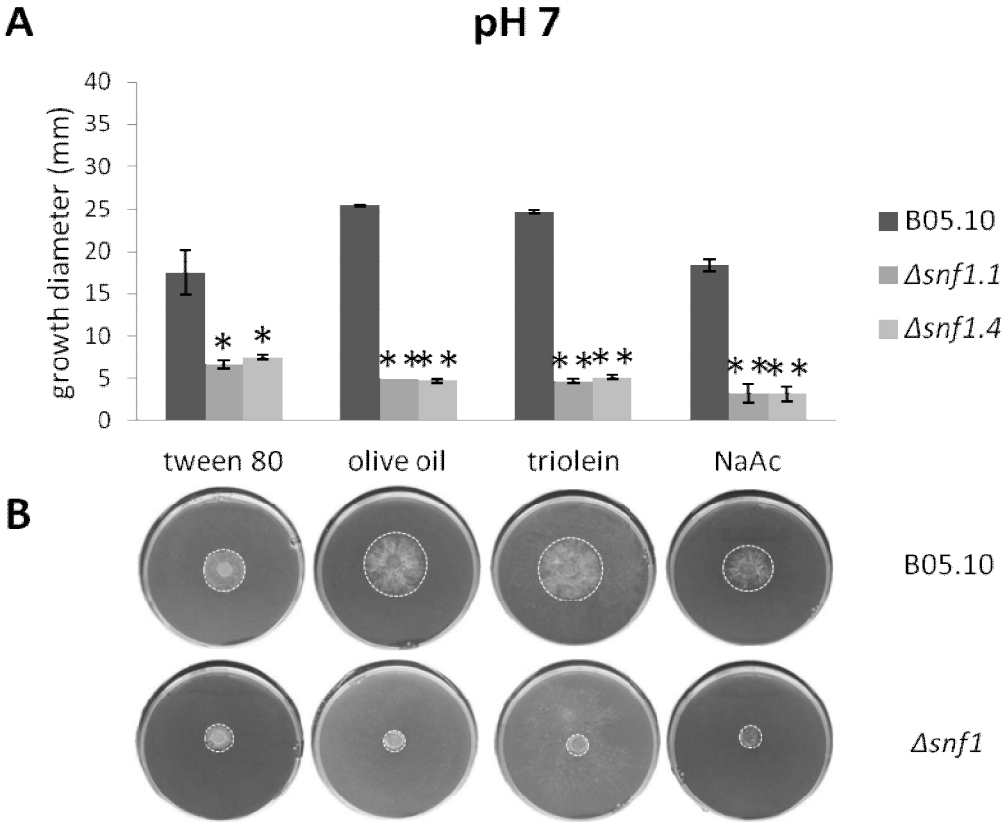

Figure 2.11 - Growth of the *B. cinerea* wild type B05.10 and the Δ*snf1* mutants on lipidic non-fermentable carbon sources at pH 7. (**A**) Growth of 4-day-old mycelium was measured (excluding 7 mm, the diameter of the mycelium plug). Bars indicate the standard error calculated from three independent experiments. (6 growth diameter measurements of each strain per experiment were done.) Asterisks mean significant difference of growth between the wild type and the mutant strains according to Student's *t*-test (*, p<0.05; **, p<0.01). (**B**) Photos of plates were taken at 4 dpi.

2.3.4 Determination of enzymatic activity

The enzymatic, activity produced by the wild type and the *Δsnf1.1* mutant at 4 dpi, was determined at pH 5 and pH 7 by 4-hydroxybenzoic acid hydrazide (PAHBAH) method. While at pH 5 the xylanase activity of the Δ*snf1.1* mutant was significantly lower than that of the wild type strain (Figure 2.12), surprisingly this mutant produced a higher PG activity (Figure 2.13). At pH 7, both enzyme activities decreased drastically, and only the xylanase activity - produced by the wild type - was still detectable. No significant difference among the wild type and the mutant strain was observed in cellulase secretion, which was very low at both pHs.

The complemented strain, tested in a preliminary experiment, showed a restored xylanase activity (Figure S2.3), but was still producing PG activity higher than the wild type and comparable to that of the mutant (Figure S2.4).

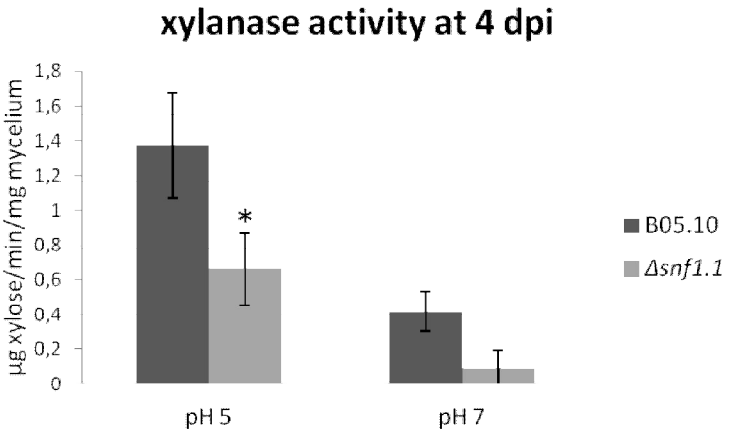

Figure 2.12 – Xylanase activity of *B. cinerea* wild type B05.10 and Δ*snf1.1* mutant strains grown on 1 % (w/v) xylan for 4 days. The xylanase activity was determined at pH 5 and pH 7. Bars indicate the standard deviation calculated from three independent experiments. At pH 5, the difference of enzyme activity between the wild type and the mutant strain was significant according to Student's *t*-test (*, p<0.05).

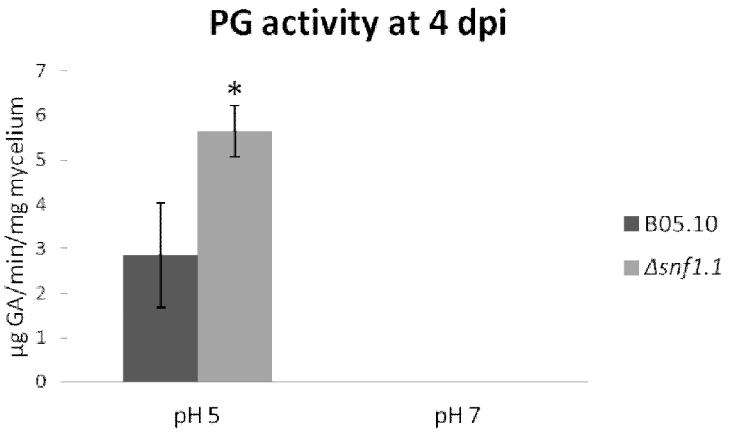

Figure 2.13 – Polygalacturonase (PG) activity of *B. cinerea* wild type B05.10 and Δ*snf1.1* mutant strains grown on 1 % (w/v) PGA for 4 days. The PG activity was determined at pH 5 but was undetectable at pH 7. Bars indicate the standard deviation calculated from three independent experiments. At pH 5, the difference of enzyme activity between the wild type and the mutant strain was significant according to Student's *t*-test (*, p<0.05).

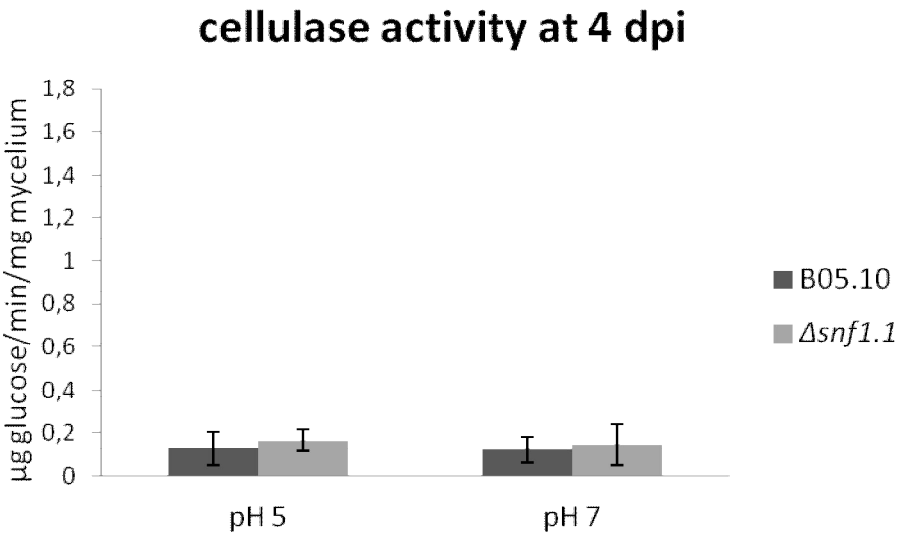

Figure 2.14 - Cellulase activity of *B. cinerea* wild type B05.10 and Δ*snf1.1* mutant strains grown on 1 % (w/v) cellulose for 4 days. No significant difference between the wild type and the mutants strain was observed.

2.3.5 Virulence of *Δsnf1* mutants on different plant tissues

To define the role of *B. cinerea snf1* gene in pathogenicity, apple fruits, French bean leaves, and gherkin cotyledons were inoculated with mycelium plugs of the wild type and *Δsnf1* mutant strains. It was not possible to inoculate plants with macroconidia because asexual sporulation is strongly impaired in Δ*snf1* mutants. Surface lesions were measured daily up to 4 dpi. At 4 dpi, on apple fruits, the mutant strains showed a 60 % reduction of the lesion size (Figure 2.15) and the weight of the rotten tissue was 70 % less in comparison to the wild type (data not shown). On French bean leaves, the lesion area produced by the mutant strains was 80 % lower than that of the wild type at 4 dpi (Figure 2.16). Lesions caused by the mutant strains were even more reduced on gherkin cotyledons, and only a small infected tissue was visible just around the mycelium plugs (Figure 2.18).

One biological replicate was done with the complemented strain infecting bean leaves or gherkin cotyledons, and it showed a partial restoration of virulence (about 25 % on bean leaves and about 40 % on gherkin cotyledons). (Figure S2.5 and Figure S2.6).

Infection cushions were observed for both wild type and Δ*snf1* mutant at 1, 2, 3 and 4 dpi (Figure 2.17).

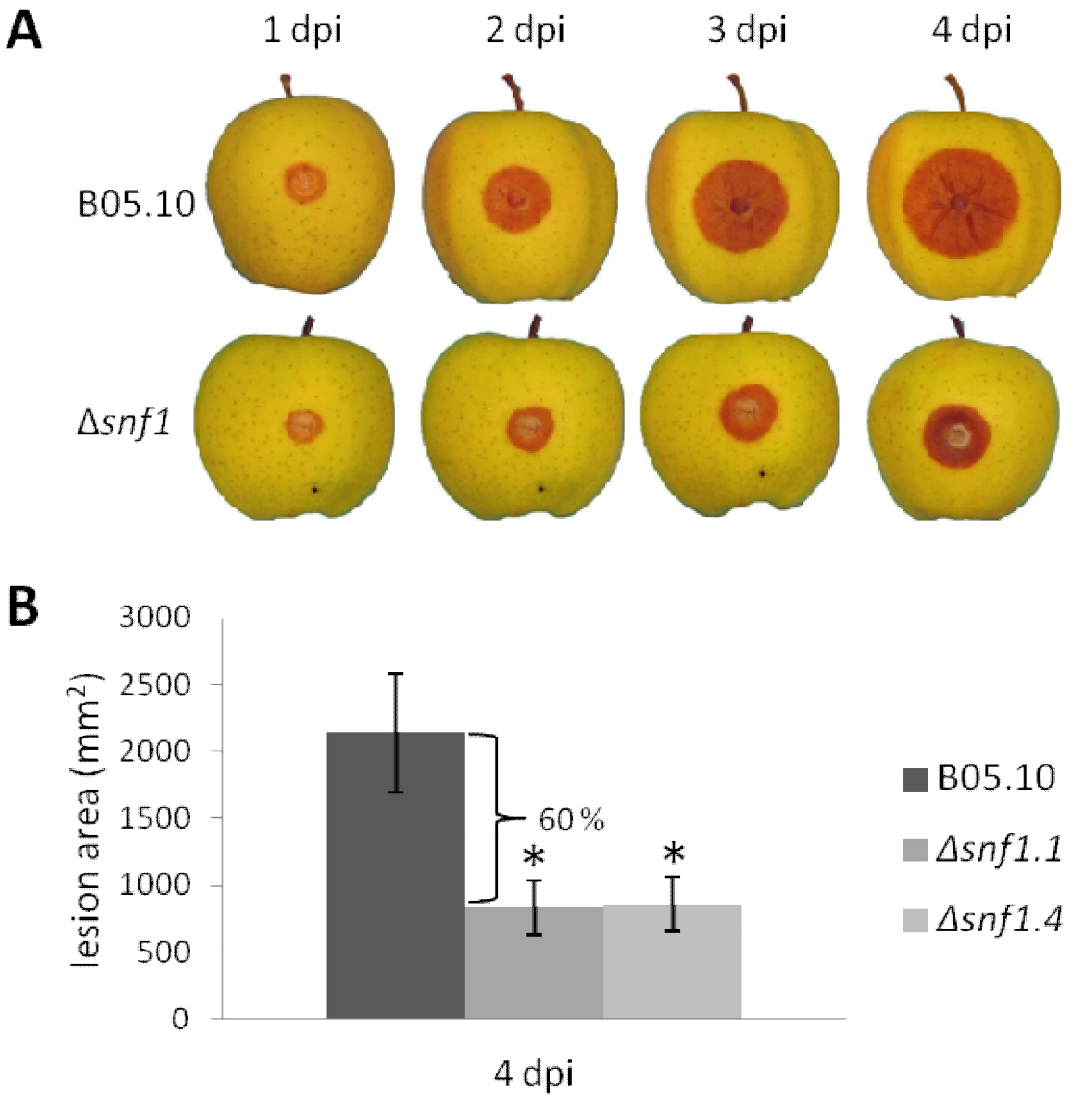

Figure 2.15 - Virulence of *B. cinerea* wild type B05.10 and *Δsnf1* mutants at 1, 2, 3, and 4 dpi on wounded apple fruits (cv. Golden Delicious) inoculated with 7 mm of diameter plugs containing actively growing mycelium. (**A**) Representative samples of infected apple fruits. (**B**) Histogram showing the measurement of the lesions area at 4 dpi. Bars indicate the standard error calculated from three independent experiments each performed by infecting 10 fruits for each strain. Asterisks mean significant difference between the mutants and the wild type, according to Student's *t*-test (*, $p<0.05$).

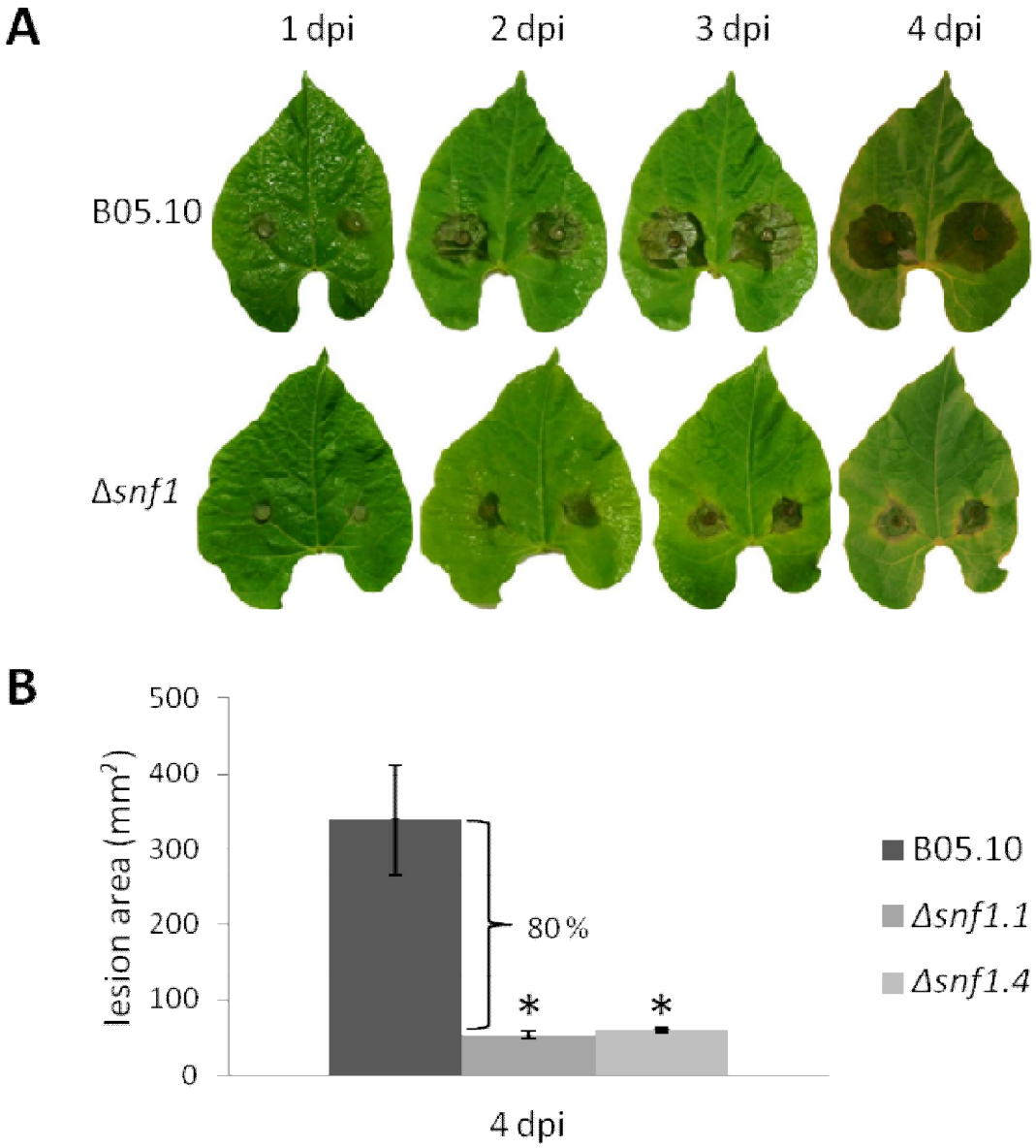

Figure 2.16 - Virulence of *B. cinerea* wild type B05.10 and *Δsnf1* mutants at 1, 2, 3, and 4 dpi on French bean leaves (cv. Saxa) inoculated with 3 mm of diameter plugs containing actively growing mycelium. (**A**) Representative samples of infected bean leaves. (**B**) Histogram showing the measurement of the lesions area at 4 dpi. Bars indicate the standard error calculated from three independent experiments each performed by infecting 14 leaves (two inoculation points per leaf) for each strain. Asterisks mean significant difference between the mutants and the wild type, according to Student's *t*-test (*, $p<0.05$).

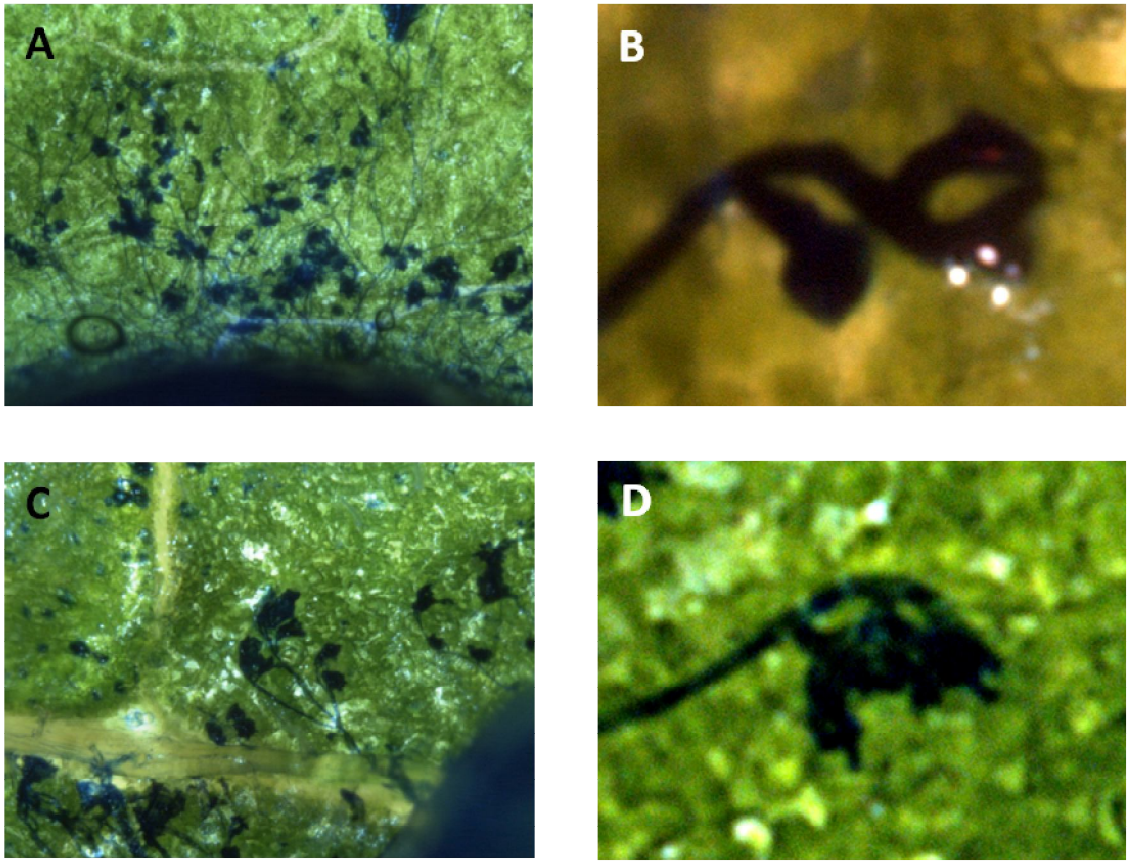

Figure 2.17 – Infection of *B. cinerea* wild type B0.510 and *Δsnf1.1* mutant on French bean leaf. Mycelium on the leaf surface was coloured with lactic blue cotton solution and photos were taken with stereo microscope at 2 dpi. (**A**) Mycelium and infection cushions of the wild type strain growing from the plug. (**B**) Enlarged infection cushion of the wild type. (**C**) Mycelium and infection cushions of the Δ*snf1.1* mutant growing from the plug. (**B**) Enlarged infection cushion of the Δ*snf1.1* mutant.

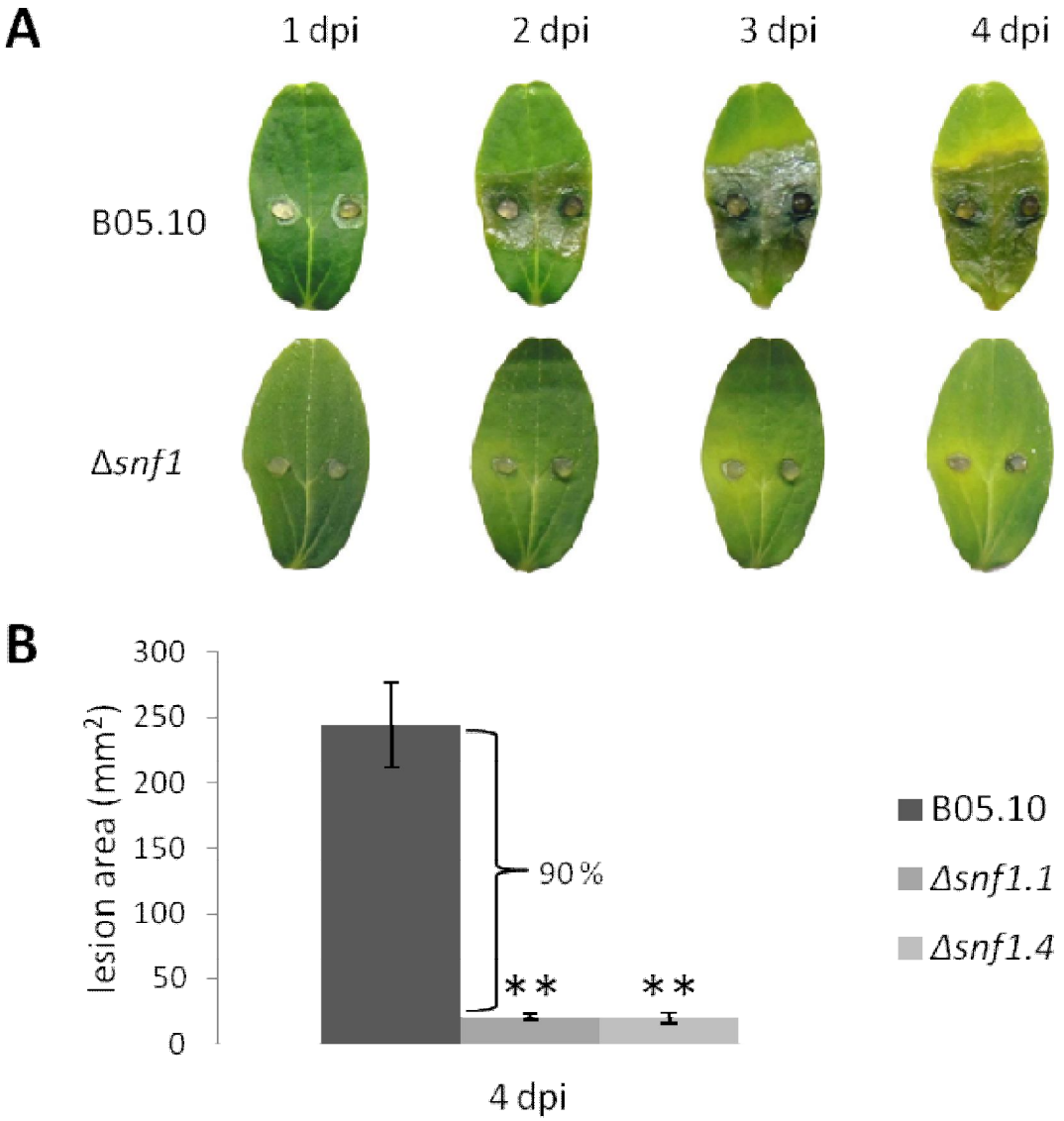

Figure 2.18 - Virulence of *B. cinerea* wild type B05.10 and *Δsnf1* mutants at 1, 2, 3, and 4 dpi on gherkin cotyledons (cv. Petit vert de Paris) inoculated with 3 mm of diameter plugs containing actively growing mycelium. (**A**) Representative samples of infected gherkin cotyledons. (**B**) Histogram showing the measurement of the lesions area at 4 dpi. Bars indicate the standard error calculated from three independent experiments each performed by infecting 18 cotyledons (two inoculation points per cotyledon) for each strain. Asterisks mean significant difference between the mutants and the wild type, according to Student's *t*-test (*, $p<0.05$).

2.3.6 Monitoring pH modulation caused by the fungus

2.3.6.1 pH of liquid culture modulated by *B. cinerea*

To measure the pH changes during *B. cinerea* growth, mycelia of the wild type and the two mutant strains were grown in modified Gamborg medium adjusted at pH 6 (but not buffered) and the pH of the cultures was measured up to 3 dpi (Table 2.4). The Δ*snf1* mutants were able to initially acidify the medium and then to increase the pH to neutral values as well as the wild type. Nevertheless the mutants appeared to increase the pH of the medium to a higher value than the wild type did.

Table 2.4 – pH measurement of *in vitro* cultures

strain	1 dpi	2 dpi	3 dpi
B05.10	pH 4.95	pH 5.58	pH 6.78
Δ*snf1.1*	pH 4.85	pH 7.03	pH 7.53
Δ*snf1.4*	pH 4.64	pH 6.56	pH 7.39

2.3.6.2 pH of plant tissues infected by *B. cinerea*

To examine the pH changes during the infection process, detached French bean leaves and apple fruits were inoculated with mycelium plugs of *B. cinerea* wild type and Δ*snf1.1* mutant strain (Table 2.5). Although the Δ*snf1.1* mutant caused smaller lesions than the wild type at 4 dpi, there was no significant difference between the pHs of the plant tissues infected by wild type and mutant.

Table 2.5 – pH measurement of lesion at 4 dpi

	bean leaf	apple fruit
healthy tissue	pH 6.8	pH 3.9
B05.10	pH 6.5	pH 3.4
Δ*snf1.1*	pH 6.4	pH 3.3

2.3.7 Conidiation

The *B. cinerea* Δ*snf1* mutants did not show normal conidiophores and macroconidia. In fact, only microconidia and occasionally very few macroconidia could be observed. Complementation restored the conidiophore and conidia formation.

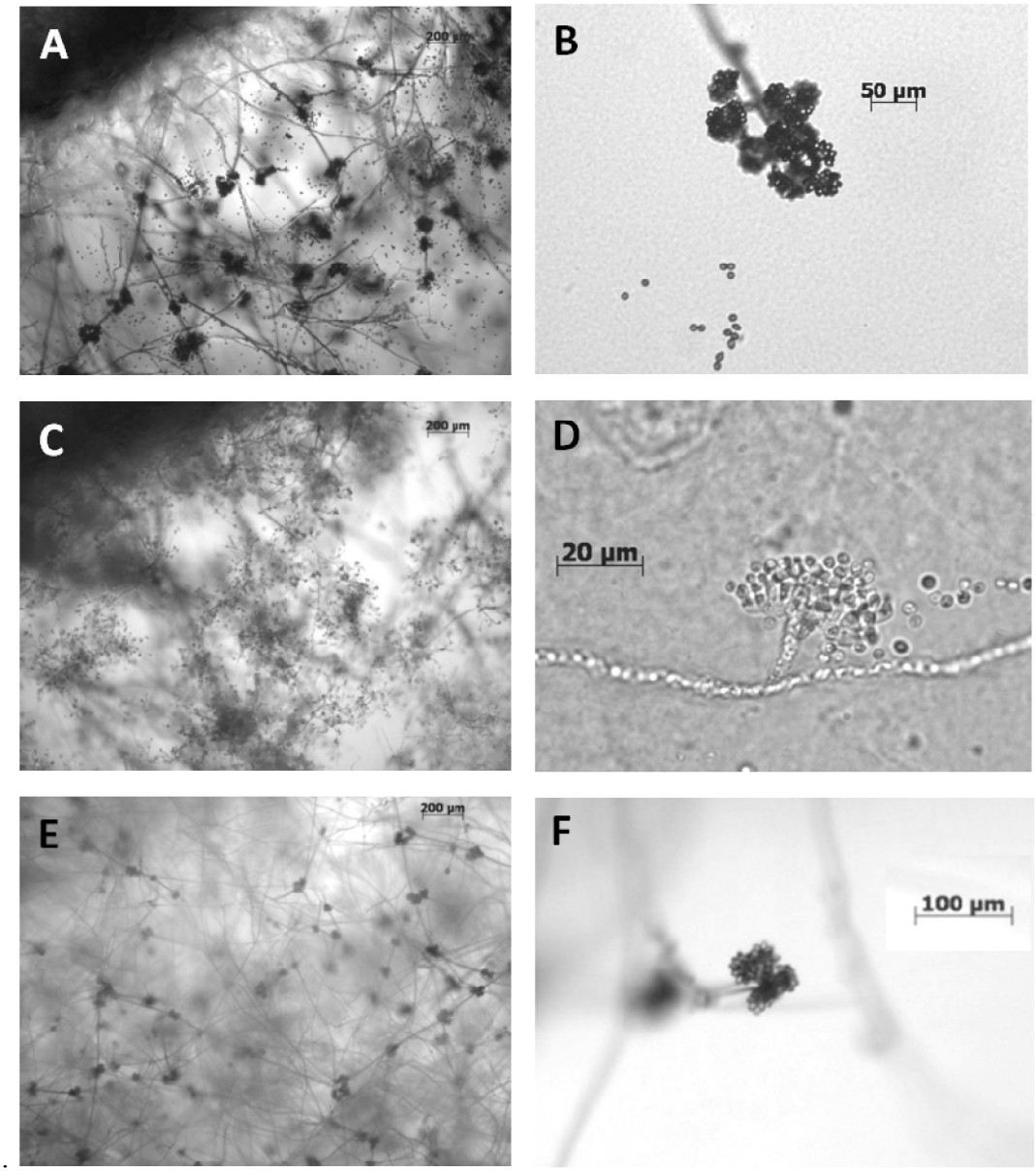

Figure 2.19 – Difference in conidiation between the wild type, Δ*snf1* mutant and complemented strain. (**A**) Wild type producing normal conidiophores with macroconidia. (**B**) Enlarged conidiophores of the wild type. (**C**) The mutant without conidiphores and macroconidia; only microspores are visible. (**D**) Enlarged microconidia. (**E**) The complemented strain is restored in macroconidia formation. (**F**) Enlarged conidiphore with macroconidia of the complemented strain.

2.4 Discussion

Signalling cascades mediate the morphogenesis, differentiation, sexual development, as well as the communication between pathogens and plants during infection (Tudzynski and Gronover, 2007, Williamson *et al*., 2007). In yeast, the Snf1 protein kinase plays an important role in a glucose signalling pathway controlling the response to nutritional and environmental stresses by regulating approximately 400 genes (Young *et al*., 2003). At high glucose concentration, s*nf1* gene is repressed; when this preferable carbon source is scarce or absent, this gene is expressed and releases the transcription factor Mig1 [*creA* in filamentous fungi (Ronne, 1995)], a repressor of several CWDE encoding genes (Tonukari *et al*., 2003). Snf1 activates other transcription factors too, e.g. Cat8, Adr1, and Sip4, which regulate genes involved in peroxisome biosynthesis, gluconeogenesis, glyoxylate cycle and β-oxidation (Zeng *et al*., 2014). Although the *snf1* gene is highly conserved in filamentous fungi (Hedbacker and Carlson, 2008), phenotypical analyses of Δ*snf1* mutants of various species showed some differences (Table 2.6).

In order to characterize the role of *B. cinerea* Snf1 kinase, deletion mutants of the encoding gene were obtained and analyzed *in vitro* and *in vivo*.

The growth of two independent mutants was tested *in vitro* on simple sugars and polysaccharides from plant cell wall and on other non-fermentable carbons at pH 5 and 7. The choice of these pH values is justified by the need to mimic *in vitro* the pH conditions of two typical *B. cinerea* host tissues, leaves and fruits, respectively. In addition, in the closely related fungus *S. sclerotiorum*, it was observed that pH can affect the expression of *creA* which is a target of Snf1 (Vautard-Mey and Fèvre, 2003).

In general, the growth of wild type and Δ*snf1* mutants was higher on all carbon sources at pH 5, but in comparison with the wild type, the growth of mutants was much less affected at pH 5 than at pH 7. At pH 5 no significant difference of growth between the mutants and the wild type was observed on glucose and GA and this result is in agreement to the fact that *snf1* gene in the wild type is repressed in the presence of glucose. On sucrose and xylose the growth of mutants was significantly lower than that of the wild type. These results could be owed to a reduced ability to uptake these simple sugars in Δ*snf1* mutants, probably through defects in sugar transporters. This phenomenon seems to be exacerbated at pH 7 where the growth of the Δ*snf1* mutants was significantly reduced on all simple sugars. A reduced uptake of simple sugars is in agreement with the demonstration that the

Saccharomyces cerevisiae Snf1 has been shown to mediate, at least in part, the activation of genes encoding high-affinity hexose transporters (Casamayor *et al*., 2012).

The decreased growth of mutants on PGA can not be explained easily, because at this pH the PG activity produced by the Δ*snf1.1* mutant was higher than that of the wild type. This observation is in contrast to what observed with other filamentous fungi (*C. carbonum, F. oxysporum,* and *M. oryzae*) where the *snf1* gene deletion resulted in a reduction of PG activity; however, the assay used for PG activity measurement did not discriminate between endo- and exo-activity. Then it is possible that the s*nf1* gene deletion can affect differentially the expression of the two types of PG genes, and a lack of exo-PG activity - which is responsible for the release of the GA simple sugar - can result in a reduced growth of the fungus also in presence of a high endo-PG activity. A similar explanation may be invoked for the reduced growth on carboxymethylcellulose where glucanase and cellobiohydrolase may be differentially expressed although no significant difference in cellulose activity between the wild type and the mutants was observed. More consistent are the results obtained with xylan where a decreased xylanase activity may be responsible for the reduced growth. The decreased xylanase activity seems to be common in Δ*snf1* fungal mutants. A lower xylanase activity was measured in *C. carbonum* Δ*snf1* mutant (Tonukary *et al*., 2000) and in mutants of *F. graminearum*, *V. dahliae* and *P. digitatum* a lower expression level of one or two genes was detected (Lee *et al*., 2009, Tzima *et al*., 2011, and Zhang *et al*., 2013); besides, three *M. oryzae* xylanase encoding genes showed down-, up- and stable expression in the Δ*snf1* mutant compared to the wild type (Yi *et al*., 2008). Taken together, the enzymatic activity results of *B. cinerea* seem to be partially in contrast with the putative role ascribed to Snf1 as general activator of CWDE expression.

Since *M. oryzae* Δ*snf1* mutants showed enlarged peroxisomes and inability to metabolize fatty acids and NaAc (Zheng *et al*., 2014), we tested the role of *B. cinerea snf1* gene also in lipid metabolism. With this aim, the wild type and the mutant strains were tested for growth on lipidic non-fermentable carbon sources: the *B. cinerea* Δ*snf1* mutants exhibited reduced growth rate on all fatty acids and on NaAc at both pHs compared to the wild type. In particular, the largest growth reduction (about 80 %) was observed at pH 7 on olive oil, triolein and NaAc.

On the whole, our results indicate not only the importance of *snf1* gene in uptake of simple sugars and in lipid metabolism, but also in a possible pH dependent regulation. In fact, the *B. cinerea* Δ*snf1* mutant is impaired in growth mostly at pH 7 on all the carbon sources

tested. This behaviour is similar to what was observed with *S. cerevisiae* where about 75 % of the genes induced by high pH were also induced when glucose was depleted. Therefore, the function of Snf1 protein kinase appears to be crucial not only in adaptation to glucose scarcity but also for alkaline pH tolerance (Casamayor *et al*., 2012).

Interestingly, the ability of utilization of other non-fermentable carbons was restored in the complemented strain only at pH 7, suggesting that the homologous recombination of the *snf1* ORF could have produced some mutations in its endogenous promoter with misregulation of pH regulation for Snf1. In fact, the 5'-GCCARG-3' sequence recognized by PacC transcription factor and involved in alkaline pH regulation is also present in the promoter region of the *B. cinerea snf1* gene.

The hypothesis that the homologous recombination could have determined some mutations in the promoter region leading to a partial misregulation of Snf1 is reinforced by the observation that the complemented strain showed only a partial restoration of xylanase activity and failed to restore PG activity to wild type levels.

Previously, pathogenicity tests demonstrated that the *snf1* gene is an important virulence factor in many plant pathogenic fungi; significant reduction in plant tissue colonization was observed with *C. carborum*, *F. oxysporum*, *M. grisae*, *F. graminearum*, *V. dahliae* and *P. digitatum* Δ*snf1* mutants (Tonukary *et al*., 2000; Ospina-Giraldro *et al* 2003; Yi *et al*., 2008; Tzima *et al*., 2011; Zhang *et al*., 2013). In the case of *B. cinerea*, the Δ*snf1* mutants did not lose completely their ability to infect plant tissues, but their virulence was strongly reduced (from 60 % to 90 % of reduction according to the plant tissues tested). In particular, the lesion produced by the mutants slowed down or stoped just after the early stage of infection, when infection cushions were usually observed for both mutant and wild type. These results suggest that *B. cinerea Δsnf1* mutants are not affected in the penetration process, but more likely in the colonization of plant tissues. Interestingly, the *Δsnf1* mutants were more impaired in the colonization of tissues with neutral pH (about 6.5), such as bean leaf and gherkin cotyledon, than on tissues with acidic pH, such as apple fruit. This is in agreement with the *in vitro* growth tests where the reduction in growth of the *Δsnf1* mutants compared to wild type was stronger at pH 7 than at pH 5, thus confirming the possible involvement of Snf1 kinase in a pH dependant regulation.

During colonization of plant tissues, the pH profile of *B. cinerea* can be divided in two parts: in the first stage, the pH decreases because of accumulation of citric and succinic acids; in the second stage, the pH increases because of fungal ammonia production (Billon-Grand *et*

al., 2012). In order to determine if the *B. cinerea Δsnf1* mutants have defect in acidification or alkalization during colonization, *in vitro* tests were performed; pH measurements showed that mutants were not impaired in acidification and alkalization, although they appeared to increase the pH medium faster than the wild type. However this behaviour needs to be further investigations in order to determine the involvement of Snf1 kinase in pH regulation and adaptation.

Finally, the absence of *snf1* gene strongly affected conidiation. Mutants did not produce normal conidiophores with macroconidia, but only microconidia, whereas the complemented strain was restored for these characteristics.

In conclusion, we confirmed the importance of *B. cinerea* Snf1 protein kinase in conidiation, carbon source utilization and virulence, in accordance to other Ascomycota plant pathogenic fungi (Table 2.6). In particular, Snf1 appears to be involved in simple sugars uptake and in lipid metabolism. On the contrary, Snf1 does not act as general activator of *B. cinerea* CWDE expression, since we observed differences in xylanase, PG, and cellulase activity secretion. Finally, *B. cinerea* Snf1 kinase seems to play a role in a possible pH dependent regulation, especially at alkaline pHs.

2.5 Conclusion and perspectives

In plant pathogenic fungi, signal transduction pathways regulated by glucose content in the ambient have been deeply investigated (Turrà *et al*., 2014). While the cAMP-PKA pathway, activated by the presence of glucose, is well studied in *B. cinerea* (Dub *et al*., 2013; Tudzynski and Gronover, 2007; Schumacher *et al*., 2008; Gronover *et al*., 2001), the *B. cinerea* Snf1 pathway, activated when glucose is scarce, was still unexplored. Therefore, in this study, we investigated growth, enzymatic activity, sporulation, and pathogenicity of *B. cinerea snf1* gene deletion mutants in order to determine the role of this protein kinase. The results obtained indicate an important function of Snf1 kinase in invasive growth and sporulation; this could be the starting point for subsequent researches aimed at establishing if this protein could be a target for new fungicides.

In perspective, since on all the carbon sources tested the radial growth of the Δ*snf1*mutants was more reduced at pH 7 than at pH 5 compared to the wild type, the regulation of *snf1* gene expression should be verified by qRT-PCR at different pHs. Besides, since the *snf1*complementation restored fungal ability to metabolize lipidic carbon sources only at pH 7 and restoration of fungal virulence was only partial, sequencing of the promoter region of the *snf1* ORF re-inserted in the *B. cinerea* genome could help to identify possible alterations involved in a pH dependent regulation.

Table 2.6 – Role of Snf1 protein kinase in different plant pathogenic fungi

		Cochliobolus carbonum Tonukary *et al.*, 2000	*Fusarium oxysporum* Ospina-Giraldo *et al.*, 2003	*Magnaporthe oryzae* Yi *et al.*, 2008	*Gibberella zeae (Fusarium graminearum)* Lee *et al*, 2009	*Verticillium dahlmiae* Tzima *et al.*, 2011	*Ustilago maydis* Nadal *et al.*, 2010	*Penicillium digitatum* Zhang *et al.*, 2013	*Magnaporthe oryzae* Zeng *et al.*, 2014	*Botrytis cinerea* This study	
										pH 5	pH 7
growth on different carbon sources	glucose	=	=	--	=	=	=	-	=	=	--
	sucrose	-		--	--	=	=	-	nd	-	--
	xylose	--	-	--	=	=	nd	nd	nd	--	-
	galacturonic acid	--	nd	nd	nd	nd	nd	nd	nd	=	--
	PGA	nd	nd	nd	nd	nd	nd	---	nd	-	--
	xylan	--	-	--	-	nd	=	nd	nd	=	--
	cellulose	nd	nd	nd	nd	nd	nd	nd	nd	-	--
	Tween 80	nd	nd	nd	nd	nd	nd	nd	---	--	--
	Olive oil	nd	nd	nd	nd	nd	nd	nd	---	-	---
	Triolein	nd	nd	nd	nd	nd	nd	nd	---	-	---
	NaAC	nd	nd	nd	nd	nd	nd	nd	---	--	---
	endo-PG	-	-	=	nd	nd	-	nd	nd	+	nd
	xylanase	-	nd	-/=/+	-	-	++	---	nd	-	-
pathogenicity		-	---	--	---	---	=	---	nd	--/---	
sporulation		=	nd	---	--	nd	nd	---	nd	---	

2.6 Supplementary data

(including the results obtained with complemented strain)

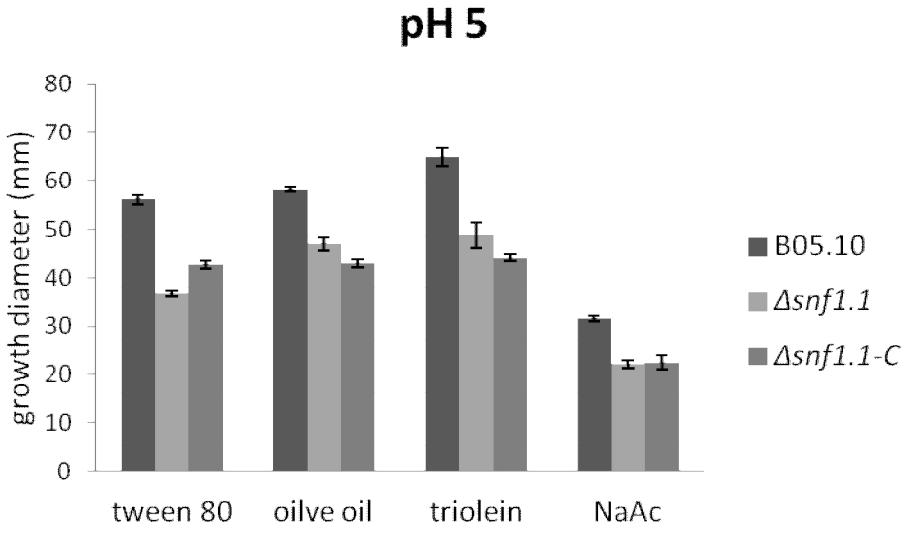

Figure S2.1 – Growth test of *B. cinerea* B05.10 wild type, Δ*snf1.1* mutant and Δ*snf1.1-C* complemented strain on lipidic non-fermentable carbon sources at pH 5. Growth of 4-day-old mycelium was measured (excluding 7 mm, the diameter of the mycelium plug) in one experiment, containing three replicates. Bars indicate the standard deviation calculated from six measurements.

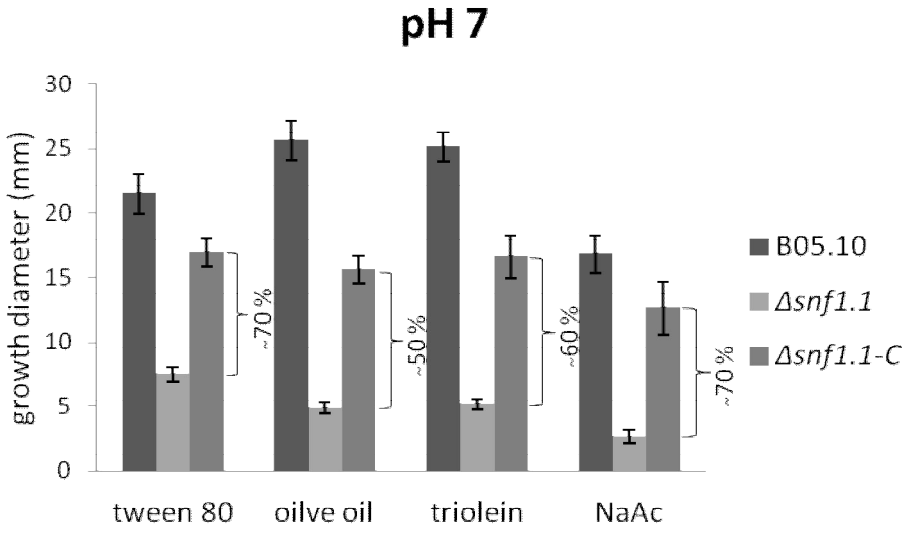

Figure S2.2 - Growth test of *B. cinerea* B05.10 wild type, Δ*snf1.1* mutant and Δ*snf1.1-C* complemented strain on lipidic non-fermentable carbon sources at pH 7. Growth of 4-day-old mycelium was measured (excluding 7 mm, the diameter of the mycelium plug) in one experiment, containing three replicates. The ability to metabolize lipidic components was partially restored in the complemented strain. Bars indicate the standard deviation calculated from six measurements.

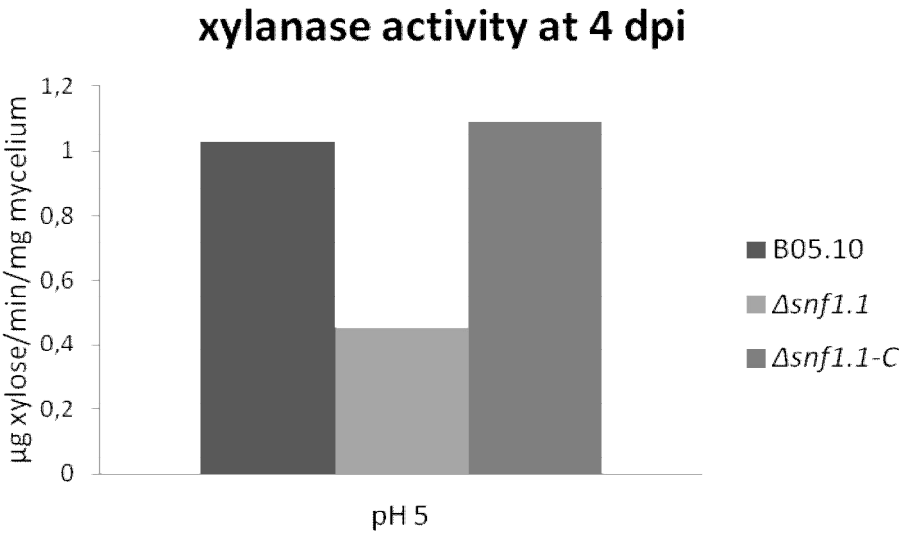

Figure S2.3 - Xylanase activity of *B. cinerea* wild type B05.10, Δ*snf1.1* mutant and Δ*snf1.1-C* complemented strains grown on 1 % (w/v) xylan. The xylanase activity was determined at pH 5 and at 4 dpi. The complemented strain restored the xylanase activity according to one experiment.

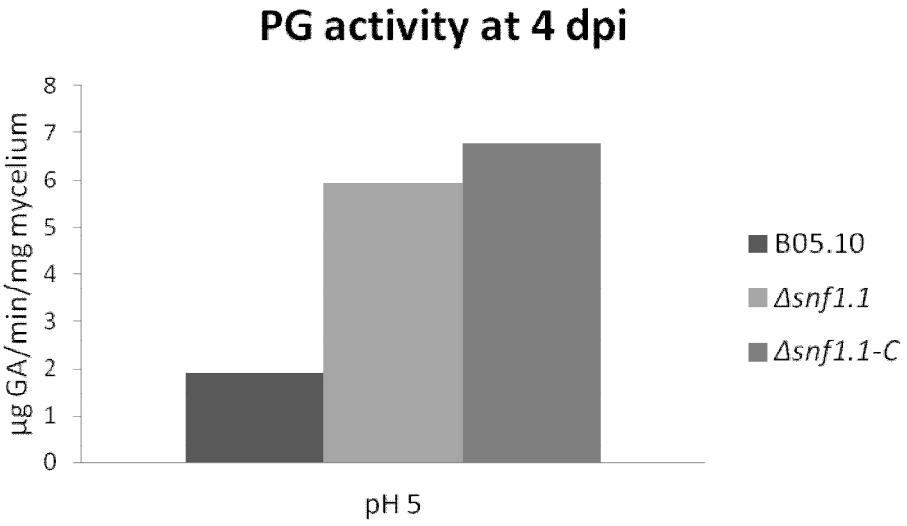

Figure S2.4 – Polygalacturonase (PG) activity of *B. cinerea* wild type B05.10, Δ*snf1.1* mutant and Δ*snf1.1-C* complemented strains grown on 1 % (w/v) PGA. The PG activity was determined at pH 5 and at 4 dpi. The complemented strain showed an activity equal to that of the mutant, according to one experiment.

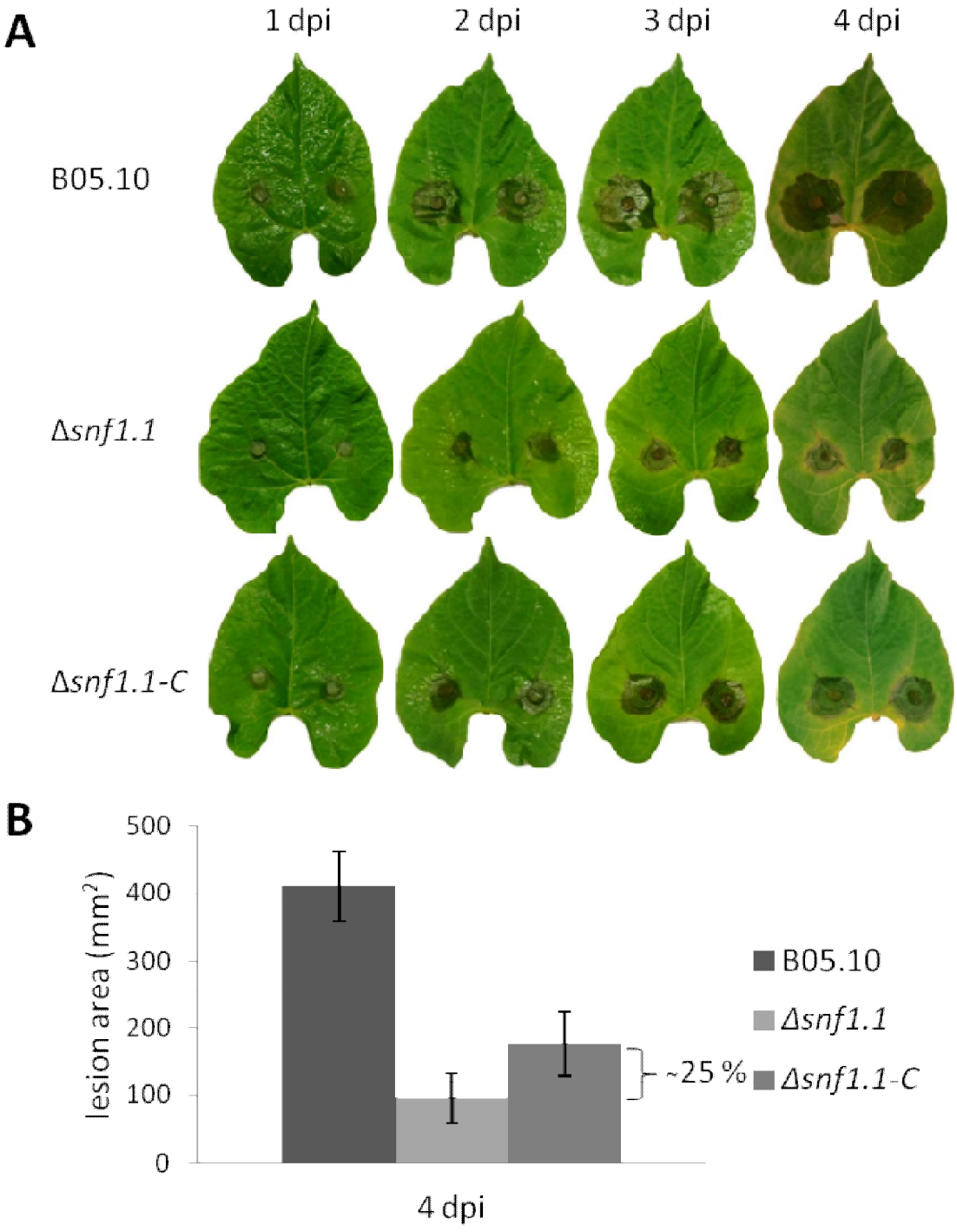

Figure S2.5 - Virulence of *B. cinerea* wild type B05.10, *Δsnf1.1* mutant and *Δsnf1.1-C* complemented strains at 1, 2, 3, and 4 dpi on French bean leaves (cv. Saxa) inoculated with 3 mm of diameter plugs containing actively growing mycelium. (**A**) Representative samples of infected bean leaves. (**B**) Histogram showing the measurement of the lesions area at 4 dpi. Bars indicate the standard deviation calculated from one experiments performed by infecting 8 leaves (two inoculation points per leaf) for each strain.

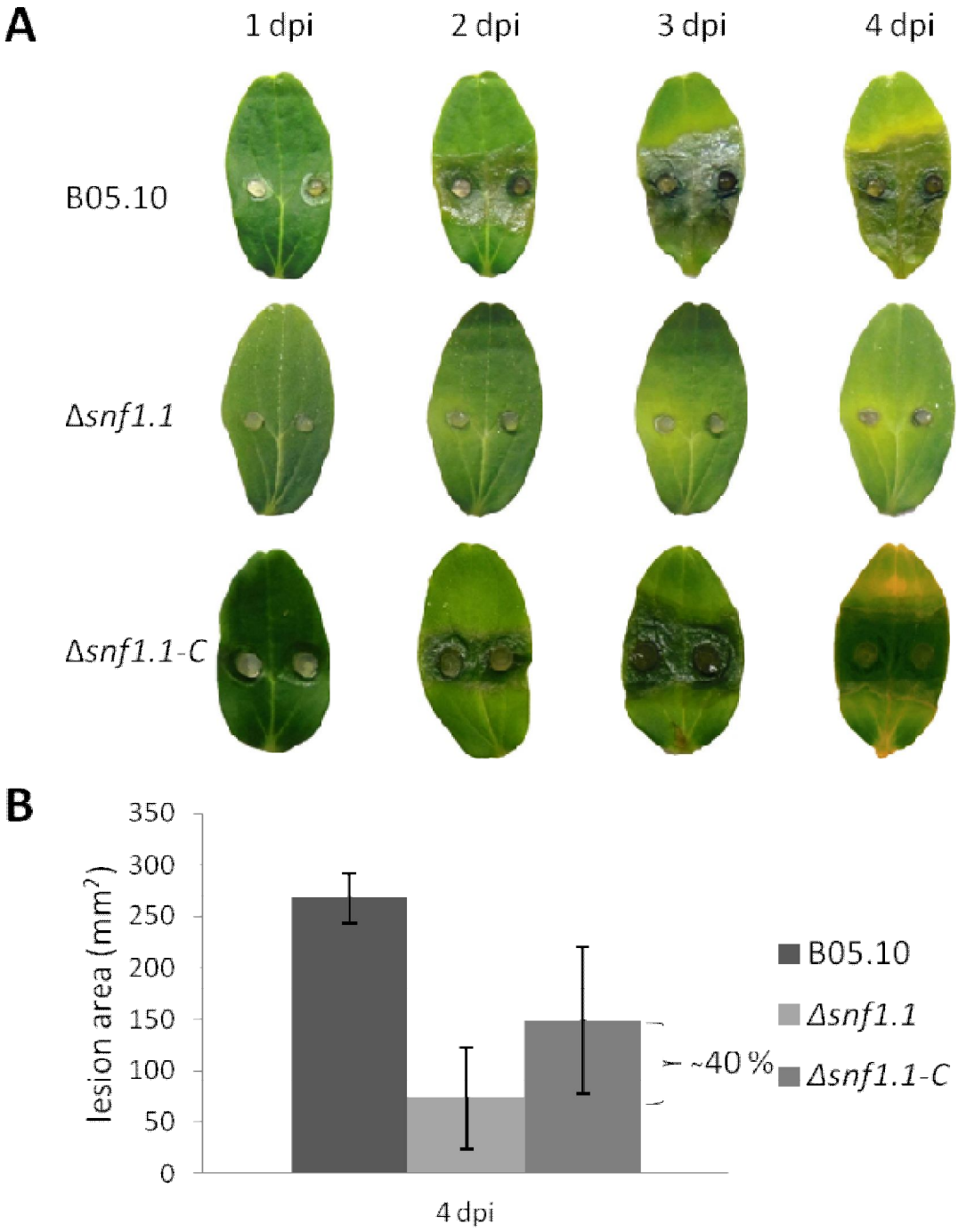

Figure S2.6 - Virulence of *B. cinerea* wild type B05.10, *Δsnf1.1* mutant and *Δsnf1.1-C* complemented strains at 1, 2, 3, and 4 dpi on gherkin cotyledons (cv. Petit vert de Paris) inoculated with 3 mm of diameter plugs containing actively growing mycelium. (**A**) Representative samples of infected gherkin cotyledons. (**B**) Histogram showing the measurement of the lesions area at 4 dpi. Bars indicate the standard deviation calculated from one experiments performed by infecting 20 leaves (two inoculation points per leaf) for each strain.

Bibliography

Ahuja, N., H. P. Singh, D. R. Batish, and R. K. Kohli. 2014. "Eugenol-Inhibited Root Growth in Avena Fatua Involves ROS-Mediated Oxidative Damage." *Pesticide Biochemistry and Physiology*.

Aminifard, M. H. and S. Mohammadi. 2013. "Efficacy of Plant Essential Oils to Control Post-Harvest Decay of Sweet Cherry (Prunus Avium L.) Fruit." *Journal of Horticultural Science and Biotechnology* 88 (1): 79-84.

Amiri, A., Dugas, R., Pichot, A. L., & Bompeix, G. (2008). In vitro and in vitro activity of eugenol oil (eugenia caryophylata) against four important postharvest apple pathogens. *International Journal of Food Microbiology, 126*(1-2), 13-19.

Amselem, J., C. A. Cuomo, J. A. L. van Kan, M. Viaud, E. P. Benito, A. Couloux, P. M. Coutinho, *et al*. 2011. "Genomic Analysis of the Necrotrophic Fungal Pathogens Sclerotinia Sclerotiorum and *Botrytis cinerea*." *PLoS Genetics* 7 (8).

Ashburner, M., C. A. Ball, J. A. Blake, D. Botstein, H. Butler, J. M. Cherry, A. P. Davis, *et al*. 2000. "Gene Ontology: Tool for the Unification of Biology." *Nature Genetics* 25 (1): 25-29.

Bennis, S., F. Chami, N. Chami, T. Bouchikhi, and A. Remmal. 2004. "Surface Alteration of Saccharomyces Cerevisiae Induced by Thymol and Eugenol." *Letters in Applied Microbiology* 38 (6): 454-458.

Billon-Grand, G., C. Rascle, M. Droux, J. A. Rollins, and N. Poussereau. 2012. "PH Modulation Differs during Sunflower Cotyledon Colonization by the Two Closely Related Necrotrophic Fungi *Botrytis cinerea* and Sclerotinia Sclerotiorum." *Molecular Plant Pathology* 13 (6): 568-578.

Blanco-Ulate, B., A. Morales-Cruz, K. C. H. Amrine, J. M. Labavitch, A. L. T. Powell, and D. Cantu. 2014. "Genome-Wide Transcriptional Profiling of *Botrytis cinerea* Genes Targeting Plant Cell Walls during Infections of Different Hosts." *Frontiers in Plant Science* 5 (SEP).

Brito, N., J. J. Espino, and C. González. 2006. "The Endo-β-1,4-Xylanase Xyn11A is Required for Virulence in *Botrytis cinerea*." *Molecular Plant-Microbe Interactions* 19 (1): 25-32.

Bullerman, L. B., Lieu, F. Y. and S. A. Seier. 1977. "Inhibition of Growth and Aflatoxin Production by Cinnamon and Clove Oils. Cinnamic Aldehyde and Eugenol". *Journal of Food Science* 42: 1107–1109.

Casamayor, A., R. Serrano, M. Platara, C. Casado, A. Ruiz, and J. Ariño. 2012. "The Role of the Snf1 Kinase in the Adaptive Response of Saccharomyces Cerevisiae to Alkaline pH Stress." *Biochemical Journal* 444 (1): 39-49.

Catlett, N. L., B-N. Lee, O. C. Yoder, and B. Gillian. 2003. "Split-Marker Recombination for Efficient Targeted Deletion of Fungal Genes." *Fungal Genet. Newsl.* (50):9-11

Choquer, M., E. Fournier, C. Kunz, C. Levis, J. -M Pradier, A. Simon, and M. Viaud. 2007. "*Botrytis cinerea* Virulence Factors: New Insights into a Necrotrophic and Polyphageous Pathogen." *FEMS Microbiology Letters* 277 (1): 1-10.

Colmenares, A. J., J. Aleu, R. Durán-Patrón, I. G. Collado, and R. Hernández-Galán. 2002. "The Putative Role of Botrydial and Related Metabolites in the Infection Mechanism of Botrytis Cinerea." *Journal of Chemical Ecology* 28 (5): 997-1005.

Cools, H. J. and K. E. Hammond-Kosack. 2013. "Exploitation of Genomics in Fungicide Research: Current Status and Future Perspectives." *Molecular Plant Pathology* 14 (2): 197-210.

Dalmais, B., J. Schumacher, J. Moraga, P. Le Pêcheur, B. Tudzynski, I. G. Collado, and M. Viaud. 2011. "The Botrytis Cinerea Phytotoxin Botcinic Acid Requires Two Polyketide Synthases for Production and has a Redundant Role in Virulence with Botrydial." *Molecular Plant Pathology* 12 (6): 564-579.

De Oliveira Pereira, F., J. M. Mendes, and E. De Oliveira Lima. 2013. "Investigation on Mechanism of Antifungal Activity of Eugenol Against Trichophyton Rubrum." *Medical Mycology* 51 (5): 507-513.

De Waard, M. A., A. C. Andrade, K. Hayashi, H. -J Schoonbeek, I. Stergiopoulos, and L. -H Zwiers. 2006. "Impact of Fungal Drug Transporters on Fungicide Sensitivity, Multidrug Resistance and Virulence." *Pest Management Science* 62 (3): 195-207.

Deighton, N., I. Muckenschnabel, A. J. Colmenares, I. G. Collado, and B. Williamson. 2001. "Botrydial is Produced in Plant Tissues Infected by *Botrytis cinerea*." *Phytochemistry* 57 (5): 689-692.

Dias, P. J., M. C. Teixeira, J. P. Telo, and I. Sá-Correia. 2010. "Insights into the Mechanisms of Toxicity and Tolerance to the Agricultural Fungicide Mancozeb in Yeast, as Suggested by a Chemogenomic Approach." *OMICS A Journal of Integrative Biology* 14 (2): 211-227.

Dub, A. M., L. Kokkelink, B. Tudzynski, P. Tudzynski, and A. Sharon. 2013. "Involvement of *Botrytis cinerea* Small GTPases BcRAS1 and BcRAC in Differentiation, Virulence, and the Cell Cycle." *Eukaryotic Cell* 12 (12): 1609-1618.

FRAC Code List©*2014: Fungicides sorted by mode of action (including FRAC Code numbering)

Fu, J., J. Wu, J. Jiang, Z. Wang, and Z. Ma. 2013. "Cystathionine Gamma-Synthase is Essential for Methionine Biosynthesis in Fusarium Graminearum." *Fungal Biology* 117 (1): 13-21.

Gamborg, O. L., R. A. Miller, and K. Ojima. 1968. "Nutrient Requirements of Suspension Cultures of Soybean Root Cells." *Experimental Cell Research* 50 (1): 151-158.

Gronover, C. S., D. Kasulke, P. Tudzynski, and B. Tudzynski. 2001. "The Role of G Protein Alpha Subunits in the Infection Process of the Gray Mold Fungus *Botrytis cinerea*." *Molecular Plant-Microbe Interactions* 14 (11): 1293-1302.

Hahn, M. 2014. "The Rising Threat of Fungicide Resistance in Plant Pathogenic Fungi: Botrytis as a Case Study." *Journal of Chemical Biology*.

Hedbacker, K. and M. Carlson. 2008. "SNF1/AMPK Pathways in Yeast." *Frontiers in Bioscience* 13 (7): 2408-2420.

Hong, S. -P and M. Carlson. 2007. "Regulation of Snf1 Protein Kinase in Response to Environmental Stress." *Journal of Biological Chemistry* 282 (23): 16838-16845.

Jacometti, M. A., S. D. Wratten, and M. Walter. 2010. "Review: Alternatives to Synthetic Fungicides for *Botrytis cinerea* Management in Vineyards." *Australian Journal of Grape and Wine Research* 16 (1): 154-172.

Kagan, I. A., A. Michel, A. Prause, B. E. Scheffler, P. Pace, and S. O. Duke. 2005. "Gene Transcription Profiles of Saccharomyces Cerevisiae After Treatment with Plant Protection Fungicides that Inhibit Ergosterol Biosynthesis." *Pesticide Biochemistry and Physiology* 82 (2): 133-153.

Kalemba, D. and A. Kunicka. 2003. "Antibacterial and Antifungal Properties of Essential Oils." *Current Medicinal Chemistry* 10 (10): 813-829.

Kamatou, G. P., I. Vermaak, and A. M. Viljoen. 2012. "Eugenol - from the Remote Maluku Islands to the International Market Place: A Review of a Remarkable and Versatile Molecule." *Molecules* 17 (6): 6953-6981.

Kars, I. and J. A. L. Van Kan. 2007. *Extracellular Enzymes and Metabolites Involved in Pathogenesis of Botrytis*. Botrytis: Biology, Pathology and Control.

Kitagawa, E., J. Takahashi, Y. Momose, and H. Iwahashi. 2002. "Effects of the Pesticide Thiuram: Genome-Wide Screening of Indicator Genes by Yeast DNA Microarray." *Environmental Science and Technology* 36 (18): 3908-3915.

Lee, S. -H, J. Lee, S. Lee, E. -H Park, K. -W Kim, M. -D Kim, S. -H Yun, and Y. -W Lee. 2009. "GzSNF1 is Required for Normal Sexual and Asexual Development in the Ascomycete Gibberella Zeae." *Eukaryotic Cell* 8 (1): 116-127.

Leroux, P. 2007. *Chemical Control of Botrytis and its Resistance to Chemical Fungicides*. Botrytis: Biology, Pathology and Control.

Leroux, P. and A. -S Walker. 2013. "Activity of Fungicides and Modulators of Membrane Drug Transporters in Field Strains of *Botrytis cinerea* Displaying Multidrug Resistance." *European Journal of Plant Pathology* 135 (4): 683-693.

Lever, M. 1972. "A New Reaction for Colorimetric Determination of Carbohydrates." *Analytical Biochemistry* 47 (1): 273-279.

Livak, K. J. and T. D. Schmittgen. 2001. "Analysis of Relative Gene Expression Data using Real-Time Quantitative PCR and the 2-ΔΔCT Method." *Methods* 25 (4): 402-408.

Myers, Ashley L. 2015. http://www.arec.vaes.vt.edu/alson-h-smith/grapes/pathology/extension/factsheets/botrytis-bunch-rot.pdf

Nadal, M., M. D. Garcia-Pedrajas, and S. E. Gold. 2010. "The snf1 Gene of Ustilago Maydis Acts as a Dual Regulator of Cell Wall Degrading Enzymes." *Phytopathology* 100 (12): 1364-1372.

Noda, J., N. Brito, and C. González. 2010. "The *Botrytis cinerea* Xylanase Xyn11A Contributes to Virulence with its Necrotizing Activity, Not with its Catalytic Activity." *BMC Plant Biology* 10.

Oe, T., T. Ohyagi, and A. Naganuma. 1998. "Determination of γ-Glutamylglutathione and Other Low-Molecular-Mass Biological Thiol Compounds by Isocratic High-Performance Liquid Chromatography with Fluorimetric Detection." *Journal of Chromatography B: Biomedical Applications* 708 (1-2): 285-289.

Ospina-Giraldo, M. D., E. Mullins, and S. Kang. 2003. "Loss of Function of the Fusarium Oxysporum SNF1 Gene Reduces Virulence on Cabbage and Arabidopsis." *Current Genetics* 44 (1): 49-57.

Özkan, A. and A. Erdoğan. 2013. "Membrane and DNA damaging/protective Effects of Eugenol, Eucalyptol, Terpinen-4-Ol, and Camphor at various Concentrations on Parental and Drug-Resistant H1299 Cells." *Turkish Journal of Biology* 37 (4): 405-413.

Parks, L. W., S. J. Smith, and J. H. Crowley. 1995. "Biochemical and Physiological Effects of Sterol Alterations in Yeast-A Review." *Lipids* 30 (3): 227-230.

Patel, R. M., M. N. Heneghan, J. A. L. van Kan, A. M. Bailey, and G. D. Foster. 2008. "The pOT and pLOB Vector Systems: Improving Ease of Transgene Expression in *Botrytis cinerea*." *Journal of General and Applied Microbiology* 54 (6): 367-376.

Pearson, M. N. and A. M. Bailey. 2013. *Viruses of Botrytis*. Advances in Virus Research. Vol. 86.

Penninckx, M. 2000. "A Short Review on the Role of Glutathione in the Response of Yeasts to Nutritional, Environmental, and Oxidative Stresses." *Enzyme and Microbial Technology* 26 (9-10): 737-742.

Pinedo, C., C. -M Wang, J. -M Pradier, B. Dalmais, M. Choquer, P. Le Pêcheur, G. Morgant, I. G. Collado, D. E. Cane, and M. Viaud. 2008. "Sesquiterpene Synthase from the Botrydial Biosynthetic Gene Cluster of the Phytopathogen *Botrytis cinerea*." *ACS Chemical Biology* 3 (12): 791-801.

Pócsi, I., R. A. Prade, and M. J. Penninckx. 2004. *Glutathione, Altruistic Metabolite in Fungi*. Advances in Microbial Physiology. Vol. 49.

Poinssot, B., E. Vandelle, M. Bentéjac, M. Adrian, C. Levis, Y. Brygoo, J. Garin, F. Sicilia, P. Coutos-Thévenot, and A. Pugin. 2003. "The Endopolygalacturonase 1 from *Botrytis cinerea* Activates Grapevine Defense Reactions Unrelated to its Enzymatic Activity." *Molecular Plant-Microbe Interactions* 16 (6): 553-564.

Polge, C. and M. Thomas. 2007. "SNF1/AMPK/SnRK1 Kinases, Global Regulators at the Heart of Energy Control?" *Trends in Plant Science* 12 (1): 20-28.

Popper, Z. A., G. Michel, C. Hervé, D. S. Domozych, W. G. T. Willats, M. G. Tuohy, B. Kloareg, and D. B. Stengel. 2011. *Evolution and Diversity of Plant Cell Walls: From Algae to Flowering Plants*. Annual Review of Plant Biology. Vol. 62.

Priebe, S., J. Linde, D. Albrecht, R. Guthke, and A. A. Brakhage. 2011. "FungiFun: A Web-Based Application for Functional Categorization of Fungal Genes and Proteins." *Fungal Genetics and Biology* 48 (4): 353-358.

Ronne, H. 1995. "Glucose Repression in Fungi." *Trends in Genetics* 11 (1): 12-17.

Ruepp, A., A. Zollner, D. Maier, K. Albermann, J. Hani, M. Mokrejs, I. Tetko, *et al*. 2004. "The FunCat, a Functional Annotation Scheme for Systematic Classification of Proteins from Whole Genomes." *Nucleic Acids Research* 32 (18): 5539-5545.

Schneider, C.A., Rasband, W.S., Eliceiri, K.W. "NIH Image to ImageJ: 25 years of image analysis". Nature Methods 9, 671-675, 2012.

Schumacher, J., L. Kokkelink, C. Huesmann, D. Jimenez-Teja, I. G. Collado, R. Barakat, P. Tudzynski, and B. Tudzynski. 2008. "The cAMP-Dependent Signaling Pathway and its Role in Conidial Germination, Growth, and Virulence of the Gray Mold *Botrytis cinerea*." *Molecular Plant-Microbe Interactions* 21 (11): 1443-1459.

Shin, J. -H, Y. -M Kim, J. -W Park, J. -E Kim, and I. -K Rhee. 2003. "Resistance of Saccharomyces Cerevisiae to Fungicide Chlorothalonil." *Journal of Microbiology* 41 (3): 219-223.

Siegmund, U., J. Heller, J. A. L. van Kan, and P. Tudzynski. 2013. "The NADPH Oxidase Complexes in Botrytis Cinerea: Evidence for a Close Association with the ER and the Tetraspanin Pls1." *PLoS ONE* 8 (2).

Simon A, Biot E. (2010). ANAIS: Analysis of NimbleGen Arrays Interface. Bioinformatics 2010 Oct; 26(19):2468-9.

Slameňová, D., E. Horváthová, L. Wsólová, M. Šramková, and J. Navarová. 2009. "Investigation of Anti-Oxidative, Cytotoxic, DNA-Damaging and DNA-Protective Effects of Plant Volatiles Eugenol and Borneol in Human-Derived HepG2, Caco-2 and VH10 Cell Lines." *Mutation Research - Genetic Toxicology and Environmental Mutagenesis* 677 (1-2): 46-52.

Spellman, P. T., G. Sherlock, M. Q. Zhang, V. R. Iyer, K. Anders, M. B. Eisen, P. O. Brown, D. Botstein, and B. Futcher. 1998. "Comprehensive Identification of Cell Cycle-Regulated Genes of the Yeast Saccharomyces Cerevisiae by Microarray Hybridization." *Molecular Biology of the Cell* 9 (12): 3273-3297.

Staats, M., P. Van Baarlen, and J. A. L. Van Kan. 2005. "Molecular Phylogeny of the Plant Pathogenic Genus Botrytis and the Evolution of Host Specificity." *Molecular Biology and Evolution* 22 (2): 333-346.

Temme, N. and P. Tudzynski. 2009. "Does Botrytis Cinerea Ignore H2O2-Induced Oxidative Stress during Infection? Characterization of Botrytis Activator Protein 1." *Molecular Plant-Microbe Interactions* 22 (8): 987-998.

Ten Have, A., W. Mulder, J. Visser, and J. A. L. Van Kan. 1998. "The Endopolygalacturonase Gene Bcpg1 is Required to Full Virulence of *Botrytis cinerea*." *Molecular Plant-Microbe Interactions* 11 (10): 1009-1016.

Ten Have, A., W. O. Breuil, J. P. Wubben, J. Visser, and J. A. L. Van Kan. 2001. "*Botrytis cinerea* Endopolygalacturonase Genes are Differentially Expressed in various Plant Tissues." *Fungal Genetics and Biology* 33 (2): 97-105.

Tonukari, N. J., J. S. Scott-Craig, and J. D. Walton. 2000. "The Cochliobolus Carbonum SNF1 Gene is Required for Cell Wall-Degrading Enzyme Expression and Virulence on Maize." *Plant Cell* 12 (2): 237-247.

Tonukari, N. J., J. S. Scott-Craig, and J. D. Walton. 2003. "Isolation of the Carbon Catabolite Repressor (CREA) Gene from the Plant-Pathogenic Fungus Cochliobolus Carbonum." *DNA Sequence - Journal of DNA Sequencing and Mapping* 14 (2): 103-107.

Tudzynski, B. and C. S. Gronover. 2007. *Signalling in Botrytis cinerea*. Botrytis: Biology, Pathology and Control.

Turrà, D., D. Segorbe, and A. Di Pietro. 2014. *Protein Kinases in Plant-Pathogenic Fungi: Conserved Regulators of Infection*. Annual Review of Phytopathology. Vol. 52.

Tzima, A. K., E. J. Paplomatas, P. Rauyaree, M. D. Ospina-Giraldo, and S. Kang. 2011. "VdSNF1, the Sucrose Nonfermenting Protein Kinase Gene of Verticillium Dahliae, is Required for Virulence and Expression of Genes Involved in Cell-Wall Degradation." *Molecular Plant-Microbe Interactions* 24 (1): 129-142.

Valero, D., F. Guillén, D. Martínez-Romero, S. Castillo, P. J. Zapata, and M. Serrano. 2010. *A Novel Active Packaging to Maintain Quality and Increase Shelf Life and Safety of Table Grapes*. Acta Horticulturae. Vol. 858.

Valette-Collet, O., A. Cimerman, P. Reignault, C. Levis, and M. Boccara. 2003. "Disruption of *Botrytis cinerea* Pectin Methylesterase Gene Bcpme1 Reduces Virulence on several Host Plants." *Molecular Plant-Microbe Interactions* 16 (4): 360-367.

Valverde, J. M., Guillén, F., Martínez-Romero, D., Castillo, S., Serrano, M., & Valero, D. (2005). Improvement of table grapes quality and safety by the combination of modified atmosphere packaging (MAP) and eugenol, menthol, or thymol. *Journal of Agricultural and Food Chemistry, 53*(19), 7458-7464.

van Kan, J. A. L. 2006. "Licensed to Kill: The Lifestyle of a Necrotrophic Plant Pathogen." *Trends in Plant Science* 11 (5): 247-253.

Vautard-Mey, G. and M. Fèvre. 2003. "Carbon and pH Modulate the Expression of the Fungal Glucose Repressor Encoding Genes." *Current Microbiology* 46 (2): 146-150.

Waechter, F., E. Weber, T. Hertner, and U. May-Hertl. 2010. *Cyprodinil: A Fungicide of the Anilinopyrimidine Class*. Hayes' Handbook of Pesticide Toxicology.

Wang, C., Zhang, J., Chen, H., Fan, Y., & Shi, Z. (2010). Antifungal activity of eugenol against *Botrytis cinerea*. *Tropical Plant Pathology, 35*(3), 137-143.

Williamson, B., B. Tudzynski, P. Tudzynski, and J. A. L. Van Kan. 2007. "*Botrytis cinerea*: The Cause of Grey Mould Disease." *Molecular Plant Pathology* 8 (5): 561-580.

Wilson, C. L., J. M. Solar, A. El Ghaouth, and M. E. Wisniewski. 1997. "Rapid Evaluation of Plant Extracts and Essential Oils for Antifungal Activity Against *Botrytis cinerea*." *Plant Disease* 81 (2): 204-210.

Wubben, J. P., A. Ten Have, J. A. L. Van Kan, and J. Visser. 2000. "Regulation of Endopolygalacturonase Gene Expression in *Botrytis cinerea* by Galacturonic Acid, Ambient pH and Carbon Catabolite Repression." *Current Genetics* 37 (2): 152-157.

Yasokawa, D. and H. Iwahashi. 2010. "Toxicogenomics using Yeast DNA Microarrays." *Journal of Bioscience and Bioengineering* 110 (5): 511-522.

Yen, T. -B and S. -T Chang. 2008. "Synergistic Effects of Cinnamaldehyde in Combination with Eugenol Against Wood Decay Fungi." *Bioresource Technology* 99 (1): 232-236.

Yi, M., J. -H Park, J. -H Ahn, and Y. -H Lee. 2008. "MoSNF1 Regulates Sporulation and Pathogenicity in the Rice Blast Fungus Magnaporthe Oryzae." *Fungal Genetics and Biology* 45 (8): 1172-1181.

Young, E. T., K. M. Dombek, C. Tachibana, and T. Ideker. 2003. "Multiple Pathways are Co-Regulated by the Protein Kinase Snf1 and the Transcription Factors Adr1 and Cat8." *Journal of Biological Chemistry* 278 (28): 26146-26158.

Yu, J., H. Son, A. R. Park, S. -H Lee, G. J. Choi, J. -C Kim, and Y. -W Lee. 2014. "Functional Characterization of Sucrose Non-Fermenting 1 Protein Kinase Complex Genes in the Ascomycete Fusarium Graminearum." *Current Genetics* 60 (1): 35-47.

Zeng, X. -Q, G. -Q Chen, X. -H Liu, B. Dong, H. -B Shi, J. -P Lu, and F. Lin. 2014. "Crosstalk between SNF1 Pathway and the Peroxisome-Mediated Lipid Metabolism in Magnaporthe Oryzae." *PLoS ONE* 9 (8).

Zhang, T., X. Sun, Q. Xu, C. Zhu, Q. Li, and H. Li. 2013. "PdSNF1, a Sucrose Non-Fermenting Protein Kinase Gene, is Required for Penicillium Digitatum Conidiation and Virulence." *Applied Microbiology and Biotechnology* 97 (12): 5433-5445.